

## **Article**



https://doi.org/10.11646/zootaxa.5258.2.1 http://zoobank.org/urn:lsid:zoobank.org:pub:33F922CD-6372-427A-912E-DC3CF4641F8D

# Three new species of the *Synapturanus rabus* complex (Microhylidae: Otophryninae) in Colombia with a review of the genus *Synapturanus*

MARIELA OSORNO-MUÑOZ<sup>1,5</sup>, DORIS L. GUTIÉRREZ-LAMUS<sup>1,6</sup>, JOHN LYNCH<sup>2</sup>, RACHEL KEEFFE<sup>3</sup>, JOSÉ RANCÉS CAICEDO-PORTILLA<sup>1,7</sup>, KIN NOK CHAN<sup>4</sup>, JOÃO F. R. TONINI<sup>4,8\*</sup> & RAFAEL O. DE SÁ<sup>4,9\*</sup>

<sup>1</sup>Instituto Amazónico de Investigaciones Científicas SINCHI, Bogotá, Colombia.

#### **Abstract**

The Neotropical microhylid genus *Synapturanus* was represented by only three species for almost five decades and remains poorly known. Recently two new species were described from the Eastern Guyana Shield, one from Peru, and one from Brazil. We describe three new species related to the *S. rabus* species complex with known distribution only in western Amazonia, Colombia. The *S. rabus* complex consists of the smallest species in the genus; one of the new species is slightly larger than *S. rabus* and we describe its full osteology; the other two new species are smaller than *S. rabus*. We also described the call and larvae of one of the new species. We provide an updated diagnosis and review the available molecular and phenotypic data for the genus.

Key words: Synapturanus, osteology, diagnosis, Synapturanus rabus species complex

## Introduction

The family Microhylidae currently consist of 12 recognized subfamilies, three of which are found in the New World: the monotypic Adelastinae, Gastrophryninae (i.e., the largest neotropical radiation with 81 currently described species), and Otophryninae with six known species (Frost, 2021). Diversity of Otophryninae remains poorly known and the subfamily currently consists of two widely distributed and morphologically distinct genera in larval and adult morphology; *Otophryne* Boulenger, 1900 and *Synapturanus* Carvalho, 1954. Both genera remained poorly studied because specimens are not common in collections. Recently, an integrative analysis of genetic, acoustic, and morphometric data, significantly increased the account of species of these two genera and described three new species of *Synapturanus* (Fouquet *et al.*. 2021a,b).

Historically, the placement and relationships of *Synapturanus* has been controversial; it was considered closely related to *Elachistocleis* and *Myersiella* (Carvalho 1954), basal to Microhylidae (Frost *et al..*, 2006), closely related to Scaphiophryninae (Van Bocxlaer *et al.*. 2006), associated with Asterophryninae (van der Meijden *et al.*. 2007) and as the sister taxon to *Otophryne* in the Otophryninae (Pyron and Wiens, 2011, de Sá *et al.*. 2012, Fouquet *et al.*. 2021a). Several more recent studies, including those based on phylogenomic evidence, have recovered a Neotropical clade consisting of Otophryninae and Gastrophryninae (Feng *et al.*. 2017; Tu *et al.*. 2018; Streicher *et al.*. 2020; Hime *et al.*. 2020).

The nomenclatural history of *Synapturanus* is characterized by extensive confusion with that of the current genus *Myersiella*. Parker (1934) differentiated the two genera based on external traits; subsequently, Carvalho (1954)

<sup>&</sup>lt;sup>2</sup>Instituto de Ciencias Naturales, Universidad Nacional de Colombia, Bogotá, Colombia. <sup>6</sup> https://orcid.org/0000-0002-6358-1610

<sup>&</sup>lt;sup>3</sup>Florida Museum of Natural History, University of Florida, Gainesville, FL 32611. © https://orcid.org/0000-0002-5062-2866

<sup>&</sup>lt;sup>4</sup>Department of Biology, University of Richmond, Richmond, VA, 23173, USA

<sup>&</sup>lt;sup>5</sup> https://orcid.org/0000-0001-9333-068X

<sup>6</sup> https://orcid.org/0000-0002-9801-4544

<sup>&</sup>lt;sup>7</sup> https://orcid.org/0000-0001-5689-5657

<sup>8</sup> https://orcid.org/0000-0002-4730-3805

<sup>&</sup>lt;sup>9</sup> https://orcid.org/0000-0002-6137-962X

<sup>\*</sup>Corresponding authors. 🖃 rdesa@richmond.edu; 🖃 jfrtonini@gmail.com

designated the type species and recognized the two genera based on osteological characters. However, Nelson and Lescure (1975) reviewed the two genera and noted that osteological data did not match the corresponding taxa and provided a osteological diagnosis for each genus. Previous work provided the following combination of diagnostic characters for *Synapturanus*: prevomer divided, posterior part absent; ethmoid fused to parasphenoid; no palatine; premaxillary without medial notch; quadratojugal reduced and not in contact with maxilla; vertebral column diplasiocoelous; clavicles and procoracoids absent; urostyle with well-developed transverse processes; terminal phalanges pointed; fingers and toes with disk-like expansions, subarticular tubercles absent; toes without webbing; snout acuminate, elongate, projecting beyond the lower jaw (Carvalho, 1954; Pyburn, 1975; Nelson and Lescure, 1975, see discussion).

Synapturanus currently consists of seven described species: Synapturanus mirandariberoi Nelson and Lescure, 1975, S. salseri Pyburn, 1975, S. rabus Pyburn, 1977, S. zombie Fouquet et al.. 2021b, S. mesomorphus Fouquet et al.. 2021b, S. ajuricaba Fouquet et al.., 2021b, and S. danta Chávez et al.. 2022. Speciation in the genus seems to occur through allopatric speciation where rivers may be barriers for microhylids and small distributions are probably associated with low dispersal ability and ecological requirements of the genus Synapturanus (de Sá et al.., 2019; Fouquet et al.., 2021a). Synapturanus rabus is the smallest species in the genus and the S. rabus complex consists of a cluster of cryptic species.

Herein, we describe three additional species of the *Synapturanus rabus* species complex based on genetic, morphometric, and morphological data. The complete osteology is described for one of the new species and compare it with the osteology of other species in the genus.

## Materials and methods

Morphological methodology. Specimens, tissues, and comparative material used herein are deposited in the amphibian collection of the Instituto Amazónico de Investigaciones Científicas—SINCHI, Bogotá, Instituto de Ciencias Naturales de la Universidad Nacional de Colombia, Bogotá, and Instituto Alexander von Humboldt, Villa de Leyva, Colombia. We also examined specimens deposited at the American Museum of Natural History, the Amphibian Collection of the University of Texas in Arlington, and the National Museum of Natural History, Smithsonian (including the Holotype of *Synapturanus rabus* USNM 199674). List of examined materials is provided in Appendix 1. Acronyms and morphometric data are provided in Appendix 2 and samples, localities, and Genbank accession numbers use in the analyses are given in Appendix 3. Specimens used in the manuscript are from: SIN-CHI-A: Colección Anfibios Instituto Amazónico de Investigaciones Científicas (SINCHI), Bogotá, Colombia; ICN: Instituto de Ciencias Naturales de la Universidad Nacional de Colombia; IAvH: Instituto Alexander von Humboldt, Colombia; AMNH-A: American Museum of Natural History; UTA-A: Amphibian collection of the University of Texas in Arlington. In addition, voucher material has the following collector code: MOM: Mariela Osorno Muñoz; JARM: Julián Andrés Roja Morales; JDL: John D. Lynch; SNC-H: Filed number of material deposited at SINCHI.

The following measurements were taken with a digital caliper under a stereo microscope to the nearest 0.05 mm: SVL (snout–vent length); HL (head length; from snout to angle of the jaw); HW (head width; between the angle of jaws); ED (eye diameter; between anterior and posterior corner of the eye); IOD (inter–orbital distance; minimum distance between eyelids); END (eye–nostril distance; from the anterior corner of the eye to the posterior margin of nostril); ESD (eye–snout distance, from the anterior corner of the eye to the tip of the snout); SL (snout length from the anterior edge of the upper jaw to the tip of the snout), SW (snout width where the upper jaw meets the lower jaw), TD (tympanum diameter), TBL (tibia length; from the outer edge of the flexed knee to the heel). Fingers and toes are numbered and abbreviated as follows: Fingers I–IV, Toes I–V. Measurements are given in Tables 1 and 2, where means are reported as  $\pm$  one standard error of the mean; raw data are given in Appendix 2. Acoustic parameters of advertisement calls given in Table 3.

**Morphometric analysis.** Principal Component Analysis (PCA) based on a covariance matrix was used to assess the morphometric differentiation among adult individuals (Appendix 4a and 4b). The species of *Synapturanus* currently known as closely related to *S. rabus* and the three new species collected in the Colombian Amazon (i.e., *Synapturanus* sp. "Caquetá", *Synapturanus* sp. "Amazonas", and *Synapturanus* sp. "Jirijirimo") were included in the analysis. To remove the effect of body size, we use the residuals of the linear regressions between SVL and the morphometric variables to generate a PCA. Overall, these analyses discriminate and visualize species groupings in

multidimensional space and the absence of overlap indicates morphometric discrimination among groups. The measurements included in the analysis were: SVL, HL, HW, IO, END, ED, and TBL; measurements of *S. ajuricaba*, *S. mesomorphus*, and *S. zombie* were extracted from Fouquet *et al.*. (2021b). All analyses were performed using PAST 4.06b (Hammer *et al.*, 2001).

Osteological analyses. Osteological observations were performed using cleared and stained for bone and cartilage (Dingerkus and Uhler, 1977) and we produced μCT scans from fluid-preserved museum specimens. These methodologies allow us to corroborate characters included in the diagnosis of the genus *Synapturanus* (Nelson and Lescure, 1975) and identify additional diagnostic characters. Two adult males of *Synapturanus* sp. "Caquetá" (SINCHI-A 2679, SINCHI-A 842) and an adult female of *Synapturanus* sp. "Jirijirimo" (ICN 56893) were cleared and stained for bone and cartilage (Dingerkus and Uhler, 1977). We describe the osteology of *Synapturanus* sp. "Caquetá" and compare it with that of *Synapturanus* sp. "Jirijirimo", *S. rabus* (type specimens AMNH A92969), *S. mirandariberoi* (AMNH A909350, AMNH A90936), and with a specimen tentatively assigned to *S. salseri* (AMNH A118800).

For the three previously known species, we produced µCT scans from fluid-preserved museum specimens using a Phoenix v|tome|x M (GE's Measurement & Control business, Boston, USA) at the University of Florida's Nanoscale Research Facility. The scanner settings were as follows: *S. rabus* (AMNH A92969), 70 kV, 200 mA, 18.56 µm voxel resolution; *S. salseri* (AMNH A118800), 75 kV, 200 mA, 23.66 µm voxel; and *S. mirandaribeiroi* (AMNH A909350), 70 kV, 300 mA, 24.21µm voxel resolution. The raw x-ray data were processed in GE's proprietary Datos|x Software v.2.3 to produce tomogram stacks which were then read into VG StudioMax v.3.4 (Volume Graphics, Heidelberg, Germany) where the skeletal elements were segmented and then exported as image files. Final figures were assembled in Photoshop CS6 (CS6, Adobe).

**Molecular Analysis.** The molecular analysis included all 16S sequences available for *Synapturanus* in Genbank at the time of submission of the manuscript. We included sequences of *S. salseri* and *S. rabus* collected close to their type localities, and sequences of *Synapturanus* collected in Amazonia, but distant from the localities of the described species from Vaupés (Pyburn 1975, 1976). We preliminary label these specimens based on the geographic area they were collected, i.e., *Synapturanus* sp. "Caqueta", *Synapturanus* sp. "Amazonas", and *Synapturanus* sp. "Jirijirimo".

Total genomic DNA was extracted from ethanol preserved muscle or liver tissues using standard Qiagen DNeasy kit (Valencia, California, USA). Primers used in amplification were standard primers used in amphibians (16SAr 5'-CGCCTGTTTACCAAAAACAT-3' and 16sBr 5'-CTCCGGTCTGAACTCAGATCACGTAG-3') under the following thermal protocol: initial denaturation at 94°C for 2 min followed by 34 cycles of 94°C for 1 min, 58°C for 1 min, and 72°C for 1 min 30 s. Amplified segments were purified by heating samples at 80°C for 15 min using USB ExoSap-IT (US78201, Amersham Biosciences, Piscataway, New Jersey, USA) and sequenced (in both primer directions) by Eurofins Genomics (www.eurofinsgenomics.com, Louisville, KY, USA;). Resulting chromatograms were visualized, aligned, and cleaned using Sequencher 5.1 (Gene Codes Corp., Ann Arbor, Michigan, USA). Each sequence was searched against NCBI database using BLAST (Basic Local Alignment Search Tool, http://blast.ncbi. nlm.nih.gov/Blast.cgi; Altschul *et al...*, 1990) to eliminate potential contamination. Sequence alignment for each locus was initially produced in SATé-II (Liu *et al...*, 2012) and subsequently examined visually to identify potential problematic areas. We estimated p-uncorrected genetic distances using MEGA 11 (Tamura *et al...*, 2021).

**Phylogenetic Analyses.** We used IQ-TREE (Nguyen *et al.*. 2015) to generate the molecular phylogeny of *Synapturanus* using the 16S alignment. The best-fit substitution model was chosen using ModelFinder (Kalyaanamoorthy *et al.*. 2017). Support values were estimated using the Shimodaira-Hasegawa-like approximate likelihood ratio test (SH-alrt; Guindon *et al.*. 2010) and the Ultrafast Bootstrap approximation (UFBoot; Hoang *et al.*. 2018) with ten thousand replicates. Values above 90% are considered good support for the evolutionary relationships. In the phylogenetic analysis we included *O. robusta* and *O. steyermarki* as outgroups and we used *Adelastes hylonomos* to root the Otophryninae phylogeny following de Sá *et al.*. (2012) and Streicher *et al.*. (2020). We ran 10 phylogenetic analyses in IQTREE on the high performance computer cluster Spydur at the University of Richmond, VA and chose the phylogenetic tree with highest likelihood score. The resulting tree was visualized in FigTree v1.4.4 (Rambaut 2014).

Molecular data generated in this manuscript is deposited in Genbank and accession numbers for specimens included in the phylogenetic analyses are provided in Appendix 3. In addition, the final 16S alignment and Maximum Likelihood tree are deposit in Zenodo (10.5281/zenodo.7646925).

|               | SEX | u  | SVL                      | HL                  | HW                    | ED                   | IOD                    | END                  | ESD                     | ST                   | SW                  | TBL                   | Source                   |
|---------------|-----|----|--------------------------|---------------------|-----------------------|----------------------|------------------------|----------------------|-------------------------|----------------------|---------------------|-----------------------|--------------------------|
| S. latebrosus | 0+  | ∞  | 20.86 0.26 (20.0–22.0)   | 5.320.11 (4.8–5.8)  | 5.410.13 (4.9–5.9)    | 1.060.02 (1.0–1.15)  | 2.50.06 (2.2–2.7)      | 2.020.04 (1.85–2.2)  | 3.30.08 (3.0–3.65)      | 1.40.04 (1.25–1.65)  | 1.8 0.06 (1.55–2.1) | 7.90.2 (7.3–8.4)      | This<br>work             |
| S. latebrosus | 50  | 3  | 18.70.3<br>(18.1–19.0)   | 4.80.2 (4.55–5.15)  | 5.130.16 (4.85–5.4)   | 1.120.09 (0.95–1.25) | 2.30.11 (2.1–2.5)      | 1.950.0<br>1.95      | 3.290.08<br>(2.75–2.95) | 1.40.03 (1.35–1.45)  | 1.70.04 (1.6–1.75)  | 7.90.16 (6.35–7.2)    | This<br>work             |
| S. sacratus   | 0+  | 2  | 16.95<br>(16.6, 17.3)    | 4.5<br>(4.45,4.55)  | 4.22 (4.15, 4.3)      | 1.13 (1.1, 1.15)     | 1.97 (1.9, 2.05)       | 1.50.1 (1.4, 1.6)    | 2.50.00 (2.55)          | 1.020.12 (0.9, 1.15) | 2.00.1 (1.9, 2.1)   | 6.90.05<br>(6.8, 6.9) | This<br>work             |
| S. sacratus   | 50  | 2  | 14.5<br>(14.0, 15.0)     | 4.20.12 (3.9, 4.15) | 4.10.12 (3.95, 4.2)   | 1.150.1 (1.0, 1.25)  | 1.870.025 (1.8, 1.9)   | 1.50.025 (1.5, 1.55) | 2.250.1<br>(2.1, 2.3)   | 1,150.15 (1.0, 1.3)  | 1.650.15 (1.5,1.8)  | 6.30.35 (6.0, 6.7)    | This<br>work             |
| S. artifex    | 0+  | 3  | 17.260.18 (17.2–17.6)    | 4.680.28 (4.15–5.1) | 4.780.14 (4.5–4.95)   | 1.280.07 (1.15–1.4)  | 1.980.17 (1.7–2.3)     | 1.580.04 (1.5–1.65)  | 2.50.1 (2.35–2.7)       | 1.20.1 (1.0–1.2)     | 1.10.13 (0.9–1.35   | 7.10.29 (7.05–7.15)   | This<br>work             |
| S. artifex    | 50  | 6  | 15.570.07<br>(15.2–15.9) | 4.150.34 (4.0–4.4)  | 4.550.13<br>(4.1–5.1) | 1.070.04 $(0.9-1.3)$ | 1.930.08 (1.6,–2.25)   | 1.430.03 (1.35–1.6)  | 2.40.04 (2.3,-2.6)      | 1.080.03 (0.9–1.15)  | 1.30.07 (1.0–1.6)   | 6.60.04 (6.4–6.75)    | This<br>work             |
| S. rabus      | 50  | 1  | 16.4                     | 4.65                | 4.2                   | 1.05                 | 1.9                    | 1.3                  | 2.8                     | 1.25                 | 1.35                | 7.15                  | This<br>work             |
| S. rabus      | 0+  | 3  | 18.50.45<br>(17.2–19.0)  | 5.000.12 (4.8–5.2)  | 4.70.03 (4.7–4.8)     | 1.20.06 (1.1–1.3)    | ı                      | 1.050.06 (1.5–1.6)   | ŀ                       | I                    | ŀ                   | 7.40.10 (7.2–7.5)     | Pyburn,<br>1976          |
| S. salseri    | 50  | 13 | 24.40.28<br>(22.65–26.0) | 6.20.09 (5.7–6.8)   | 6.20.11<br>(5.8–6.95) | 1.250.04 (1.05–1.45) | 2.850.05<br>(2.55–3.2) | 2.130.04 (1.95–2.5)  | 3.70.04<br>(3.45–3.9)   | 1.70.04 (1.4–1.95)   | 2.440.44 (2.3–2.85) | 10.10.16 (9.15–11.05) | This<br>work             |
| S. danta      | 60  | 7  | 17.8<br>(18.0, 17.6)     | 4.3<br>(4.4, 4.2)   | 5.6<br>(5.6, 5.6)     | 2.1 (1.0,1.1)        | 2.35<br>(2.3, 2.4)     | 1.5 (1.5, 1.5)       | I                       | I                    | I                   | 5.05<br>5.1, 5.0      | Chávez<br>et al,<br>2021 |

#### **Results**

The phylogenetic analysis recovered three distinct clades (Fig. 1, Appendix 5). One clade consists of two undescribed putative species labeled *Synapturanus* sp. "Iça1" and *Synapturanus* sp. "Juami" occurring in Amazonas, Brazil (Fouquet *et al.*. 2021a); this clade splits from a basal node and is the sister group of all other *Synapturanus*. The second clade consists of species of the *S. rabus* species complex and includes several undescribed putative species, including one from Peru labeled *S.* sp. "Nanay", one from Amazonas, Brazil labeled *S.* sp. "Iça2", and another from Acre, Brazil labelled as *S.* sp. "Divisor", as well as the three new species from Colombia described in here. The third clade consists of *S. mesomorphus*, *S. salseri*, *S. mirandaribeiroi*, *S. zombie*, *S. ajuricaba*, and two undescribed putative species, one endemic of the Neblina National Park labeled *S.* sp. "Neblina" and another distributed in Amazonas and Pará, Brazil labelled as *S.* sp. "Taboca, Tapajós, Purus" (Fouquet *et al.*. 2021a, b).

Specimens morphologically identified as *Synapturanus salseri* included in our analyses are from two localities close to the type locality, Timbó, Vaupés, Colombia, 1°6′ N 69°55′ W (Pyburn, 1975; Kizirian & McDiarmid, 1998). One locality is to the east, about 62 km, and the second one to southeast about 92 km. The two populations lack significant genetic divergence between them (Fig. 1).

The clade herein referred as the "Synapturanus rabus complex" includes a specimen morphologically identified as S. rabus and collected close to its type locality, i.e., about 55 km south of Yapima -1° 03′ N, 69° 28′ W (Pyburn, 1976); a locality that is also found south of the Vaupes River. This specimen is placed in a larger clade consisting of various lineages morphologically close to S. rabus in the Colombian Amazon; i.e., Synapturanus sp. "Caquetá", Synapturanus sp. "Amazonas", and Synapturanus sp. "Jirijirimo". The locality of specimens of Synapturanus sp. "Jirijirimo" is about 204 km southwest to the type locality of S. rabus and south of the Apaporis River; those populations were previously reported as S. rabus (Fouquet et al.., 2021a). Our morphological examination of the specimens and the phylogenetic molecular analysis identified, with strong nodal support, three distinct lineages, i.e., Synapturanus sp. "Caquetá", Synapturanus sp. "Amazonas", and Synapturanus sp. "Jirijirimo".

Phylogenetically, relationships among the various lineages in the *S. rabus* complex are poorly resolved (Fig. 1)—support values for relationships between species are mostly below 95. The "*Synapturanus rabus* complex" contains two nominal species, *S. rabus* and *S. danta*. Genetic distances (uncorrected pairwise distances in the 16S gene) between these species and the three putative species considered herein are in all cases higher than 3%. *Synapturanus* sp. "Caquetá" and *S.* sp. "Jirijirimo" have the lowest distances to *S. rabus* (4.2% and 5.0%, respectively) and to each other (3.5%), while *S.* sp. "Amazonas" has the lowest distance to *S. danta* (3.5%), while *S. rabus* and *S. danta* differ by 6.6%.

Morphometric differences between the three putative species considered here (*Synapturanus* sp. "Caquetá", *Synapturanus* sp. "Amazonas", and *Synapturanus* sp. "Jirijirimo"; all belonging to the *S. rabus* complex) are compared to described and undescribed species in the *Synapturanus rabus* species complex are visible in the PCA based on raw morphometric measurements (Fig. 2). The first two principal components account for 83.44% of the total variation. The highest loading for PC 1 is for body length (Appendix 4a), showing a discrimination between *S. rabus*, *Synapturanus* sp. "Caqueta", *Synapturanus* sp. "Amazonas", *Synapturanus* sp. "Jirijirimo", and the other species related to *S. rabus*. PC1 illustrates size differences of the species grouped in the "*S. rabus* species complex" (Fig. 2), in which *Synapturanus* sp. "Amazonas", *Synapturanus* sp. "Jirijirimo", and *S. rabus* are the smallest size species, followed by *Synapturanus* sp. "Caquetá"; species in this clade are smaller than all currently described species in the genus. There is a size overlap between *Synapturanus* sp. "Amazonas" and *Synapturanus* sp. "Jirijirimo" (Appendix 4c); nevertheless, males and females of *Synapturanus* sp. "Jirijirimo" are smaller than *Synapturanus* sp. "Amazonas" (Appendix 4c). In PC II, tibia length is the most important variable explaining the variation (Appendix 4a). Size corrected data show tibia length (PC1) and head width and length (PC2) as the most important variables for the PCA (Appendix 4b), with overlap among species in the morphospace (Appendix 4d).

Based on the adult morphology, morphometrics, genetic distances, and phylogenetic analyses we here recognize, describe, and name the three lineages referred as *Synapturanus* sp. "Caquetá", *Synapturanus* sp. "Amazonas", and *Synapturanus* sp. "Jirijirimo" as new species. The distribution of the most recently described species, *S. danta*, is allopatric relative to the new species described herein. In addition, *S. danta* was reported to have a "glandular unpigmented supracarpal pad" (Chavez *et al..*, 2022) whereas in other species the glad is distinct and elongated.

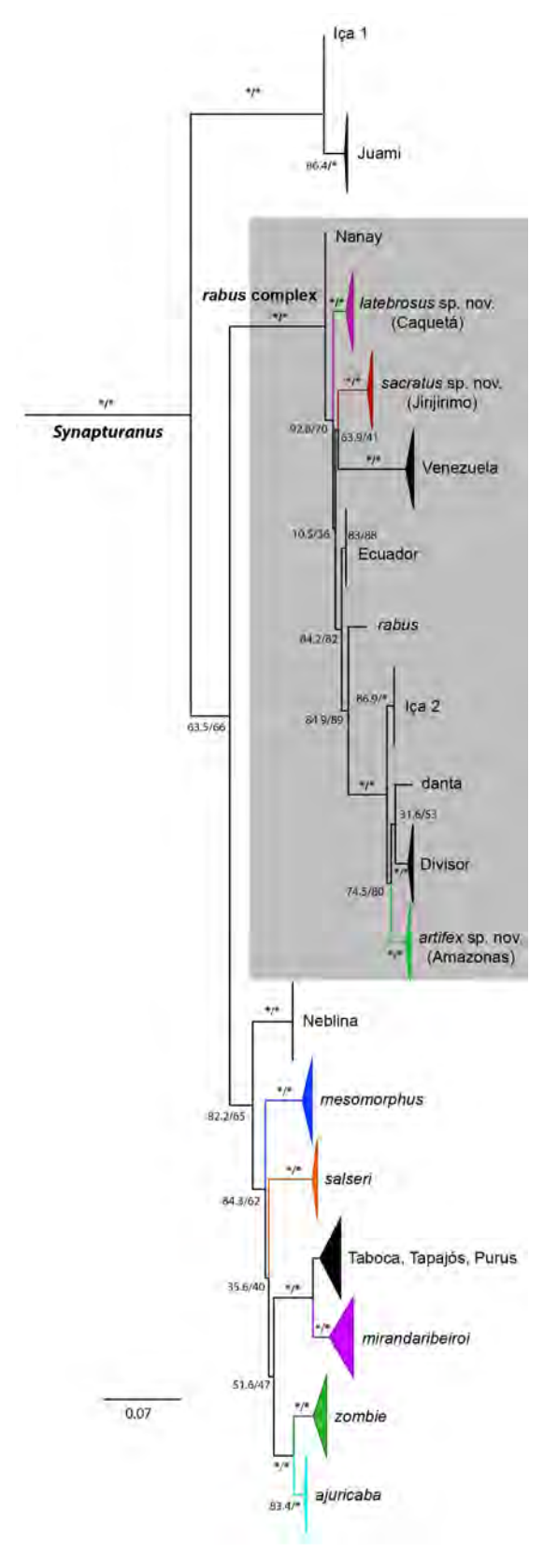


**FIGURE 1.** Maximum Likelihood phylogenetic tree of *Synapturanus* Carvalho, 1954 estimate using 16S (583 bp). The molecular phylogenetic analysis included the three new species describe here and all species currently describe and potential new species mentioned in the literature and with available Genbank sequences. Node values represent SH-aLRT support (%) / ultrafast bootstrap support (%). Asterisks indicate values equal or above 95% for both support metrics. Species in the "*Synapturanus rabus* complex" are highlighted in shade of gray.

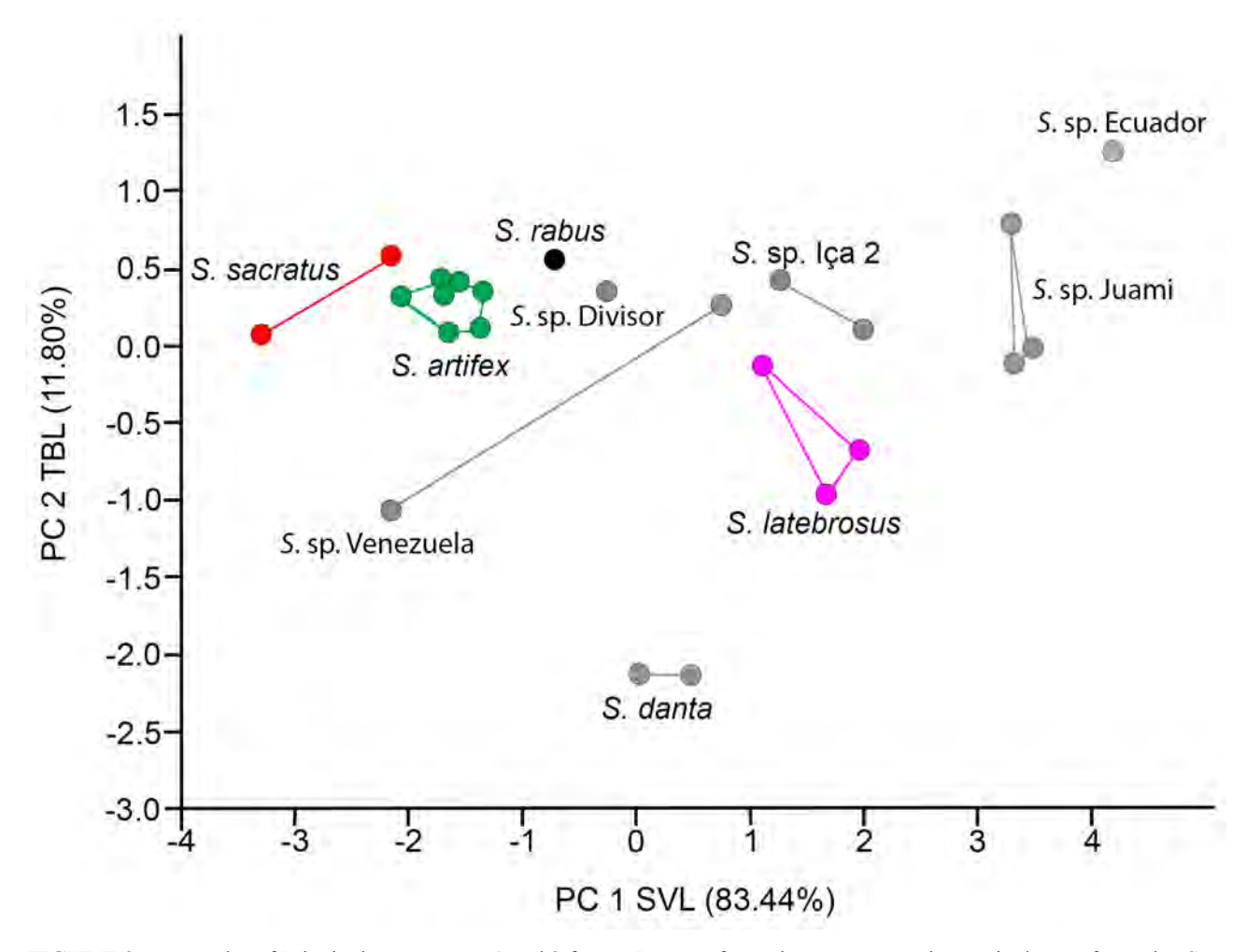


**FIGURE 2**. Scatterplot of Principal components 1 and 2 from a PCA performed on a raw morphometric dataset for males *Synapturanus rabus* species complex.

#### **Description of New Species**

Synapturanus latebrosus sp. nov.

Synapturanus sp. "Caquetá"

**Holotype** (Fig. 3). SINCHI-A 839 (MOM 2517), adult female, collected at finca El Cairo, vereda Sinaí, Municipio Morelia, Departamento Caquetá, Colombia, (01°23′31.7″ N, 75°45′06.2″ W), ca. 278 m., on August 4, 2011 by Yunner Fabian González, Diego Huseth Ruiz, Doris Laurinette Gutiérrez, and Mariela Osorno-Muñoz.

**Paratopotypes.** SINCHI-A 840-841 (MOM 2518-2519), adult females, and SINCHI-A 842 (MOM 2520), cleared and double-stained specimen, SINCHI-A 843-845 (MOM 2521-2523) adult males, all collected with the holotype.

**Paratypes.** Female SINCHI-A 2678 (JARM 139) (Fig. 3B) and male SINCHI-A 2679 (JARM 140) a cleared and double-stained specimen, collected at hacienda Villa Mery, vereda Sinaí, Municipio Morelia, Departamento Caquetá, Colombia (01°24′00.1″ N, 75°43′52.3″ W), 218 m., on December 16, 2015; female SINCHI-A 2703 (JARM 172), collected at vereda La Mono, Municipio Belén de los Andaquíes, Departamento Caquetá, Colombia, (01°18′27.8″ N, 75°48′13.9″ W), ca. 262 m., on February 18, 2016; females: SINCHI-A 5642–5643 (JARM 220-221) collected at vereda Alto Caldas, Municipio Florencia, Departamento Caquetá, Colombia (01°39′N, 75°37′W), ca. 560 m., on 01 April, 2016; female SINCHI-A 5671 (JARM 254) collected at finca Alsacia, vereda la Primavera, Municipio Florencia, Departamento Caquetá, Colombia (01°39′ 4.87″ N 75°37′4.7″ W), ca. 530 m., on

April 23, 2016, by Julián Andrés Rojas Morales, and Fabián Andrés Cabrera Vargas. Females: SINCHI-A 258–259 (MOM 1840 -1841) (Fig.3A),-collected at vereda La Recreo, Municipio Solita, Departamento Caquetá, Colombia (0°55′39.2″ N, 75°40′35″ W), ca. 220 m., collected by Hernándo Trujillo on October 09, 2009.

**Referred specimens.** Males SINCHI-A 846–847 (MOM 2524-2525), female SINCHI-A 848 (MOM 2526), all juveniles collected along with the type series, male SINCHI-A 5665 (JARM 248) collected at finca Alsacia, vereda la Primavera, Municipio Florencia, Departamento Caquetá, Colombia (01°39′ 4.87″ N 75°37′4.7″ W), ca. 530 m. on April 23, 2016, by Julián Andrés Rojas Morales, and Fabián Andrés Cabrera Vargas.



**FIGURE 3**. Synapturanus latebrosus **sp. nov.** Preserved holotype female SINCHI-A 839 (SVL=21.5 mm), (A) dorsal, (B) ventral, and (C) lateral views; specimens in life paratype female SINCHI-A 2678, (D) ventral, and (E) lateral view paratype female SINCHI-A 258.

Diagnosis. A species of Synapturanus diagnosed by the following combination of characters: 1) SVL median size: adult females 20.0–22.0 mm ( $\chi = 20.9 \pm 0.3$ , n = 8), adult males 18.1–19.0 ( $\chi = 18.7 \pm 0.3$ , n = 3 mm), 2) stout and elongated body, 3) head narrower than body, snout pointed in dorsal view, rounded in lateral view, and ventrally distinctly projecting beyond the anterior edge of the upper jaw, 4) symphysis of lower jaw with an unpigmented notch and external nares bear a wide and unpigmented rim, 5) tympanum indistinct, tympanic annulus visible below the skin, particularly its anteroventral edge, 6) vocal slits absent, 7) choanae rounded, larger in diameter than the unpigmented rim of the external nares, 8) vomerine teeth absent, 9) hand formula III>IV>II>I, digits becoming thinner towards their distal ends, rounded or slightly pointed finger tips, fingers bordered by a thin fringe, interdigital membrane absent, 10) subarticular tubercles absent; thenar tubercle elongated, palmar tubercle rounded with undefined edges, 11) adult males bear an elongated gland on the internal surface of the anterior forearm extending half of its length and broader at the wrist, 12) toe lengths IV>III>V>II>I, toes are thin and subcylindrical with a slight distal rounded or lanceolate widening, except toe I which is pointed, toes narrowly fringed, fringes more distinct distally and around the distal expansion, toes without webs, 13) inner metatarsal tubercle small and elongated, outer metatarsal tubercle absent, subarticular tubercles absent, subarticular spots unpigmented on toes, 14) skin folds on knee, heel, and wrist, 15) cephalic groove distinct, extending over the tympanum reaching and slightly extending beyond the lower jaw, 16) in life, upper surfaces of body uniformly brown, lighter brown on the area of the cephalic groove, tympanum brownish, and body flanks orange with a greyish brown ventral area, 17) light canthal stripe

present or absent; if present, dorsal to the nares and the eyes, canthal stripe continuous or broken into a series of variable size spots; confluent or not on the distal tip of snout; posteriorly, the canthal stripe could reach the area over the tympanum or above the shoulder, 18) ventral surfaces overall brown, darker on edges of mandible, snout, arms, and hidden surfaces of legs and feet; lighter on thighs, chest, and edges of abdominal region; medially the belly has a narrow and irregular shaped whitish and translucent area, hands and feet dark brown; thenar, internal metatarsal tubercles, subarticular surfaces and distal digits without coloration, 19) elongated forearm gland cream-colored in preserved specimens extending from the wrist to half the length of the forearm.

Synapturanus latebrosus **sp. nov.** differs from *S. rabus* (traits in parenthesis) by its larger size, adult females SVL 20.0-22.0 mm (vs. 17.2-19.0 mm), adult males SVL 18.1-19.0 mm (vs. 16.2-16.6 mm), a shorter tibia length TBL/SVL 38% in females and 37% in males (vs. 41% in both sexes). Eyes are smaller in *S. latebrosus* **sp. nov.** ED/SVL is 54% (vs. 73%) and the ratio of the eye diameter to the eye-nare distance is also smaller, ED/END females  $\chi = 0.5$  (vs. 0.8), ED/END males  $\chi = 0.6$  (vs. 0.9) (Tables 2 and 3). In life, *S. latebrosus* **sp. nov.** has greyish ventral flanks (vs. overall dark brown); canthal stripe, if present, extending to the shoulder area (vs. canthal stripe may extend onto the body); posterior limbs without spotting (vs. most specimens have irregular light spots on one or both legs), tympanum partially hidden (visible tympanum).

Synapturanus latebrosus **sp. nov.** males are smaller (SVL 18.1-19.0 mm) than *S. mirandariberoi* (SVL males 27.0-31.7 mm), *S. salseri*, (SVL males 23.7-26.4 mm), *S. zombie* (SVL males 37.0-40.6 mm), *S. mesomorphus* (SVL males 22.9-26.0 mm), and *S. ajuricaba* (SVL males 29.3-33.2 mm); *S. latebrosus* is larger than *S. danta* (SVL males 17.6-17.9). Adults of *Synapturanus danta* and *S. latebrosus* **sp. nov.** have a uniform dark brown dorsal coloration in life whereas the dorsum of *S. mirandariberoi*, *S. salseri*, *S. zombie*, *S. mesomorphus*, and *S. ajuricaba* have noticeable mottled patterns made up of speckles, spots, or blotches.

The forearm gland is not conspicuous in life in *Synapturanus latebrosus* **sp. nov.** and *S. rabus* (i.e., gray-brown, similar to the rest of the arm), whereas in *S. salseri* and *S. mirandariberoi* it was described as a pale wrist gland contrasting with the darker coloration of the rest of the arm (Pyburn, 1976). Furthermore, the gland of *S. salseri* is protuberant on the dorsal and inner area of the distal forearm and becoming slightly triangular with its apex towards the posterior forearm; in *S. latebrosus* the gland is slightly wider on the wrists and narrowing posteriorly, in some specimens reaching the midpoint of forearm.

**Description of the Holotype.** An adult female with two large, unpigmented ovarian eggs (3.6 and 4.0 mm diameter), body smooth, slightly ovoid in dorsal view, SVL = 21.5 mm; head triangular in shape, broader than longer (HW = 5.9 mm, HL = 5.5 mm); snout tip acuminate, snout projects beyond the anterior edge of the upper jaw (SL/SW = 0.6), nostrils with a distinct light rim, directed laterally, the distance from the eye to the nostril is 2.0 mm, being twice the diameter of the eye; canthus rostralis defined, slightly concave, loreal region marked by a distinct groove that extends from the anteroventral edge of eye to the posteroventral edge of nostril, eyes small and slightly protruding, interorbital area concave, IOD = 2.5 mm; occipital groove indistinct across the head and tympanum and visible just beyond the jaw; tympanum mostly concealed, anteroventral edge of tympanic ring barely visible, upper jaw distinctly projecting beyond lower one, with an unpigmented median notch in the anterior end of the lower jaw; the tongue is as wide as the oral cavity, its posterior edges are thin and wide; vomerine teeth absent; choanae round and widely separated. Anterior and posterior limbs short and robust, hands without interdigital membranes, finger relative lengths III>IV>II>I, fingers narrowing distally with distal tips pointed or rounded, slightly fringed, subarticular tubercles absent, subarticular area light colored, thenar tubercle elongated to oval, light colored and located at the base of finger I; distinct fold on knee and heel, less distinct folds also on wrist and metatarsal area; toes overall subcylindrical and slightly broader and rounded distally, fringes noticeable in toes I, II and distally in toes III, IV, V, interdigital membrane absent, in lateral view the distal tip of the digits are slightly flattened, subarticular areas light colored without subarticular tubercles, inner metatarsal tubercle very small, elongated, placed at base of toe I, outer metatarsal tubercle absent, toe formula IV>III>V>III>I; tibia length 8.3 mm, about 39% of snout-vent length.

Live coloration. Dorsal surfaces uniformly brown, except the cephalic groove that is lighter; ventral body flank greyish brown; lateral head anterior to the arm light brown, rim of nares and tip of snout grey; tympanum brown/slightly orange; iris dark brown, canthal stripe formed by very small and discontinuous cream spots that do not reach the shoulder, ventral surface brown, belly with a narrow, medial, and unpigmented area; dorsal surfaces of hands and feet brown, articulation and distal tips of digits unpigmented, ventrally dark brown with unpigmented subarticular areas; a black spot on the external region of the right wrist.

Coloration of Preserved Specimens. Dorsal surfaces brown, light brown around the occipital groove on top

head, anterior body flank brown, medial and posterior body flank brown-cream, ventral surfaces of throat, chest, arms and legs light brown cream, central belly light cream, ventral surfaces of hands and feet dark brown, unpigmented subarticular surfaces, and tips of digits cream-colored (Fig. 4).

**Measurements of Holotype (mm).** SLV 21.5, HL 5.5, HW 5.9, HL/ESD 1.6, SL/SW 0.6, ESD 3.5, END 2.0, ED 1.0, ED/END 0.5, IOD 2.5, TBL 8.3, TBL/SVL 0.4

Variation in the type series. Measurement data of the type series are given in Table 2 and Table S2. Overall, the type series agrees with the holotype coloration. Two adult females (SINCHI-A 840 and SINCHI-A 5643) lack canthal stripes, three adult males (SINCHI-A 843-845) and five females (SINCHI-A 841, SINCHI-A 2678, SINCHI-A 2703, SINCHI-A 5642 and SINCHI-A 5671) have a canthal stripe being less distinct in the holotype. The medial unpigmented area of belly is variable, in two females (SINCHI-A 840 and SINCHI-A 841) it extends toward the ventral flanks, in males the unpigmented medial area bears a few small brownish dots.

**Etymology**. Latin adjective, meaning ignored, alluding to the ecological and behavioral habits that make the species imperceptible and probably even allow it to live in forest fragments, as small as those found in the type locality.

**Distribution (Fig. 4).** The northernmost locality currently known for *Synapturanus latebrosus* **sp. nov.** is the Municipio Florencia, Departamento Caquetá; likely the species has a continuous distribution from the Municipio Morelia and Belén de los Andaquíes to Municipio Solita, north of the Caquetá River.

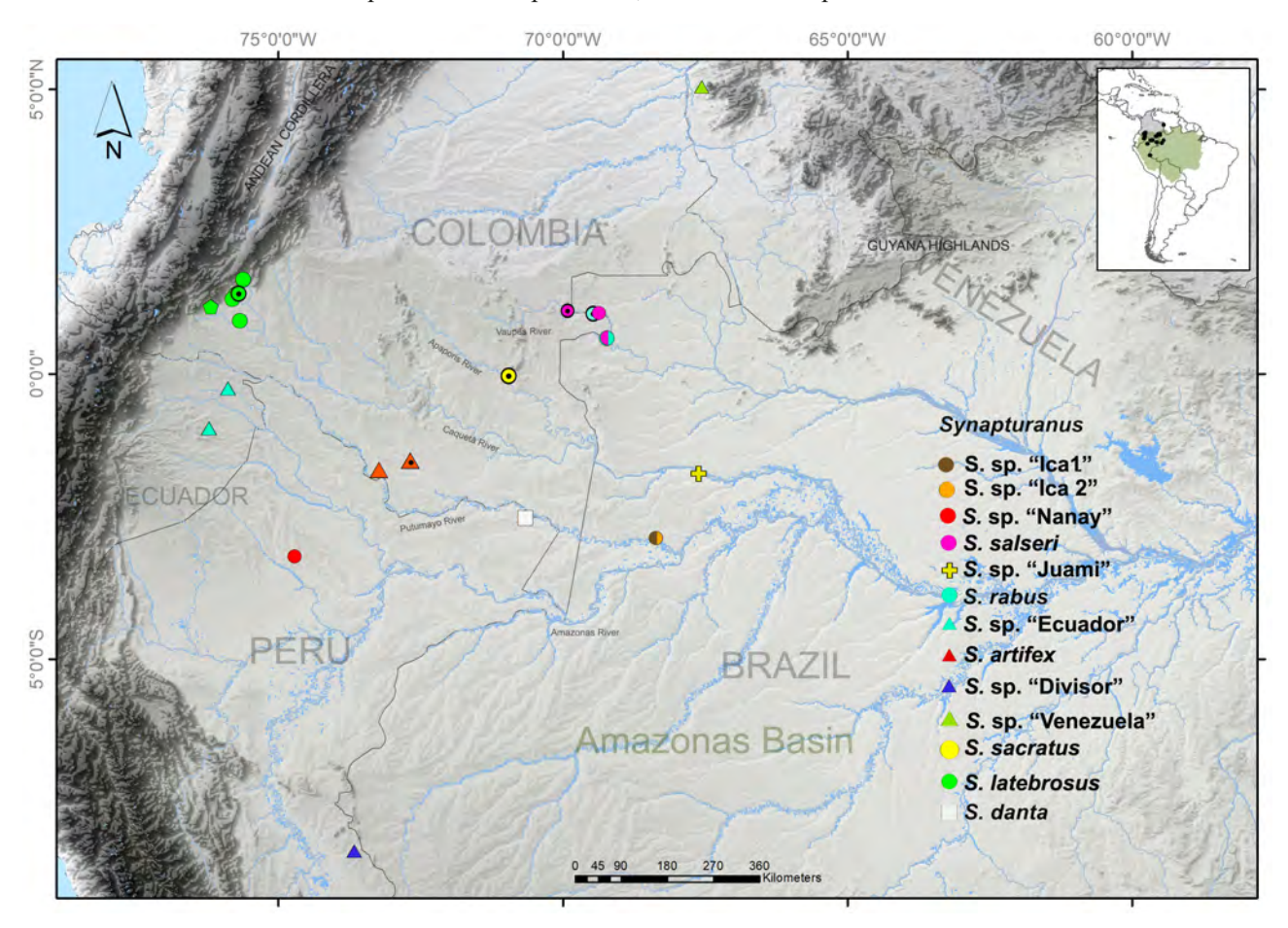


**FIGURE 4.** Current known distribution of new species of *Synapturanus*; symbols with black edges and a black dot identify type localities; the pentagon corresponds to *S.* sp. "Colombia" (Fouquet *et al.*. 2021a) which was homogenized as *S. latebrosus* in this study.

#### **Tadpole and Advertisement Call.** Unknown

**Natural History**. The holotype and paratopotypes of *Synapturanus latebrosus* **sp. nov.** were collected in a fragment of primary forest (< 10 hectares), surrounded by meadows for livestock and located on the top of a low hill. A few specimens were found in the afternoon moving over the leaf litter. At night, in the same place, we selected an area of about 1x2 mts, removed the fallen leaves and cut the network of fine roots into a rectangle; we carefully

rolled the rectangle and lifted it exposing the clay substrate where we found and collected additional specimens. At the time of collection, all the specimens were placed together; consequently, we do not know if the specimens moving around in the afternoon were males or females. Of the series of paratypes and referred material, two males, SINCHI-A 5665 and SINCHI-A 2679, were found under leaf litter and among a decomposing trunk, the females were found both under and above the leaf litter.

## Synapturanus sacratus sp. nov.

Synapturanus sp. "Jirijirimo" Synapturanus rabus Fouquet et al.., 2021a

**Holotype** (Fig. 5). ICN 56890 (JDL28952), adult female, collected at the Departamento Amazonas, "area no municipalizada" La Victoria, Comunidad Jirijirimo, (00°02′30″S, 70°57′W, 136 m), within Parque Nacional Natural Yaigojé Apaporis, Colombia, collected on march 21, 2009 by John D. Lynch and Jorge Kayuanari.

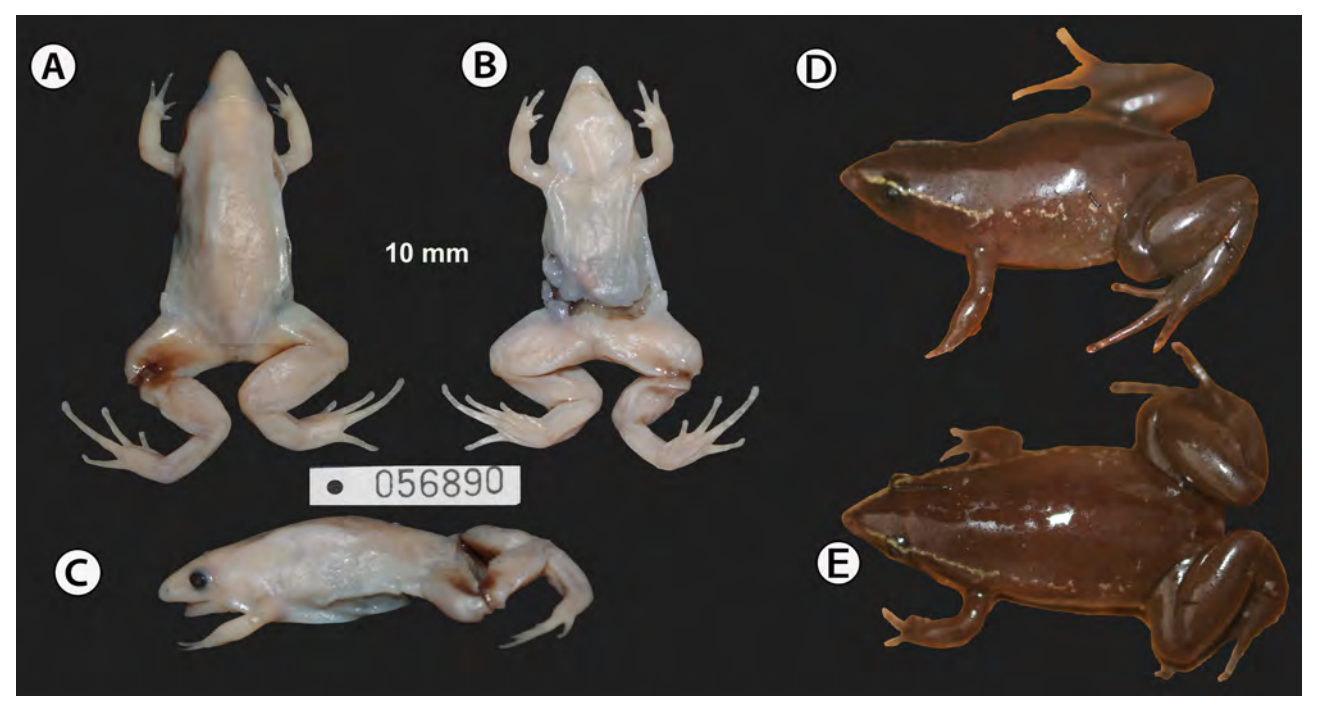


**FIGURE 5**. Synapturanus sacratus **sp. nov.** Preserved holotype female ICN 56890 (SVL=16.6 mm), (A) dorsal, (B) ventral, and (C) lateral views. Specimen in life, paratopotype female ICN 56893, (D) lateral, and (E) dorsal views.

**Paratopotypes**. Females: ICN 56893 (JDL 28935), cleared and double-stained specimen, ICN 56889 (JDL 28951) (Fig. 3); males ICN 56892 (JDL 28934) and ICN 56895 (JDL 28973), all adult specimens were collected with the holotype.

**Referred specimen**. ICN 56891(JDL 28953) and ICN 56894 (JDL 28933) juveniles collected along with the type series.

**Diagnosis:** A species of *Synapturanus* diagnosed by the following combination of characters: 1) SVL small size, adult females 16.6, 17.3 mm ( $\chi$  = 17.0, n = 2); adult males SVL 14.0, 15.0 mm ( $\chi$  = 14.5, n = 2), 2) stout and ovoid body, 3) head narrower than body, snout pointed in dorsal view, rounded in lateral view, and ventrally distinctly projecting beyond the anterior edge of the upper jaw, 4) symphysis of lower jaw with an unpigmented notch and external nares with a wide and unpigmented rim, 5) tympanum slightly visible, 6) vocal slits absent, 7) rounded choanae, equal in diameter to the unpigmented rim of the external narin, 8) vomerine teeth absent, 9) hand formula III>IV>II>I, hand digits becoming thinner towards their distal ends, rounded or slightly pointed finger-tips, fingers bordered by a thin fringe, interdigital membrane absent, 10) subarticular tubercles absent, thenar tubercle small and elongated, palmar tubercle indistinct, 11) adult males bear a gland on the distal internal surface of the anterior forearm closer to the wrist and visible dorsally, 12) relative length of toes IV>III>V>II>I, toes are thin and subcy-

lindrical, distal tip rounded, except on toe I that is distinctly pointed, fringes not evident, toe webbing absent, 13) inner metatarsal tubercle small and elongated, outer metatarsal tubercle absent, subarticular tubercles absent, 14) knee, heel, and wrist with skin folds, 15) cephalic groove distinct, across the head, over the tympanum and reaching the throat barely beyond the jaw articulation, 16) in life dorsal surfaces and flanks uniformly brown or pale brown, occipital groove light brown, 17) canthal stripe distinct and dull cream, extending continuously from the rostral tip, over the nare and eye; stripe distinct over the shoulder and then broken along the flank, 18) ventral surfaces brown to grayish, hands and feet dark brown, articular surfaces and distal tips of digits unpigmented, 19) forearm gland lighter than the background in preserved specimens, scattered along the inner forearm up to the middle.

Synapturanus sacratus sp. nov. can be distinguished from S. rabus (traits in parenthesis) by its smaller size, adult females SVL 16.9 and 17.3 mm (vs. 17.2-19.0 mm) and adult males SVL 14.0 and 15.0 mm (vs. 16.2-16.6 mm). The HL/END ratio in S. sacratus sp. nov. is 2.8 in average for both sexes, it is smaller than HL/END ratio in in S. rabus (3.4 in average for both sexes). Synapturanus sacratus sp. nov. (as recorded in J.D. Lynch's field notes) have a conspicuous and continuous canthal stripe that becomes discontinuous over the body flanks (vs. a white or pale cream line along the canthus rostralis may extend onto the body). Synapturanus sacratus sp. nov. also lacks spotting on posterior legs (vs. most specimens have irregular spots on one or both legs), and dorsal surfaces are light brown to brown (vs. dark brown).

Synapturanus sacratus sp. nov. is smaller than S. latebrosus sp. nov. (traits in parenthesis), adult females SVL 16.9 and 17.3 mm (vs. 20.0-22.0 mm) and adult males SVL 14.0 and 15.0 (vs. 18.1-19.0 mm). Synapturanus sacratus sp. nov. has a longer tibia, 42% of SVL (vs. 37%), and eyes larger judging by the ED/END ratio, 0.75 (vs. 0.55 in average for both sexes). Synapturanus sacratus sp. nov. has a conspicuous and continuous cream canthal stripe that becomes discontinuous over the body flanks (vs. canthal stripe formed by very small cream spots that does not extend beyond the arm).

Synapturanus sacratus **sp. nov.** with SVL 14.0-15.0 mm in males, is considerably smaller than *S. mirandariberoi* (SVL 27.0-31.7 mm in males), *S. salseri*, (SVL 23.7-26.4 mm in males), *S. zombie* (SVL 37.0-40.6 mm in males), *S. mesomorphus* (SVL 22.9-26.0 mm in males), and *S. ajuricaba* (SVL 29.3-33.2 mm in males) and smaller than *S. danta* (SVL 17.6-17.9 mm in males). *Synapturanus sacratus* **sp. nov.** lacks any pattern of speckles, spots or blotches on the back present to a greater or lesser extent in those species. In *S. sacratus* **sp. nov.**, the forearm gland is scattered and reaches up to the middle vs. protruding and concentrated towards the wrist in *S. salseri*.

**Description of Holotype.** An adult female with unpigmented eggs in the oviduct (the largest ca. 1.5 mm), body smooth, triangular in dorsal view and small (SVL = 16.6 mm); head triangular, but almost as wide as long (HW = 4.3 mm, HL = 4.5 mm), snout tip acuminate, snout projects beyond the anterior edge of upper jaw (SL/SW= 0.6); nostrils with a distinct and light colored rim, directed laterally; the eye-nostril distance slightly greater than the eye diameter (END = 1.6 mm, ED = 1.1 mm), canthus rostralis poorly defined dorsally, loreal region concave marked bellow by a distinct groove that reaches from the antero-ventral edge of eye to the posteroventral edge of nostril, inter-orbital area concave, IOD = 1.9 mm; lacking occipital fold, a distinct shallow groove is visible behind the eyes running over the tympanic area and barely exceeds the lower jaw; tympanum small, poorly distinguishable in life but distinct in the preserved specimen, tympanum diameter = 0.7 mm; tongue thin on free edges and as wide as the oral cavity; vomerine teeth absent; oval choanae widely separated and slightly medially slanted anteriorly. Anterior and posterior limbs short and robust, hands without interdigital membranes, finger relative length III>IV>II>I, distally pointed and with thin fringes, subarticular tubercles absent, subarticular area light colored, thenar tubercle elongated to oval, located at the base of finger I, palmar tubercles not distinct; distinct folds on knee and heel, less distinct on wrist and metatarsal area; toes cylindrical, thin, narrowly fringed, and expanded distally, distal tip rounded, toe I distally pointed; subarticular tubercles absent, inner metatarsal tubercles elongated, small, at the base of finger I; toe relative lengths IV>III>V>II>I; tibia length TBL = 6.9 mm, about 41% of snout-vent length.

Live coloration (Fig. 5). Dorsal surfaces brown, dull cream canthal stripe continuing, but interrupted, along flank, dark brown iris, cephalic groove light brown, fingers and toes dark brown with light colored articular surfaces, venter brown to grayish.

**Coloration of Preserved Specimens**. Specimens have lost their coloration; overall all specimens are white to light cream. However, we note that in specimen ICN 56890 (Fig. 5 A, B, and C) there is a light brown coloration at the site where the label was removed and which was not discolored by light.

**Measurements of Holotype (mm).** SLV 16.6; HL 4.5; HW 4.3; HL/ESD 1.8; SL/SW 0.6, TD 0.7, ESD 2.6, END 1.6, ED 1.1, ED/END 0.7, TBL 6.9, IOD 1.9, TBL/SVL 0.4.

Variation in the type series. Measurement data of the type series are given in (Table 1, Appendix 2). According to the field notes (JDL), the dorsal coloration varies in shade of brown, from almost black to pale brown. Ventral coloration is not detailed, in three specimens, one of them the holotype, is described as brown to grayish, in other two specimens as mostly gray, which probably means that the depigmented area is extensive. In two adult males (ICN 56892, 56895) glandular tissues are noticeable as white dots, although specimens are decolored.

**Etymology.** Latin, a noun in apposition, meaning sacred, alludes to the sacred sense that animals have for indigenous Amazonian peoples, particularly in the Yaigoje territory, currently designated as the Yaigojé-Apaporis National Natural Park.

**Distribution (Fig. 4).** *Synapturanus sacratus* **sp. nov.** is known only from the type locality **Tadpole and Advertisement Call.** Unknown

**Natural History**. The specimens were detected by their movements and collected among leaf litter in the afternoon, in a *terra firme* forest, that means a forest that does not flood.

## Synapturanus artifex sp. nov.

Synapturanus sp. "Amazonas"

**Holotype** (Fig. 6). SINCHI-A 6632 (SNC-H 405), adult male, collected at Departamento Amazonas, "area no municipalizada" La Chorrera, cabildo indígena Okaina, Comunidad de Puerto Oriente, Colombia (01°31′43.7″ S, 72°40′38.5″ W), 134 m., on October 18, 2019, by Marco Fidel Rochicón and Vitilio Iyokina.

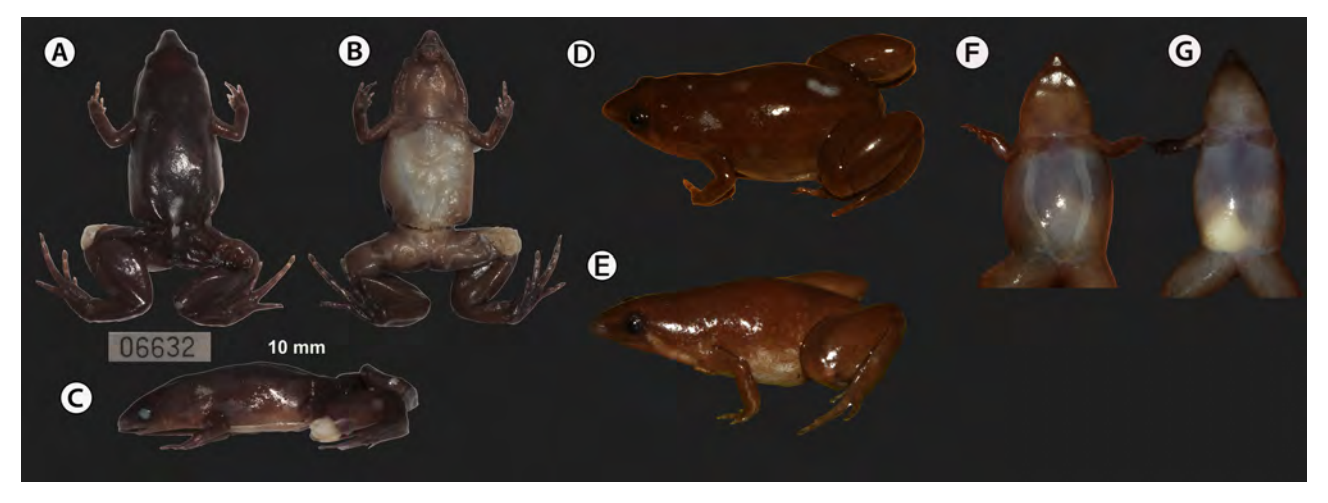


**FIGURE 6.** Synapturanus artifex **sp. nov.** Preserved holotype male SINCHI-A 6632 (SVL=15.5mm), (A) dorsal, (B) ventral, (C) lateral views; holotype in life, (D) dorsolateral, and (F) ventral views; alive paratopotype female SINCHI-A 6469, (E) lateral, and (G) ventral views.

**Paratopotypes.** Adult female SINCHI-A 6469 (MOM 7430), adult males SINCHI-A 6631 (SNC-H 404), SINCHI-A 6633 (SNC-H 406), and SINCHI-A 6518 (MOM 7479); all collected along with the holotype by Zabdiel Anderson Ciake, Alfredo Iyokina, Sofonias Iyokina, Diomedes Vigidima, and Epifanio Ciake.

**Diagnosis**: A species of *Synapturanus* diagnosed by the following combination of characters: 1) SVL small size, adult female SVL = 17.6 mm (n = 1); adult males 15.2-15.9 mm ( $\chi = 15.5 \pm 0.1$  mm, n = 4), 2) stout and body elongated, 3) head narrower than body, snout pointed in dorsal view, rounded in lateral view, and ventrally distinctly projecting beyond the edge of the anterior upper jaw, 4) symphysis of lower jaw with an unpigmented notch and external nares with a wide and unpigmented rim, 5) tympanum slightly visible, 6) vocal slits absent, 7) rounded choanae, about equal in diameter to the unpigmented edge of the external narin, 8) vomerine teeth absent, 9) hand formula III>IV>II>I, digits becoming thinner towards their distal ends, fingertips rounded or slightly pointed, fingers bordered by a thin fringe, interdigital membrane absent, 10) subarticular tubercles absent, thenar tubercle elongated, palmar tubercle rounded with undefined edges, 11) adult males with a protuberant and oval-shaped glandular area on the internal surface of distal forearm, extending from the wrist to the middle of the distal forearm and dorsally visible, 12) relative lengths of toes IV>III>V>II>I, toes are thin and subcylindrical with a distal rounded or

lanceolate widening, with thin fringes extending from the base of the digits to their distal end, digits lack webbing, 13) inner metatarsal tubercle small and elongated, outer metatarsal tubercle absent, subarticular tubercles absent, unpigmented subarticular spots on toes, 14) knee, heel, and wrist with skin folds, 15) cephalic groove distinct, extending over the head and tympanum and reaching and extending beyond the lower jaw articulation and reaching or distinctly crossing over entire throat, 16) in life dorsal body surfaces dark brown, with or without pale dorsal spots, occipital groove area light brown, edge of tympanum with small orange spots, ventral area of flanks greyish, oblique light brown to orange stripe begins posterior to the eye and extends over the tympanum and broadening towards the arm, ventrally, 17) canthal stripe present or absent, if present poorly defined; canthal stripe formed by a series of small, and discontinuous cream spots, extending from the rostral tip and dorsal to the flank, 18) in life ventral surfaces dark brown on snout and on edges of throat and its anterior surface, lighter on the posterior half of the throat; chest with two triangular-shaped spots that do not meet medially, most of the belly surface translucent, *lineae masculinae* (Davis and Law, 1935) present, ventral surfaces of thigh light brown, the remaining of ventral leg surfaces dark brown, hands and feet dark brown, thenar and inner metatarsal tubercles, subarticular surfaces, and tip of digits unpigmented, 19) forearm gland cream-colored in preserved specimens.

Synapturanus artifex sp. nov. can be differentiated from *S. rabus* (traits in parenthesis) in being somewhat smaller, SVL 17.6 mm in one female (vs. 17.2-19.0 mm) and SVL 15.2–15.9 mm in males (vs. 16.2-16.6 mm); two males have few and poorly defined pale spots on the back (absent in *S. rabus*), *S. artifex* sp. nov. lacks irregular markings on the posterior limbs (most specimens have irregular spots on one or both legs in *S. rabus*), gray flank, a light brown stripe runs obliquely posteroventral to the eye and broadening towards the arm (uniformly dark brown), entire belly, central area of chest, and proximal throat translucent gray, lacking brown pigmentation (only the central part of belly is translucent gray).

Synapturanus artifex males are smaller than S. danta (SVL 15.2-15.9 vs. 17.6-17.9). Synapturanus artifex sp. nov. is smaller than S. latebrosus sp. nov. (traits in parenthesis) SVL 17.6 mm in one female (vs. 20.0-22.0 mm) and SVL 15.2-15.9 mm in males (vs. 18.1-19.0 mm). Synapturanus artifex sp. nov. has a longer tibia, 42% of SVL (vs. 37%), and also larger eyes than S. latebrosus sp. nov. judging by the ED/END ratio, 0.7 in average for both sexes (vs. 0.6). Synapturanus artifex sp. nov. has a broad, unpigmented midventral area that extends over the chest and throat, whereas in S. latebrosus sp. nov. it is narrow and circumscribed to the belly. In S. artifex sp. nov. the cephalic groove crosses over the entire throat whereas in S. latebrosus sp. nov. it slightly extends beyond the lower jaw.

Synapturanus artifex sp. nov. differs from S. sacratus sp. nov. (traits in parenthesis) in being slightly larger, SVL 17.6 mm in one female (vs. 16.9, 17.3 mm in two females) and SVL 15.2 -15.9 mm in males (vs. 14.0, 15.0 mm in two males). Synapturanus artifex sp. nov. exhibits a poorly defined faint canthal line when present (vs. a conspicuous and continuous canthal stripe that becomes discontinuous over the body flanks); in life, S. artifex sp. nov. has a thick, light brown to orange stripe running obliquely over the tympanum toward the ventral arm (vs. not evident in S. sacratus sp. nov.); cephalic groove distinctly crosses over the entire throat (vs. cephalic groove slightly extends beyond the lower jaw).

Synapturanus artifex sp. nov. with SVL 15.2-15.9 mm in males is clearly smaller than S. mirandariberoi (SVL 27.0–31.7 mm in males), S. salseri, (SVL 23.7-26.4 mm in males), S. zombie (SVL 37.0-40.6 mm in males), S. mesomorphus (SVL 22.9-26.0 mm in males), and S. ajuricaba (SVL 29.3-33.2 mmv in males). Synapturanus artifex sp. nov. lacks any pattern of speckles, spots or blotches on the back present to a greater or lesser extent in the above-mentioned species, although the holotype and another male of S. artifex sp. nov. shows few whitish spots of diffuse contours. In S. artifex sp. nov., the forearm gland is scattered and reaches up to the middle vs. protruding and concentrated towards the wrist in S. salseri.

**Description of Holotype.** An adult male with a protruding and elongated glandular surface, broader near the wrist, on the inner distal forearm; the glandular area extends over the middle of the forearm and is dorsally visible; body smooth, ovoid in dorsal view, small (SVL = 15.5 mm); head triangular, almost as wide as long (HL = 4.2, HW = 4.1), snout tip acuminate, snout projects beyond the anterior edge of the upper jaw (SL/SW= 0.7); nostrils with a distinct light colored rim, directed laterally; the eye–nostril distance is slightly greater than the eye diameter (END = 1.5 mm, ED = 1.2 mm), *canthus rostralis* defined, loreal region concave below marked by a distinct groove that reaches from the antero–ventral edge of eye to the posteroventral edge of nostril, interorbital area concave, IOD = 2.2 mm, without occipital fold, a distinct shallow cephalic groove extending over the tympanum and barely exceeding the level of the lower jaw; tympanum visible, TD = 0.9 mm; vocal slits absent, tongue less wide than the oral cavity, tongue thin on posterior free edges; vomerine teeth absent; rounded choanae widely separated. Anterior and

posterior limbs robust and short, hands without webbing, finger relative lengths III>IV>II>I, hand digits distally pointed, with narrow fringes on digits, subarticular tubercles absent, subarticular surfaces light colored, small and oval thenar tubercle located at the base of finger I, palmar tubercle rounded with poorly defined edges; distinct folds on knee and heel, less distinct on wrist and metatarsal area; toes lack webbing, toes subcylindrical and slightly expanded distally, distal tips lanceolate and flat in lateral view, except toe I that is distally pointed, toes with narrow fringes along their length, external edge of toe I reaches the ventral edge of the internal metatarsal tubercle; subarticular tubercles absent, inner metatarsal tubercle elongated, small, at the base of toe I; toes relative lengths IV>III>V>II>I; tibia length TBL = 6.7 mm, about 43% of snout–vent length.

Live coloration. Dorsal body surfaces dark brown with few and poorly defined whitish spots, ventral flank gray, light brown band extends from behind the eye and broadening towards the arm, iris dark brown, dorsal articular surfaces and distal tips of fingers and toes unpigmented. Ventrolateral surfaces of throat dark brown distally as well as the snout, surfaces of hands and feet, forelimbs, tibia, and feet, light brown on medial and proximal areas of throat, as well as two separate patches on chest; edges of belly and thighs translucent gray, translucent, whitish central belly without brown pigmentation as in medial area of chest and over the fold between the throat and chest, *lineae masculinea* visible. Subarticular surfaces of fingers and toes unpigmented.

Coloration of Preserved Specimens. Dorsally dark brown, with diffuse white to cream dots, ventral flanks and post-ocular band broadening towards the arm cream, the translucent ventral areas in life turn into light cream. Articular surfaces on fingers and toes cream.

**Measurements of Holotype (mm).** SLV 15.5; HL 4.2; HW 4.1; HL/ESD 1.8; SL/SW 0.7, TD 0.9, ESD 2.3, END 1.5, ED 1.2, ED/END 0.8, TBL 6.7, IOD 2.2, TBL/SVL 0.4.

Variation in the type series. Measurement data for the type series are given in Table 2 and Table S2. The canthal stripe is present in the female and two males; in the female SINCHI-A 6469 it is barely visible, discontinuous, and reaches the flank; in male SINCHI-A 6631 is distinct, discontinuous, and extends only to the area above the insertion of the forearm; in male SINCHI-A 6518 consists of dots over the posterior part of the *canthus rostralis* and over the eyelid, in male SINCHI-A 6633, as well as on the holotype, the canthal stripe is absent. The posterior surface of the throat can be translucent; the translucent belly can bear areas of small brown dots. Female SINCHI-A 6469 has two visible eggs (3.5 and 1.6 mm) at their longest side.

**Etymology**. A Latin noun in aposition meaning artist, in allusion to the skills and extraordinary designs that Okaina, Uitoto, Bora, and Muinane indigenous peoples capture in their basketry in which they depict their life in nature.

**Distribution** (Fig. 4). Synapturanus artifex sp. nov. is known only from the type locality.

**Tadpole (Fig. 7).** During a sampling at Comunidad San Rafael del Caraparaná, "área no municipalizada El Encanto", on April, 2022, one clutch, with two larvae was found in the soil, when removing the rootlets layer. The two larvae at stage 35 (Gosner 1960) have a total length of 11.9 and 10.4 mm, a body width of 4.2 mm and a tail length of 6.4 and 5.7 mm respectively. Each larva is embedded in a viscous and translucent jelly about 9.5 mm in diameter and the complete posture contained in its hole in the ground measures about 19 mm. The larvae were pinkish in life, cream in preservative, with fine brown marbling on the head and along the dorsal midline extending up to the tail proximally. No opercular folds are visible. The tail is oval in cross section, without fins, and it is 54% of the total length.

Advertisement Call (Fig. 8). Calls of *Synapturanus artifex* sp. nov. were recorded from two individuals. The first individual recorded on October 19, 2019 at 20:00 hrs., air temperature of 26.9°C, and 91% relative humidity was not possible to collect with SINCHI-A 6631(https://doi.org/10.6084/m9.figshare.16943425). It was recorded from Puerto Oriente, at 134 m., "área no municipalizada" La Chorrera (1°31'43.7"S, 72°40'38.5"W), Departamento Amazonas, Colombia. The second individual corresponds to voucher SINCHI-A 7110 (Fig. 8), (https://doi.org/10.6084/m9.figshare.16943425) recorded on August 30, 2021 at 21:30 hrs., air temperature of 25.6°C, and 81% relative humidity recorded from Puerto Oriente, at 134 m., "área no municipalizada" La Chorrera (2°31'43.7"S, 72°39'53.6"W), Departamento Amazonas, Colombia (Table 3).

The call of *Synapturanus artifex* **sp. nov.** (n = 3) consists of single (one pulsed note, Guild C sensu Emmrich *et al.*. 2020) tonal notes (mean note length 0.040, range 0.029-0.052 seconds, SD=0.007) and interval between notes between 5.35 and 17.54 seconds ( $\chi$  = 7.52), dominant frequency between 1639 and 2224 Hz ( $\chi$  = 1904 Hz, SD=216.9). The calls have a descendent modulation frequency.

|               |                               |            |              |               |              | 111 /1111/   | i di         | 1/10/41        |              | U /EeD       | 100           |                  |
|---------------|-------------------------------|------------|--------------|---------------|--------------|--------------|--------------|----------------|--------------|--------------|---------------|------------------|
| Species       | Sex                           | u          | TBL/SVL      | HL/SVL        | HW/SVL       | HL/HW        | ED/END       | ED/SVL         | HL/END       | HL/ESU       | ED/TBL        | (ED/TBL)/SVL     |
| S. latebrosus | 0+                            | ∞          | 0.38 0.007   | 0.26 0.006    | 0.26 0.005   | 0.99 0.03    | 0.53 0.02    | 0.05 0.002     | 2.4 0.06     | 1.63 0.05    | 0.0130.005    | 0.0070.0003      |
| sp.nov.       |                               |            | (0.35-0.42)  | (0.23-0.29)   | (0.24-0.27)  | 0.92 - 1.16  | (0.46-0.59)  | (0.05-0.06)    | (2.4-2.9)    | (1.45-1.84)  | (0.12-0.15)   | (0.005-0.008)    |
|               | 50                            | 3          | 0.37 0.02    | 0.26 0.01     | 0.26 0.015   | 0.94 0.03    | 0.57 0.05    | 900.0 90.0     | 4.38 0.53    | 1.68 0.06    | 0.160.014     | 0.0090.0008      |
|               |                               |            | (0.33-0.40)  | (0.25-0.27)   | (0.26-0.28)  | (0.88-0.97)  | (0.49-0.64)  | (0.05-0.069)   | (3.64-5.42)  | (1.59-1.81)  | (0.13-0.18)   | (0.007-0.009)    |
|               | ED/SVL                        | N          | 1            |               | 1            | 1            | 1            | 0.05 0.014     | 1            | 1            | 1             | 1                |
|               | $\mathbb{Q}$ and $\mathbb{Q}$ | वें<br>वें |              |               |              |              |              | (0.046-0.07)   |              |              |               |                  |
|               | $\chi\!\!\pm 2SD$             | Q          |              |               |              |              |              |                |              |              |               |                  |
| S. sacratus   | 0+                            | 7          | 0.41         | 0.27          | 0.25         | 1.07         | 0.75         | 990.0          | 3.02         | 1.76         | 0.159         | 600.0            |
| sp nov        |                               |            | (0.40, 0.41) | (0.26, 0.27)  | (0.24, 0.26) | (1.03, 1.10) | (0.69, 0.82) | (0.066, 0.066) | (2.78, 3.25) | (1.75, 1.78) | (0.16, 0.165) | (0.0096, 0.0097) |
|               | 50                            | 7          | 0.44         | 0.28          | 0.28         | 66.0         | 0.75         | 0.079          | 2.64         | 1.79         | 0.18          | 0.012            |
|               |                               |            | 0.43, 0.45   | 0.28, 0.28    | 0.26, 0.3    | 0.93, 1.05   | 0.70, 0.81   | 0.075, 0.083   | 2.60, 2.68   | 1.77, 1.81   | 0.17, 0.19    | 0.0125, 0.0125   |
|               | ED/S                          | ED/SVL     | !            | 1             | !            | 1            | 1            | 0.07 0.016     | 1            | 1            | 1             | 1                |
|               | and ${\mathscr C}$            | €          |              |               |              |              |              | (0.07-0.08)    |              |              |               |                  |
|               | $\chi$ ± 2SD                  | Q          |              |               |              |              |              |                |              |              |               |                  |
| S. artifex    | 0+                            | 3          | 0.410.003    | 0.270.01      | 0.280.01     | 0.910.03     | 0.810.05     | 0.070.005      | 2.950.12     | 1.870.06     | 0.180.01      | 0.010.0007       |
| sp.nov        |                               |            | (0.41-0.413) | (0.24-0.29)   | (0.26-0.29)  | (0.85-1.13)  | (0.72-0.87)  | (0.065-0.081)  | (2.8–3.2)    | (1.8-20.)    | (0.16-02)     |                  |
|               | 50                            | 6          | 0.420.003    | 0.270.003     | 0.290.08     | 0.92 0.03    | 0.76 0.03    | 0.07 0.002     | 2.9 0.06     | 1.76 0.03    | 0.160.005     | 0.0100.0003      |
|               |                               |            | (0.41-0.43)  | (0.26 - 0.28) | (0.26-0.33)  | (0.82-1.02)  | (0.56-0.93)  | (0.058-0.082)  | (2.56-3.11)  | (1.61-1.87)  | (0.13-0.19)   | (0.009-0.012)    |
|               | ED/S                          | ED/SVL♀    | 1            | 1             | ;            | ;            | :            | 0.067 0.014    | :            | :            | ;             | ;                |
|               | and $\vec{\lhd}$              | €>         |              |               |              |              |              | (0.058-0.074)  |              |              |               |                  |
|               | $\chi\!\!\pm 2\mathrm{SD}$    | Ü          |              |               |              |              |              |                |              |              |               |                  |
| S. rabus**    | 50                            | 1          | 0.41         | 0.29          | 0.2          | 1.04         | 98.0         | 0.073          | 3.43         | ŀ            | 0.15          | 0.008            |
| S. rabus *    | 0+                            | 3          | 0.410.007    | 0.280.01      | 0.260.006    | 1.06 0.02    | 0.80 0.04    | 0.066 0.001    | 3.36 0.06    | I            | 0.1600.006    | 0.0090.00009     |
|               |                               |            | (0.39-0.42)  | (0.27-0.30)   | (0.25-0.27)  | (1.02-1.09)  | (0.73-0.86)  | (0.064-0.068)  | (3.25-3.40)  |              | (0.15-0.17)   | (0.009-0.0092)   |
|               | 50                            | 9          | 1            | ı             | 1            | ŀ            | 1            | 0.073 0.011    | 3.43         | ŀ            | 1             | 1                |
| S. salseri*   | 50                            | _          | 0.40         | 0.25          | 0.26         | 66.0         | 99.0         | 0.05           | 3.33         | ŀ            | 0.13          | 0.005            |
| S. salseri**  | 50                            | 13         | 0.4140.004   | 0.260.004     | 0.260.005    | 0.990.02     | 0.60.02      | 0.050.002      | 2.910.05     | 1.650.01     | 0.1240.005    | 0.0050.0002      |
|               |                               |            | (0.38-0.44)  | (0.39-0.43)   | (0.23-0.29)  | (0.86-1.1)   | (0.47-0.7)   | (0.04-0.06)    | (2.6-3.25)   | (1.5-1.7)    | (0.10-0.15)   | (0.004-0.006)    |
| S. danta*     | 50                            | 7          | 0.280.004    | 0.240.003     | 0.310.003    | 0.760.02     | 0.70.03      | 0.060.01       | 2.870.07     | I            | 0.210.01      | 0.010.001        |
|               |                               |            | (0.28, 0.28) | (0.24, 0.24)  | (0.31, 0.32) | (0.75, 0.78) | (0.66, 0.73) | (0.05, 0.06)   | (2.8, 2.93)  |              | (0.2, 0,22)   | (0.01, 0.01)     |

|                                     |             |                     | 1                   | -          | (11)          |                       | 9                    |
|-------------------------------------|-------------|---------------------|---------------------|------------|---------------|-----------------------|----------------------|
| Species                             | Sample size | NL (seconds)        | Dor (Hz)            | Pulses     | Det (Hz)      | Internote             | Keterences           |
| S. artifex sp. nov<br>SINCHI-A 7110 | n=1         | 0.047 (0.036–0.052) | 1.889 (1.657–2.120) | 1 (1–1)    | 28.5 (27–30)  | 7.576 (7.035–8.208)   | This study           |
| S. artifex (Unvouchured)            | n=1         | 0.036 (0.029–0.048) | 1.904 (1.639–2.224) | 1 (1–1)    | 28.3 (26–32)  | 7.561 (5. 353–17.543) | This study           |
| S. artifex<br>SINCHI-A 8134         | n=1         | 0.046 (0.039–0.053) | 1.874 (1.661-2.116) | 1 (1–1)    | 27.2 (27-28)  | 3.873 (3.631–4.113)   | This study           |
| S. danta                            | n=2         | 0.059 (0.054–0.063) | 1.763 (1.734–1.809) | 1 (1–1)    | 59 (0–94)     | 4.083 (3.777–4.552)   | Chávez et al. 2022   |
| S. ajuricaba                        | n=5         | 0.322 (0.282–0.366) | 1.064 (1.013–1.121) | 14 (12–16) | 57 (11–87)    | 6.91 (5.20–9.04)      | Fouquet et al. 2021b |
| S. mesomorphus                      | n=2         | 0.167 (0.160–0.173) | 1.093 (1.058–1.127) | 1 (1–1)    | 28 (15–40)    | 10.30 (9.66–10.93)    | Fouquet et al. 2021b |
| S.mirandariberoi                    | 6=u         | 0.167 (0.130–0.194) | 1.251 (1.100–1.471) | 7 (5–8)    | 148 (22–256)  | 6.57 (4.10–11.56)     | Fouquet et al. 2021b |
| S. rabus                            | n=1         | 0.039               | 1.642               | 1          | 169           | 11.20                 | Fouquet et al. 2021b |
| S. salseri<br>(Unvouchured)         | n=1         | 0.040 (0.029–0.05)  | 1.734 (1.481–2.148) | 1 (1–1)    | 24.1(20–27)   | 2.63 (1.66–4.46)      | This study           |
| S. salseri                          | 9=u         | 0.079 (0.071–0.090) | 1.411 (1.312–1.574) | 1 (1–1)    | 49 (14–91)    | 5.31 (2.36–9.16)      | Fouquet et al. 2021b |
| S. salseri<br>(Type locality)       | n=1         | 0.1                 | 1.400               | 1 (1–1)    | I             | I                     | Pyburn 1975          |
| S. zombie                           | n=4         | 0.154 (0.147–0.167) | 1.107 (1.059–1.190) | 1 (1–1)    | 142 (104–194) | 8.48 (6.90–9.90)      | Fouquet et al. 2021b |

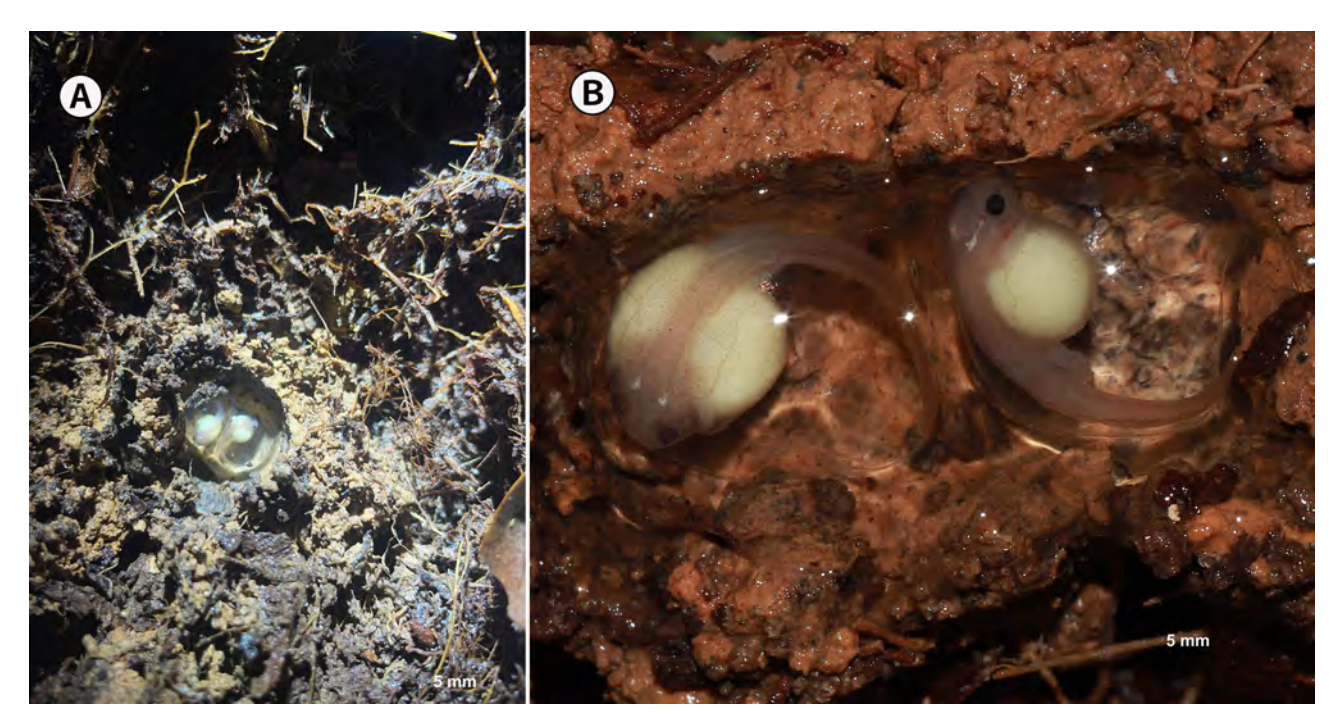


**FIGURE 7**. (A) *Synapturanus artifex* nest in a shallow hole under rootlets, Departamento, Amazonas "área no municipalizada" San Rafael de Caraparaná, (B) Tadpoles close up.

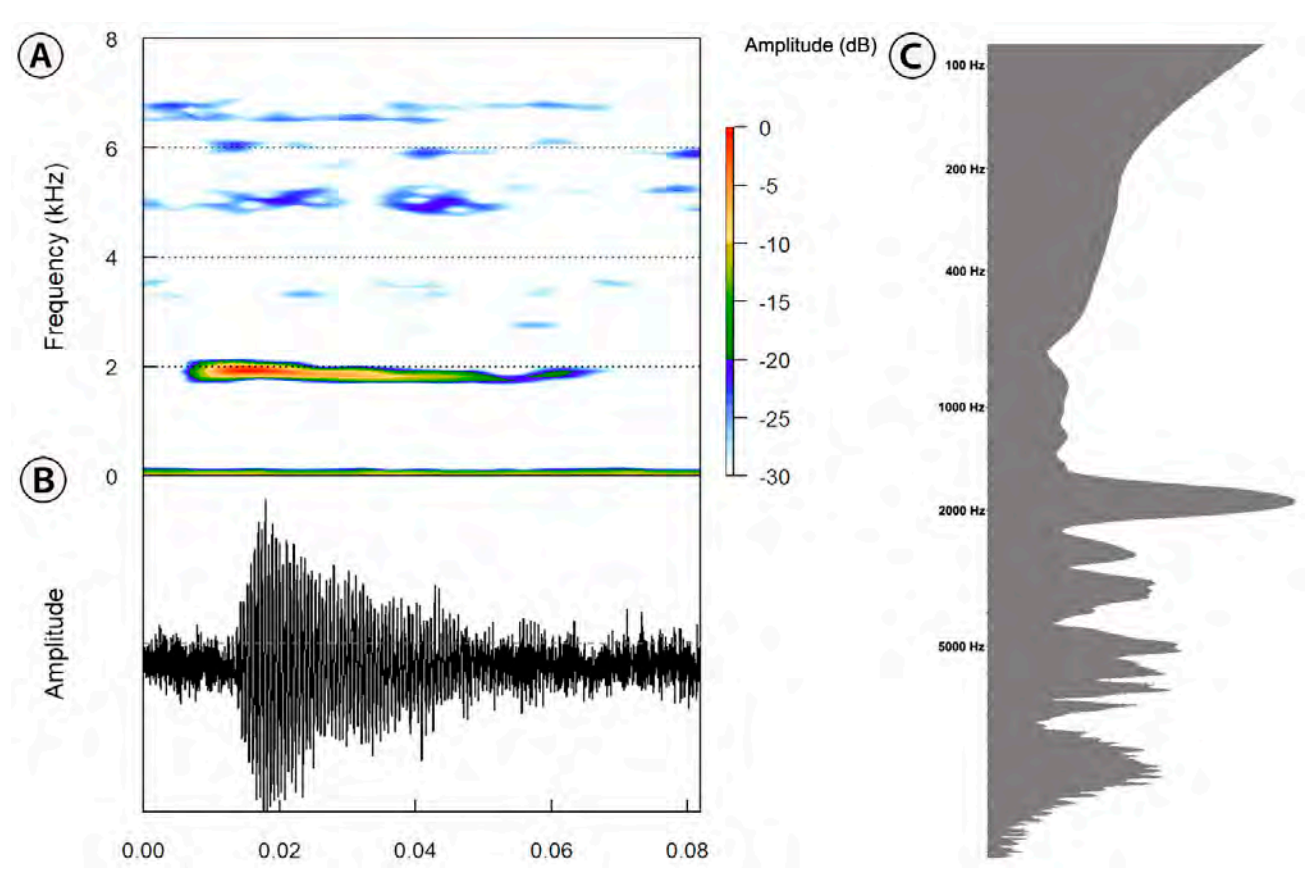


**FIGURE 8.** Advertisement call of *Synapturanus atifex* **sp. nov**. (SINCHI-A 7110, male, SVL= 15.45 mm). (A) spectrogram, (B) oscilogram, (C) power spectrum.

**Natural History**. In 2019, specimens were collected in a secondary forest during nights with light rain; we found them by gently removing the thick layer of rootlets of the floor, below the leaf litter. In 2021, specimens were collected on a night with no rain, but after a heavy downpour in the afternoon. They were calling everywhere and the

caller specimen SINCHI-A 7110 (Table 3) was collected in an "indigenous chagra" (traditional crop system), about half a hectare in size, with no trees to shade the ground in the daytime. According to the owner of the "chagra" this forest named "monte bravo" was cut down to make the settlement 40 years ago, this "chagra" area has been cut and burned several times, most recently a year ago. The male was singing in the root of a bush about 10 cm depth under the rootlets. In 2022, specimens were collected in a secondary forest which was used as a cattle breeding pasture in the 70's. The adults were found under the rootlets, about 10 cm depth; in the same microhabitat where the adults were found, one postures with two larvae was collected in a small hollow in the soil.

#### Osteology of Synapturanus latebrosus sp. nov.

Overall, the skull of the genus *Synapturanus* is well ossified, with very little cartilaginous areas, mostly restricted to the nasal capsule and tympanic ring. Osteological description of *Synapturanus latebrosus* **sp. nov.** is based on male specimen SINCHI-A 2679, variation with male SINCHI-A 842 is noted and compared with an adult female of *S. sacratus* **sp. nov.** (ICN 56893). The skull of *S. latebrosus* **sp. nov.** is overall triangular, slightly longer than wide (Fig. 9A, B, and C) and widest at the level of the jaw articulation. The jaw articulation lies at the most anterior edge to the otic capsule. The planum anterorbitalis is ossified and oriented anterolaterally forming the posterolateral walls of the nasal capsules and the anterior wall of the orbits. The auditory capsules, except its most anteroventral edge that is mostly cartilaginous, and the crista parotica are fully ossified. Between the anteroventral cartilaginous edge of the otic capsule and the crista parotica, lies a large and cartilaginous operculum; by transparency a large fenestra ovalis is clearly visible. From the most anterior edge of the operculum and running horizontally, between the crista parotica and the cartilaginous anterior edge of the otic capsule, lies the ossified columella. The columella then bends slightly ventrally towards the squamosal, before reaching the posterior edge of the squamosal, it articulates with a cartilaginous externa plectri that connects with the cartilaginous tympanic ring. The tympanic ring is not complete, but lack its dorsoposterior third.

**Endocranium**. *Sphenethmoid*. The paired sphenethmoid are well developed, fused into a single bone, ossified, and form the anterolateral wall of the neurocranium and the anterior margin of the optic fenestra. Dorsally, the sphenethmoid is mostly covered by the nasals and frontoparietals and only visible between the nasals and the frontoparietals. Ventrally, it is visible anteriorly and posteriorly on both sides of the cultriform process of the parasphenoid and forming the ventral border of a very large optic fenestra. Anteriorly it does not reach the posterior border of the choanae. Posterolaterally, the sphenethmoid indistinguishable fuses with prootic and surrounds the optic fenestra.

Prootics and exoccipitals. The prootics are fused with the exoccipitals contributing to the posterior part of the braincase, both are well ossified. The prootic ossifies on the posterolateral wall of the neurocranium, forming the dorsal and posterior margin of the optic foramen and entirely enclose the prootic foramen. Dorsally, their anteromedial margins are overlapped by the frontoparietals. Ventrally, the medial and posterior margins of the prootic are overlapped by the parasphenoid. The prootics also form the anterior and ventrolateral walls of the otic capsules; dorsally they form the epiotic eminences. The epiotic eminences are ossified, large, and visible; medially they fuse gradually to the skull. Most of the ossified crista parotica does not extend beyond the level of the otic capsule; however, a small distinct extension is found on the anterolateral corner of the crista parotica. The otic capsule is mostly ossified except in its most anteroventral area. A relatively large prootic foramen lies on the anteroventral surface of the otic capsule. In anurans, usually smaller oculomotor and trochlear foramina are found between the optic fenestra and prootic fenestra; these two foramina are not visible in *S. latebrosus*, and likely were integrated to the large optic fenestra. The exoccipitals form the posterior part of the otic capsules, the margins of the foramen magnum, and the occipital condyles. Dorsally, the exoccipitals are largely overlapped by the frontoparietals and ventrally by the alae and posteromedial process of the parasphenoid. The exoccipitals are only visible forming the dorsal and ventral edge of the foramen magnum and the occipital condyles. The occipital condyles bear oval-shaped articular surfaces.

**Plectral apparatus**. The plectral apparatus is found ventral to the crista parotica. The columella (*pars media plectri*) is a long, cylindrical bone, that proximal to the operculum has an expanded base, and runs almost horizontally and then it bends slightly and gradually ventrally towards the squamosal to about half the height of the squamosal. Distally, it connects with the cartilaginous *pars externa plectri* which is surrounded by a dorsally incomplete and wide ring, the cartilaginous tympanic annuli. The proximal end of the columella contacts with the anterodorsal edge of the cartilaginous operculum. The operculum is well developed, cartilaginous, and occludes the large fenes-

tra ovalis.

**Exocranium**. Frontoparietals. The broad, large, and paired frontoparietal bones are narrowly separated medially along their length and completely roofing the frontoparietal fenestra. The frontoparietals do not contact with the nasal bones and overlap the sphenethmoid. The anterior tip of the frontoparietals is close to the midline and from there they slant outwardly and posteriorly to the anterodorsal edge of the orbit. Posteriorly the frontoparietals extend over the prootic, partially overlap the epiotic eminences, and the exoccipitals. In specimen SINCHI 842, the separation of the frontoparietals is much narrower on its posterior 1/3.

Nasal. The paired nasals are extensive and well-ossified bones, they cover the nasal capsule and the sphenethmoid, they are medially separated, and do not contact with the frontoparietals. From the midline, they extend posteriorly slanted in a 45-degree angle to reaching the dorso-anterior edge of the orbit. The nasals cover the olfactory capsules and curve ventrolateral to about half the diameter of the external nostril (they do not reach the maxillae) and then turn upward over and dorsally surrounding the nasal capsule. Dorsally, between the anterior tip of the nasals and between the anterior tip of the cartilaginous nasal capsule, a thin ossification of the septum nasi is visible between the nasals with its apex directed posteriorly.

Parasphenoid. The large parasphenoid lacks ornamentation. The cultriform process is broad, occupying most of the floor of the brain and laterally reaching the ventral edges of the optic foramina. Overall, it is rectangular shaped, with its anterior and broad rounded tip passing and between the anterior edge of the neopalatines; medially the anterior tip of the parasphenoid is notched. The parasphenoid alae are broad, rectangular shaped, oriented posterolateral and underlying the otic capsules in about ½ their ventral width and they are widely separated from the medial ramus of the pterygoid. The posteromedial process of the parasphenoid is distinct, overall rounded, and its posterior medial edge bears a medial notch. The parasphenoid does not reach the edge of the foramen magnum.

*Vomer.* The small, paired anterior vomers lack articulation with other bony elements; posterior vomer are absent. Ventrally, the vomers are seen as thin ossifications on the margins of the choanae and visible, in ventral view, as a triradiate bone over the wall of the choana. The pre- and post-choanal processes support the choana's anterior and anteromedial margins. Vomerine teeth and odontoids are absent. In specimen SINCHI-A 2679, there is a thin, lateral, projection, at the mid length of the vomer, towards and close to the anterior edge of the internal choana.

*Neopalatines*. The neopalatines ossify and partially cover the planum anterorbitalis; laterally, the planum anterorbitalis remains cartilaginous in the adult. The medial tips of the neopalatines are rounded, placed slightly below the anterior tip of the parasphenoid, whereas the distal ones are bifurcated. The anterior edge of the neopalatines borders the posterior edge of internal choana.

*Premaxillae*. The edentate premaxillae are narrowly separated and embedded within the snout of the species (Fig. 9). The premaxillae are not found as the most anterior bones of the upper jaw. They are placed slightly back in the palate (i.e., the maxillae extend beyond the premaxillae) and between the anterior tips of the maxillae; laterally they do not articulate with the maxillae (Fig. 9). The alary processes of the premaxillae are well developed, inclined anteriorly, and their tip end slightly before the anterior tip of the maxillae. The pars palatina are broad, almost rectangular but their outer edge is anteriorly inclined towards the maxillae; they do not contact with the pars palatina of the maxillae. In specimens SINCHI-A 842, the pars palatina are overall broad and triangular and anteriorly, on their outer edge have a variable size projection.

Septomaxillae. The septomaxillae are small, thin, and triradiate bones that are not visible from outside; ventrally they can be seen within the nasal capsule. The anterior end of the nasal capsule is imbedded within the genus characteristic projecting 'snout'. The snout has multiple, small, and incomplete cartilaginous rings (i.e., Alcian blue positive).

Maxillae. The edentate maxillae lack pre and postorbital processes; the pars facialis is moderately developed, overall triangular at the level of the posterior half of the nasals, but remains widely separated from the nasals. The maxilla is relatively short with its posterior end found at about half the length of the optic foramen; over its posterior third, the maxillae articulates with the anterior ramus of the pterygoid. The anterior end of the maxillae lacks pars palatina, which is visible posterior to and does not contact with the pars palatina of the premaxillae; it is anteriorly expanded and tapes gradually to the posterior tip of the maxillae.

Quadratojugals. The quadratojugals are lost and the maxillary arch is incomplete.

**Suspensorium**. *Pterygoid*. The pterygoid is triradiate. The anterior ramus is long and its anterior 1/3 length overlaps with the posterior part of the maxillae and its tip reaches planum anterorbitalis. The medial ramus is short, seen only as a short, blunt, and ossified triangular blunt project which does not contact the otic capsule; the connec-

tions remain cartilaginous. The posterior ramus is short and overlaps the ventral ramus of the squamosal posteriorly; sometimes remains of the cartilaginous palatoquadrate are found between these two elements. The ventral ramus of the squamosal and the posterior ramus of the pterygoid form the articular surface for the lower jaw.

Squamosal. The squamosal is "T"-shaped consisting of ventral, otic, and zygomatic rami. The ventral ramus is well developed, broad, and robust, whereas otic and zygomatic rami are poorly developed, the zygomatic is slightly longer. The ventral ramus descends almost straight, forming a 60°–80° angle with the maxilla. The otic ramus articulates with the cartilaginous anterolateral margin of the crista parotica; the crista parotica is variably calcified.

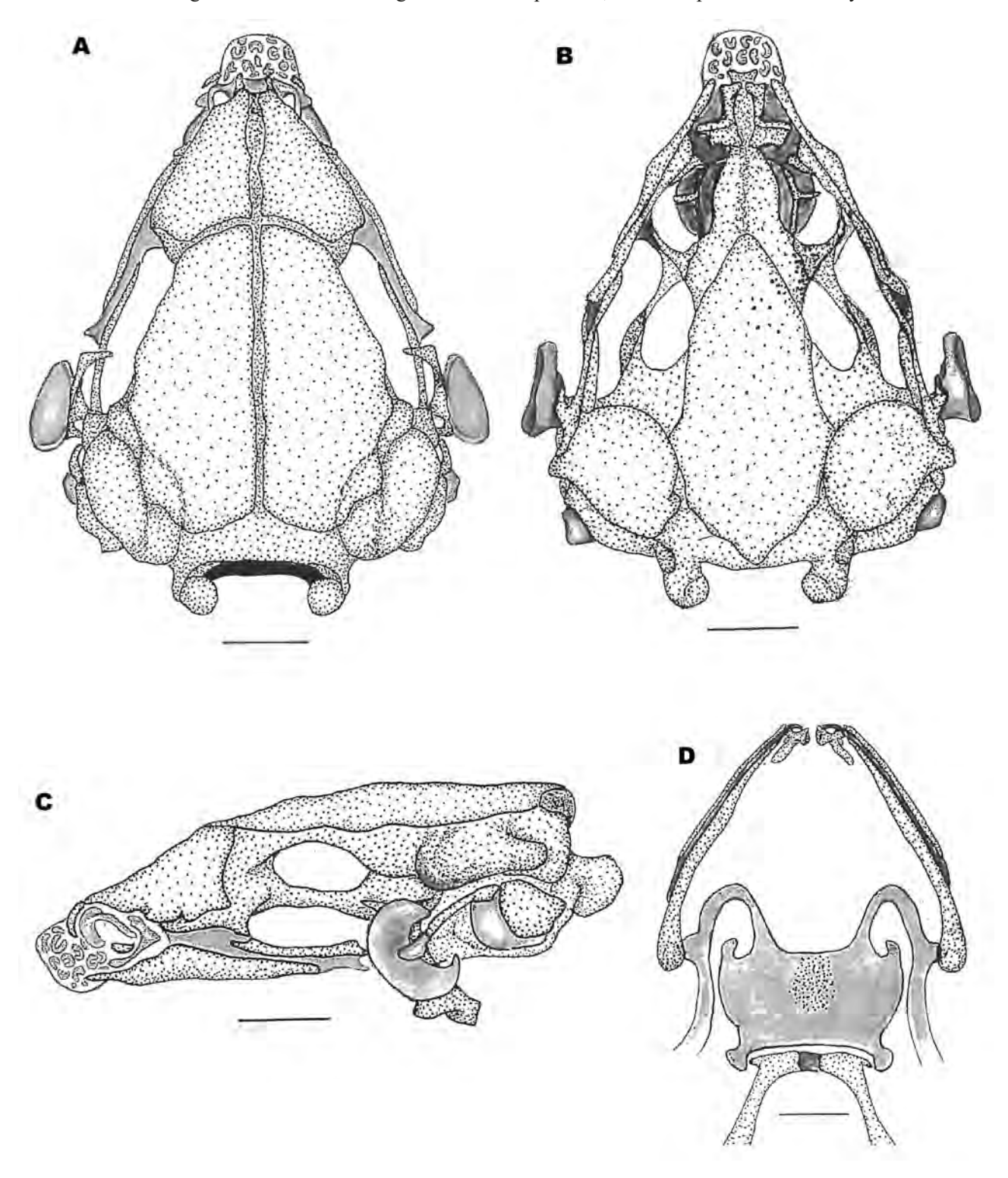


**FIGURE 9**. Synapturanus latebrosus **sp. nov.** osteology, paratype SINCHI-A 2679 (cleared and double-stained specimen, SVL=19.0mm), (A) dorsal, (B) lateral, and (C) ventral views of cranial osteology. Stippled = bone, Gray = cartilage, Stippled on gray = partially ossified cartilage

| TABLE 4. Genetic pairwise distances (lower diagonal) using 16S | e distances (le | ower diagona |         | mong Synap | oturanus spec | sies included | in the curre | among Synapturanus species included in the current analysis. Upper diagonal represent standard deviation. | represent standaı | rd deviation. |
|--|-----------------|--------------|---------|------------|---------------|---------------|--------------|---|-------------------|---------------|
| Species  | Divisor         | Ecuador      | Ica1    | Ica2       | Juami         | Nanay         | Neblina      | Purus_Taboca_Tapajos  | Venezuela         | ajuricaba     |
| Divisor  |                 | 0.0123       | 0.0279  | 6900.0     | 0.0267        | 0.0123        | 0.0254       | 0.0227  | 0.0150            | 0.0249        |
| Ecuador  | 0.0650          |              | 0.0262  | 0.0115     | 0.0262        | 0.0055        | 0.0227       | 0.0210  | 0.0132            | 0.0218        |
| lca1   | 0.1911          | 0.1701       |         | 0.0287     | 0.0058        | 0.0239        | 0.0290       | 0.0250  | 0.0272            | 0.0279        |
| Ica2   | 0.0246          | 0.0559       | 0.1964  |            | 0.0268        | 0.0113        | 0.0244       | 0.0223  | 0.0148            | 0.0246        |
| Juami  | 0.1902          | 0.1777       | 0.0175  | 0.1890     |               | 0.0231        | 0.0290       | 0.0258  | 0.0259            | 0.0289        |
| Nanay  | 0.0639          | 0.0180       | 0.1520  | 0.0558     | 0.1543        |               | 0.0211       | 0.0196  | 0.0123            | 0.0193        |
| Neblina  | 0.1760          | 0.1519       | 0.1882  | 0.1635     | 0.1984        | 0.1385        |              | 0.0147  | 0.0246            | 0.0140        |
| Purus_Taboca_Tapajos   | 0.1639          | 0.1485       | 0.1752  | 0.1569     | 0.1890        | 0.1363        | 0.0854       |   | 0.0221            | 0.0120        |
| Venezuela  | 0.0890          | 0.0751       | 0.1908  | 0.0833     | 0.1895        | 0.0667        | 0.1720       | 0.1645  |                   | 0.0229        |
| ajuricaba  | 0.1807          | 0.1408       | 0.1780  | 0.1666     | 0.1948        | 0.1202        | 0.0749       | 0.0630  | 0.1584            |               |
| artifex  | 0.0257          | 0.0716       | 0.2088  | 0.0218     | 0.2074        | 0.0748        | 0.1746       | 0.1666  | 0.0900            | 0.1703        |
| danta  | 0.0306          | 0.0735       | 0.1916  | 0.0294     | 0.1934        | 0.0712        | 0.1704       | 0.1472  | 0.0882            | 0.1548        |
| latebrosus   | 0.0669          | 0.0173       | 0.1660  | 0.0568     | 0.1665        | 0.0184        | 0.1558       | 0.1512  | 0.0722            | 0.1435        |
| mesomorphus  | 0.1565          | 0.1440       | 0.1731  | 0.1525     | 0.1842        | 0.1252        | 0.0757       | 0.0754  | 0.1533            | 0.0643        |
| mirandaribeiroi  | 0.1820          | 0.1471       | 0.17814 | 0.1764     | 0.1905        | 0.1406        | 0.0985       | 0.0401  | 0.1825            | 0.0764        |
| rabus  | 0.0609          | 0.0313       | 0.1944  | 0.0582     | 0.1996        | 0.0341        | 0.1522       | 0.1543  | 0.0853            | 0.1584        |
| sacratus   | 0.0661          | 0.0368       | 0.1509  | 0.0605     | 0.1478        | 0.0344        | 0.1372       | 0.1401  | 0.0731            | 0.1371        |
| salseri  | 0.1520          | 0.1325       | 0.1636  | 0.1409     | 0.1686        | 0.1165        | 0.0847       | 0.0705  | 0.1459            | 0.0720        |
| zombie   | 0.1713          | 0.1356       | 0.1672  | 0.1498     | 0.1759        | 0.1177        | 0.0853       | 0.0718  | 0.1522            | 0.0350        |

.....continued on the next page

| TABLE 4. (Continued) |         |        |            |             |                 |        |          |         |        |
|----------------------|---------|--------|------------|-------------|-----------------|--------|----------|---------|--------|
| Species              | artifex | danta  | latebrosus | mesomorphus | mirandaribeiroi | rabus  | sacratus | salseri | zombie |
| Divisor              | 6900.0  | 0.0075 | 0.0123     | 0.0227      | 0.0282          | 0.0117 | 0.0125   | 0.0209  | 0.0223 |
| Ecuador              | 0.0133  | 0.0131 | 0.0052     | 0.0216      | 0.0229          | 0.0075 | 0.0084   | 0.0201  | 0.0203 |
| Ica1                 | 0.0301  | 0.0292 | 0.0256     | 0.0266      | 0.0277          | 0.0290 | 0.0236   | 0.0237  | 0.0251 |
| Ica2                 | 0.0063  | 0.0076 | 0.0112     | 0.0227      | 0.0271          | 0.0112 | 0.0118   | 0.0210  | 0.0216 |
| Juami                | 0.0288  | 0.0279 | 0.0246     | 0.0262      | 0.0286          | 0.0285 | 0.0224   | 0.0232  | 0.0255 |
| Nanay                | 0.0138  | 0.0125 | 0.0059     | 0.0192      | 0.0222          | 0.0085 | 0.0083   | 0.0180  | 0.0180 |
| Neblina              | 0.0257  | 0.0251 | 0.0226     | 0.0152      | 0.0174          | 0.0238 | 0.0218   | 0.0146  | 0.0149 |
| Purus_Taboca_Tapajos | 0.0232  | 0.0208 | 0.0216     | 0.0141      | 0.0083          | 0.0219 | 0.0202   | 0.0110  | 0.0123 |
| Venezuela            | 0.0159  | 0.0148 | 0.0127     | 0.0218      | 0.0264          | 0.0144 | 0.0127   | 0.0208  | 0.0207 |
| ajuricaba            | 0.0252  | 0.0231 | 0.0221     | 0.0128      | 0.0146          | 0.0243 | 0.0212   | 0.0125  | 0.0083 |
| artifex              |         | 0.0081 | 0.0135     | 0.0224      | 0.0280          | 0.0125 | 0.0141   | 0.0211  | 0.0239 |
| danta                | 0.0347  |        | 0.0127     | 0.0225      | 0.0260          | 0.0124 | 0.0126   | 0.0198  | 0.0208 |
| latebrosus           | 0.0736  | 0.0750 |            | 0.0208      | 0.0243          | 0.0092 | 0.0079   | 0.0195  | 0.0198 |
| mesomorphus          | 0.1541  | 0.1523 | 0.1399     |             | 0.0136          | 0.0221 | 0.0202   | 0.0125  | 0.0131 |
| mirandaribeiroi      | 0.1823  | 0.1736 | 0.1554     | 0.0700      |                 | 0.0267 | 0.0237   | 0.0127  | 0.0135 |
| rabus                | 0.0680  | 0.0663 | 0.0415     | 0.1437      | 0.1664          |        | 0.0104   | 0.0193  | 0.0219 |
| sacratus             | 90800   | 0.0686 | 0.0348     | 0.1344      | 0.1473          | 0.0497 |          | 0.0188  | 0.0186 |
| salseri              | 0.1454  | 0.1369 | 0.1314     | 0.0723      | 0.0720          | 0.1285 | 0.1298   |         | 0.0113 |
| zombie               | 0.1699  | 0.1434 | 0.1333     | 0.0702      | 0.0753          | 0.1472 | 0.1275   | 0.0680  |        |

Mandible. The dentaries are smooth, lacking odontoids or ridges. The dentaries are thin and elongated bones and overlap about half of the length of the angulosplenials; anteriorly, they articulate with the main body of the mentomeckelian bones. The angulosplenial are long bones extending from almost the level of the mentomeckelian to the articulation with the upper jaw. The dentaries overlap the anterolateral outer surfaces of Meckel's cartilage and the angulosplenials the its inner and ventral surfaces. Overall, the angulosplenial are wider and longer than the dentaries. The mentomeckelian bones form the mandibular symphysis, they are well ossified but remain cartilaginous medially. The posterior tip of the mentomeckelian bones have a short, visible, posterior projection. Medially the mentomeckelian are connected by cartilage. The external margin has a distinct and long cartilaginous projection that curves and extends towards, but not contact with, the angulosplenial. These posterior projections are mostly well-ossified although their distal tips remain slightly cartilaginous

**Hyobranchial skeleton.** *Hyoid* (Fig. 9D). The hyoglossal sinus is a slightly narrow U-shaped. The hyoid is cartilaginous with an oval mineralized area located medially and anteriorly. The anterolateral processes of the hyoid plate are wide lateral expansions with small anterior projection and the posterolateral processes are slender and posteriorly curved. The hyale project anteriorly from the hyod plate and then they curve posterolateral; they are homogenous in width and at their anterior end, where they curve, they have poorly chondrified semicircular cartilaginous expansions. A narrow slit separates the hyoid plate from the posteromedial bones. The posteromedial processes are anteriorly expanded (medially connected by a small cartilaginous area) and posteriorly long, slender, narrow, and fully ossified.

## Postcranial osteology

Axial Skeleton. *Vertebral column* (Fig. 10E). The vertebral column consists of 8 presacral vertebrae (I–VII procoelous and VIII is diplasiocoelous. The atlas bears distinct and widely separated cervical cotyles. All vertebrae are non-imbricate and lack neural spines, centrum of vertebrae I–VI are wider than long, whereas that last two are more equal. Width of presacral and sacral vertebrae, including transverse processes, are: III > sacrum (including cartilaginous expansion) > IV > II > VIII> V = VI = VII > I. The transverse processes of presacral vertebrae are overall narrow with those of presacral V–VII being thinner (about than half the width of the anterior ones). The transverse processes of presacral III and V are oriented nearly perpendicular, whereas those of presacral IV are oriented slightly posteriorly, presacral II, VI–VIII are oriented anteriorly (more distinctly in II and VIII). Sacral diapophyses are perpendicular to the midline, broadly and symmetrically expanded. The lateral margins of the sacral diapophyses are continuous with a narrow cartilage that in its axial length reaches or passes the anterior tip of the transverse process of presacral VIII. This cartilage articulates with the anterior tip of the ilial shaft and shows some mineralization. The urostyle is rounded, lacking any lateral extension, and smooth; it is broader anteriorly just behind the point of articulation with the sacral vertebra.

Pectoral girdle (Fig. 10A). The firmisternal pectoral girdle lacks clavicles and procoracoid cartilages. The sternum is a broad cartilaginous plate, lacking any mineralization and continuous with the epicoracoid cartilage; the latter is restricted between the coracoids. The coracoids are in a slight angle with the body's midline; they are medially narrow. The coracoid and the scapula are robust, fully ossified, and fused with each other forming the glenoid fossa. The suprascapula is entirely cartilaginous, distally it is widely expanded and bears a distinct "hook-like" projecting posteriorly. The thin cleithrun lies on the anterior edge of the suprascapula, it is elongated and narrow, its proximal end is slightly broader.

Pelvic girdle (Fig. 10B). In dorsal view, the space between the ilial shafts is U-shaped. Anteriorly and postero-dorsally, the acetabulum is formed by the ilium and ischium, ventrally the acetabulum is bounded by a calcified pubis. A small crest is visible dorsal to the acetabulum.

**Limbs.** *Manus* (Fig. 10C). The phalangeal formula is 3-3-2-2, all phalanges well ossified; length of digits is III > IV > II > I. The terminal phalanges are overall triangular with pointed distal tips. Proximally, the carpus consists of a large radiale and medium size ulnare, no intermedium visible. Carpal elements 3–5 are fused into a single element, which lies at the base of the metacarpals III–V. A single distal carpal 2 lies at the base of metacarpal II and also articulates with metacarpal III. Element Y lies between and articulating with the radiale proximally and distally with carpal 2 and the posterior edge of the proximal element of the prepollex. The prepollex is formed by the ossified proximal and a smaller distal element.

Pes (Fig. 10D). The phalangeal formula is 2-2-3-4-3, terminal phalanges are overall triangular with pointed distal tips. Digit lengths are IV > III > V > II > I. The tarsus bears three tarsal elements: tarsal 3 is elongated and articulates mostly with digit 3 but also laterally with digit 2; tarsal 2 is minute and located between digits II, I, and tarsal 1; and tarsal 2 is large, rounded, and articulates with digit 1 and the proximal element of the prehallux, both proximal and distal elements of the prehallux are completely ossified.

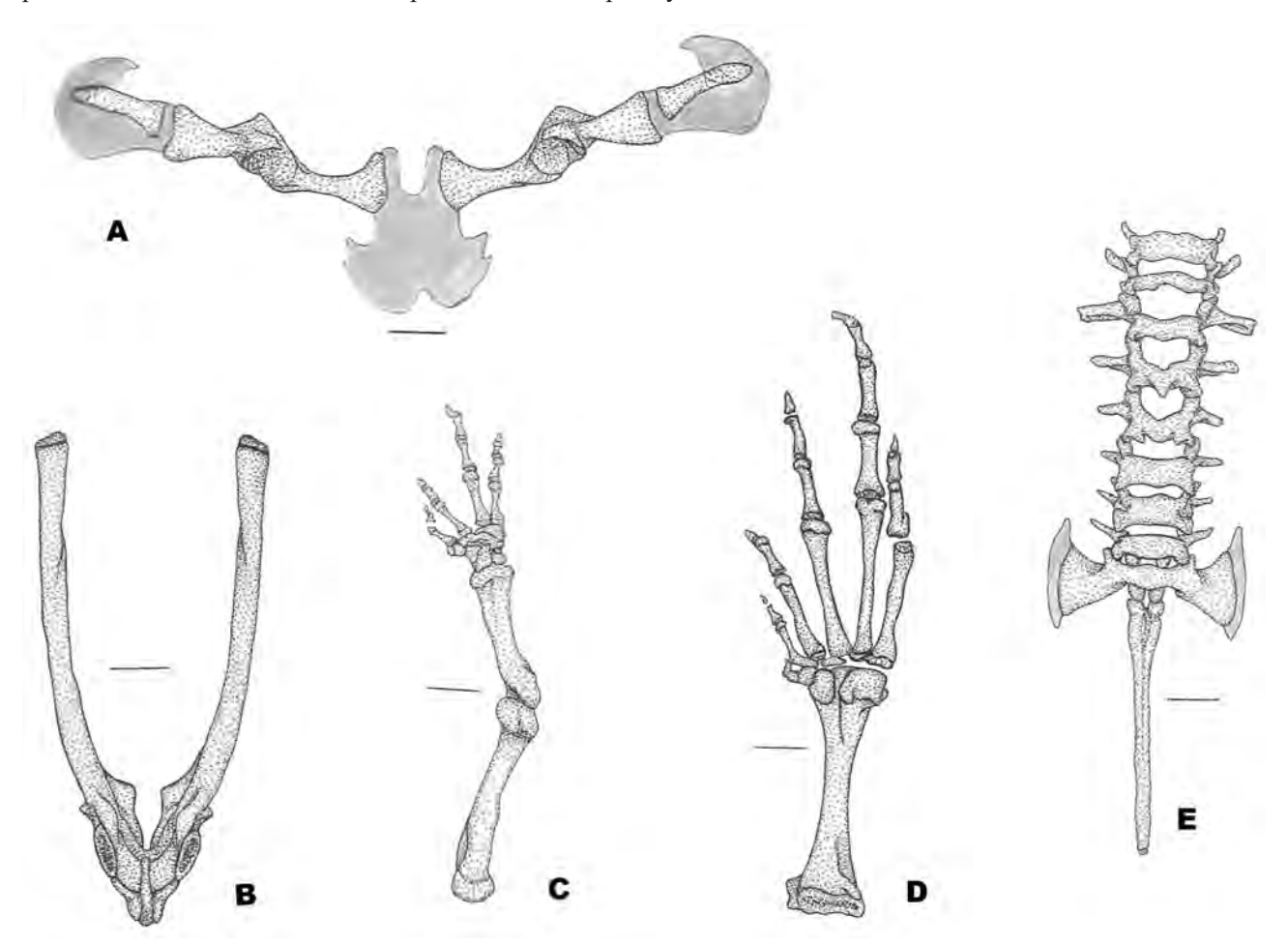


**FIGURE 10**. Synapturanus latebrosus **sp. nov.** osteology, paratype SINCHI-A 2679 (D) ventral view of pectoral girdle, (E) hand, (F) foot, (G) dorsal view of vertebral column, (H) dorsal view of lower jaw and hyobranchial skeleton, (I) dorsal view of pelvic girdle. Stippled = bone, Gray = cartilage, Stippled on gray = partially ossified cartilage

**Diagnosis of Synapturanus.** Based on the revision of S. mirandariberoi, S. salseri, S. rabus, S. latebrosus sp. nov., S. sacratus sp. nov., S. artifex sp. nov. (osteology and morphology) and the publication of further recently described species (Fouquet et al.., 2021b), we provide the following updated diagnosis for the genus: protruding snout supported by incomplete cartilaginous rings (Fig. 11A); vertebral column diplasiocoelous, eight presacral vertebrae, sacral diapophyses expanded; maxillary arch incomplete, prevomers and quadratojugal absent; pars palatina of premaxillae posteriorly notched; pars palatina of maxillae anteriorly expanded; internasal bone present; palatines present (sometimes partially or completely fused with underlying bones); procoracoid and clavicles absent; terminal phalanges pointed; distal fingers and toes rounded, lacking disk-like expansion; transverse processes of urostyle as wide as those of the third vertebrae; adult males with a distinct wrist gland; males have a single and medial testicle (Fig. 11B); W-shaped lower jaw; a small, medial, and unpigmented small area on tip of the lower jaw.

#### **Discussion**

Including the new species described here, the genus *Synapturanus* now consists of 10 described species: 5 from Colombia, 2 from Guyana, 1 from French Guyana, 1 from Peru, and 1 from Brazil. The diversity analysis of the ge-

nus *Synapturanus* suggests a species richness six times higher (Fouquet *et al..*, 2021a) and that it will increase with further sampling in the Western Amazonia, as shown by the three additional species described here. Although allopatric speciation may favor diversification in Neotropical microhylids, including *Synapturanus*, given that medium to large size rivers represent barriers triggering vicariance in small size and fossorial anurans (de Sá *et al..*, 2019), it is necessary to intensify local sampling in such hidden microhabitats, for better understanding of their distribution and speciation patterns.

Our examination of the morphology of the three new species proposed here and that of *Synapturanus rabus*, *S. salseri*, *and S. mirandariberoi* as well as osteological comparisons with *S. latebrosus* **sp. nov.**, provide additional diagnostic characters for the genus. These are: 1. protruding snout supported by cartilaginous rings (Fig.11A), also found in a cleared and double-stained specimen of *S. sacratus* **sp. nov.**, 2. adult males with a wrist gland, 3. a single testicle (i.e., not paired, Fig. 11B); examination of *Otophryne* males showed they have the common vertebrate of two testicles trait, 4. lower jaw shaped as a broad W, a small, medial, and unpigmented area on tip of the lower jaw (more evident in preserved specimens). Currently, we do not know of any report of an anuran species with a single testicle; however, Lynch (pers. comm.) is aware that *Eleutherodactylus restrepoi* shows this condition.

In anurans each testicle is associated with one kidney and they are relatively small. In *Synapturanus*, there is a single and large testicle in a medial position to both testicles. Given its larger size and medial position, we think it is likely the fusion of the two testicles into a single morphological structure. However, developmental work will be needed to determine if the single testicle of *Synapturanus* is indeed the result of a fusion of the two testicles that characterize vertebrates or corresponds to the evolutionary loss of one testicle.

Herein we discussed characters that have been erroneously considered synapomorphies for *Synapturanus*. Carvalho (1954) listed, among others, the following traits as diagnostic for *Synapturanus*: 1) prevomer fused with sphenethmoid and parasphenoid, 2) quadratojugal reduced, 3) palatines absent, and 4) fingers and toes with "disk-like expansions". Nelson and Lescure (1975) also listed fusion of prevomers and parasphenoid and maxillary arch complete in the diagnosis of *Synapturanus*. In the material examined, we did not find prevomers; either the prevomers are indistinguishable fused with other cranial elements or they were evolutionary lost. *Synapturanus salseri*, the least ossified species with a distinct lack of fusion of cranial bones, lacks prevomers. Currently, there are no cranial developmental data for *Synapturanus* to argue for a full fusion of the prevomers to other cranial elements. Palatines are present and distinct in *S. salseri* and *S. latebrosus* sp. nov., distinct and medially fused to the braincase in *S. mirandariberoi*, and indistinctly fused in *S. rabus*. Carvalho (1954) reported the absence of palatines in *S. mirandariberoi*; however, more recently Zweifel (1986) reported palatines in a cleared and stained specimen of *S. mirandariberoi*.

The septomaxillae of *Synapturanus salseri* is distinct and independent of other cranial element (Fig. 12 ventral view); in *S. mirandariberoi* (Fig. 13) and *S. rabus* (Fig. 14) only the tip of the posterior ramus of the septomaxillae fuses to the braincase at the junction between the anteromedial edge of the planum anterorbitalis and the ossified sphenethmoid. In *Synapturanus*, the maxillary arcade is incomplete due to the loss of the quadratojugal. Carvalho (1954) reported the quadratojugal present and in contact with the maxillae in *Hamptophryne*, *Hyophryne*, and *Ctenophryne*, and not in contact with the maxillae in *Relictivomer*, *Arcovomer*, *Dasypops*, and *Myersiella*. Furthermore, he noted that in *Synapturanus* the "quadratojugal is reduced, not in contact with the maxillae". The lack of quadratojugal was reported for *Syncope* (Walker, 1973). More recently, the maxillary arcade was described as incomplete in many New World microhylids but that a quadratojugal is present in all taxa except *Syncope* (Trueb *et al.*, 2011). Based on CT scans and clear and stained specimens examined herein, the quadratojugal is absent in *S. latebrosus* **sp. nov.**, *S. sacratus* **sp. nov.**, *S. mirandariberoi*, *S. salseri*, and *S. rabus*; representing a synapomorphy for the genus.

The recent description of three new species, i.e. *Synapturanus mesomorphus*, *S. ajuricaba*, and *S. zombie* included description of their osteology (Fouquet *et al..*, 2021b). Therein, it is suggested that the broad based condition of the ventral ramus of the squamosal corresponds to its fusion with quadratojugal. We see no evidence of this fusion and there is no developmental data to corroborate such a fusion. Historically, the morphology of the squamosal has been extensively studied (e.g., Griffiths, 1954; Starrett, 1968; and Lynch, 1971, Trueb, 1977); more recently the squamosal was listed among five dermal bones where hyperossification may be the results of heterochronic processes (Paluh *et al..*, 2020). Furthermore, a well-developed, broad, and robust ventral ramus is found in other anurans (e.g. *Rhinophrynus dorsalis, Rhinella acrolopha, Hemiphractus panamensis, Chacophrys pierottii, Brachycephalus ephippium, Macrogenioglottus alipioi* (Trueb 1973, Paluh *et al..*, 2020).

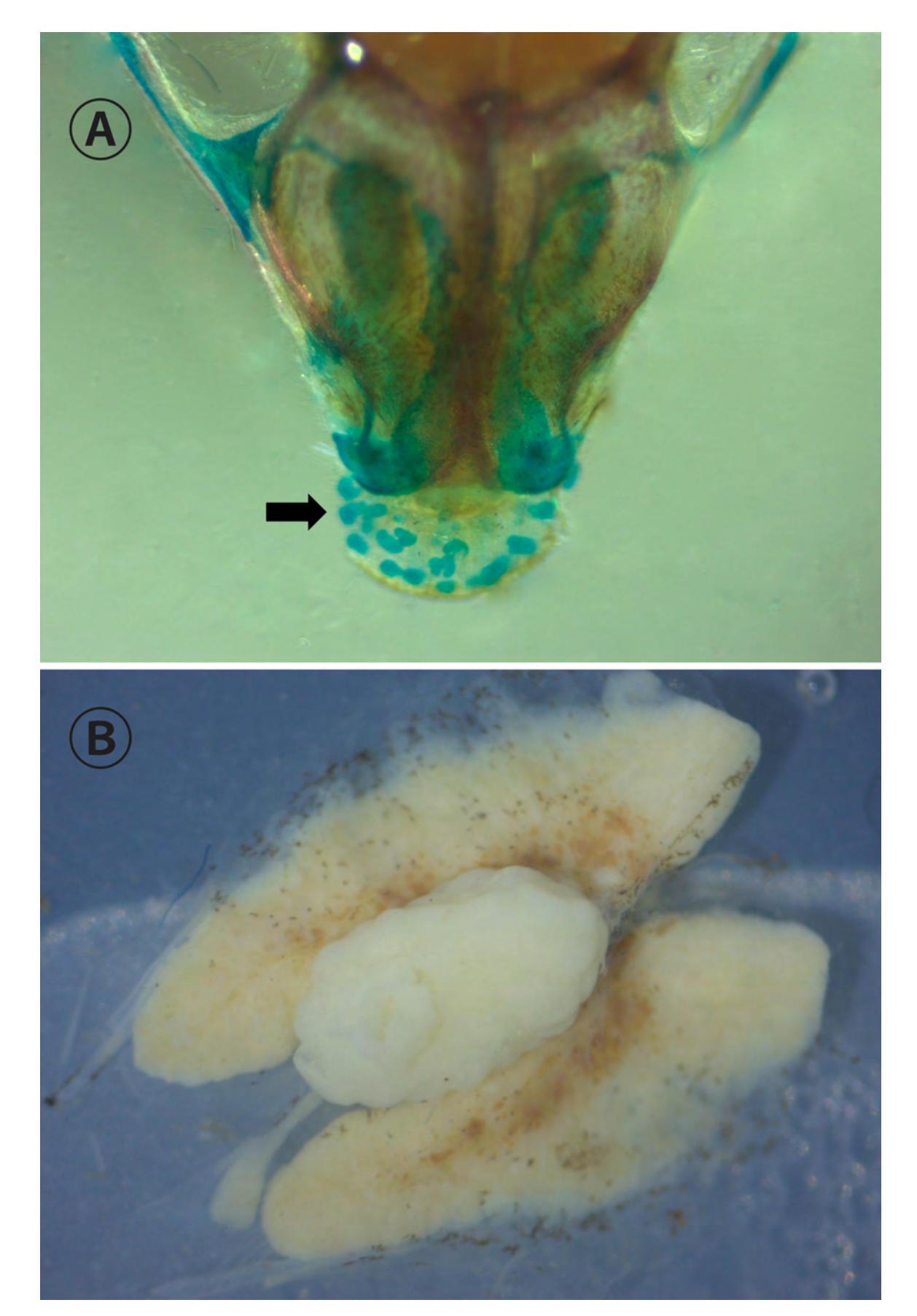


**FIGURE 11**. (A) Incomplete cartilaginous rings within the protruding snout of *Synapturanus latebrosus* **sp. nov.** SINCHI-A 2679, paratype (cleared and double-stained specimen, (B) Single and medial testicle in *Synapturanus latebrosus* **sp. nov.** adult male SINCHI-A 842, paratopotype (cleared and double-stained specimen).

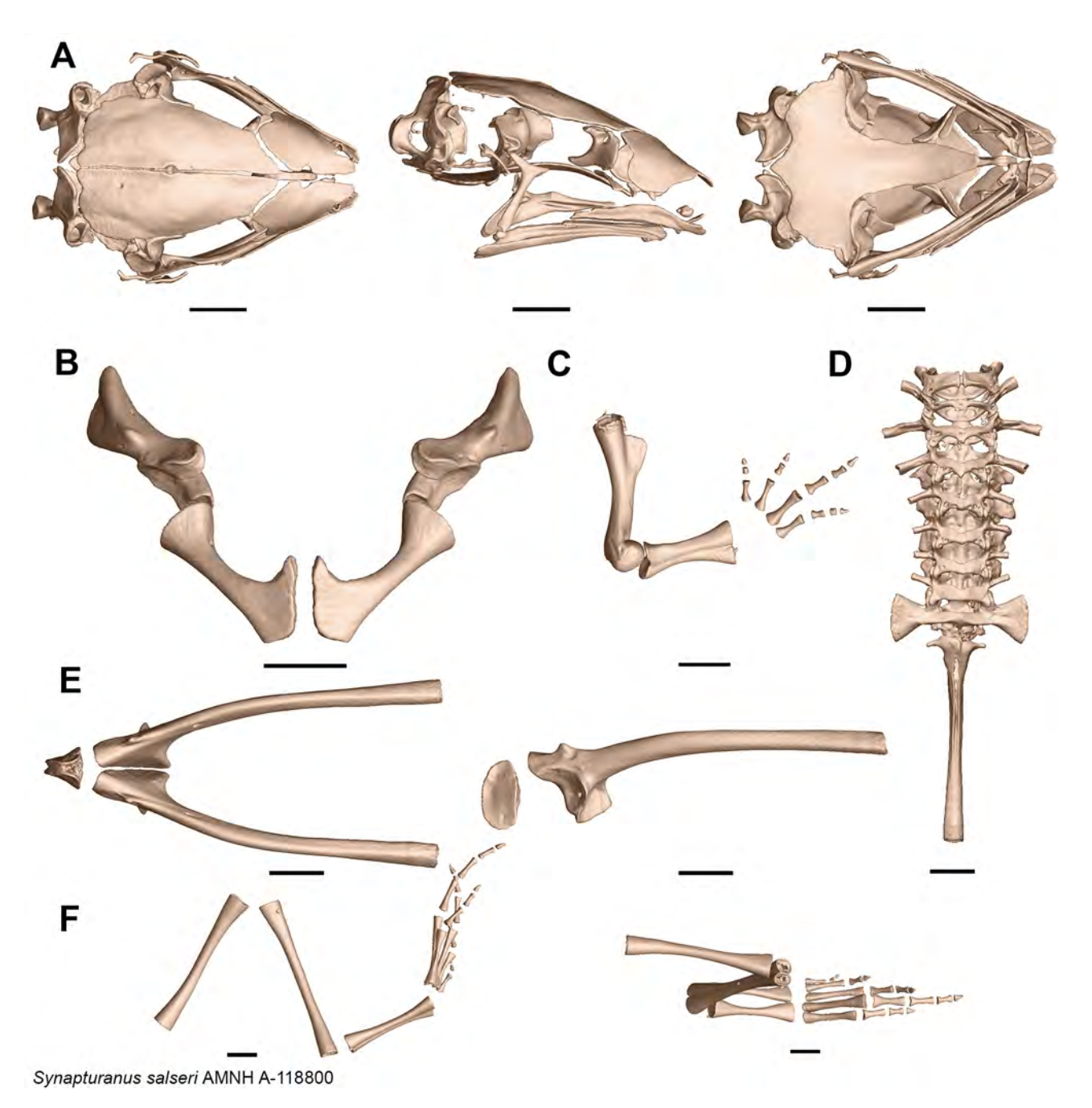


**FIGURE 12**. Colorized surface rendering of micro computed-tomography (microCT) scans of *Synapturanus salseri* (AMNH A-118800), illustrating major skeletal features. All scale bars equal 1 mm. (A) From left to right; dorsal, lateral, and ventral views of the skull; (B) ventral view of the pectoral girdle; (C) dorsal view of the right arm; (D) dorsal view of the vertebral column; (E) from left to right; dorsal and lateral views of the pelvic girdle; and (F) from left to right; dorsal and lateral views of the right leg.

Synapturanus skulls are well ossified. Among the specimens examined (Fig. 9, 12–14), S. salseri and S. latebrosus sp. nov. have frontoparietals distinctly separate from nasals and exoccipitals (narrowly separated in S. mirandariberoi, AMNH A90936 cleared and stained paratype), the parasphenoid distinct from the cranial floor. The frontoparietals are overall rectangular in shape and anteriorly narrower, whereas the nasal are triangular shaped and the lateral margin curves ventrolateral but do not contact with the pars facialis of the maxilla. Synapturanus salseri and S. latebrosus sp. nov. have narrower and slightly longer skulls than the other species in the genus. The ratio of cranial length (i.e., posterior edge of occipital condyles to the most anterior ossified cranial element) to cranial width (i.e., between posterior tips of mandible) are S. salseri and S. latebrosus sp. nov. = 1.3, S. mirandariberoi = 1.0, and

S. rabus = 1. Synapturanus rabus (Fig. 14) is the most ossified species and most cranial bones are indistinctly fused with each other. The frontoparietals, nasals, and exoccipitals are entirely fused with each other and with the sphenethmoid into a single continuous element; i.e., including the previous cartilaginous areas of the braincase found among bones in S. salseri. Synapturanus mirandariberoi is similar to S. rabus; the nasals are indistinctly fused with each other medially but their posterior edge is distinct and the frontoparietals are barely distinct from each other (mostly posteriorly) and from the nasals (Figs. 13–14). Similarly, a convergent fusion of frontoparietals, nasals, exoccipitals, and sphenethmoid was reported for Rhinophrynus and pipids (Trueb, 1973).

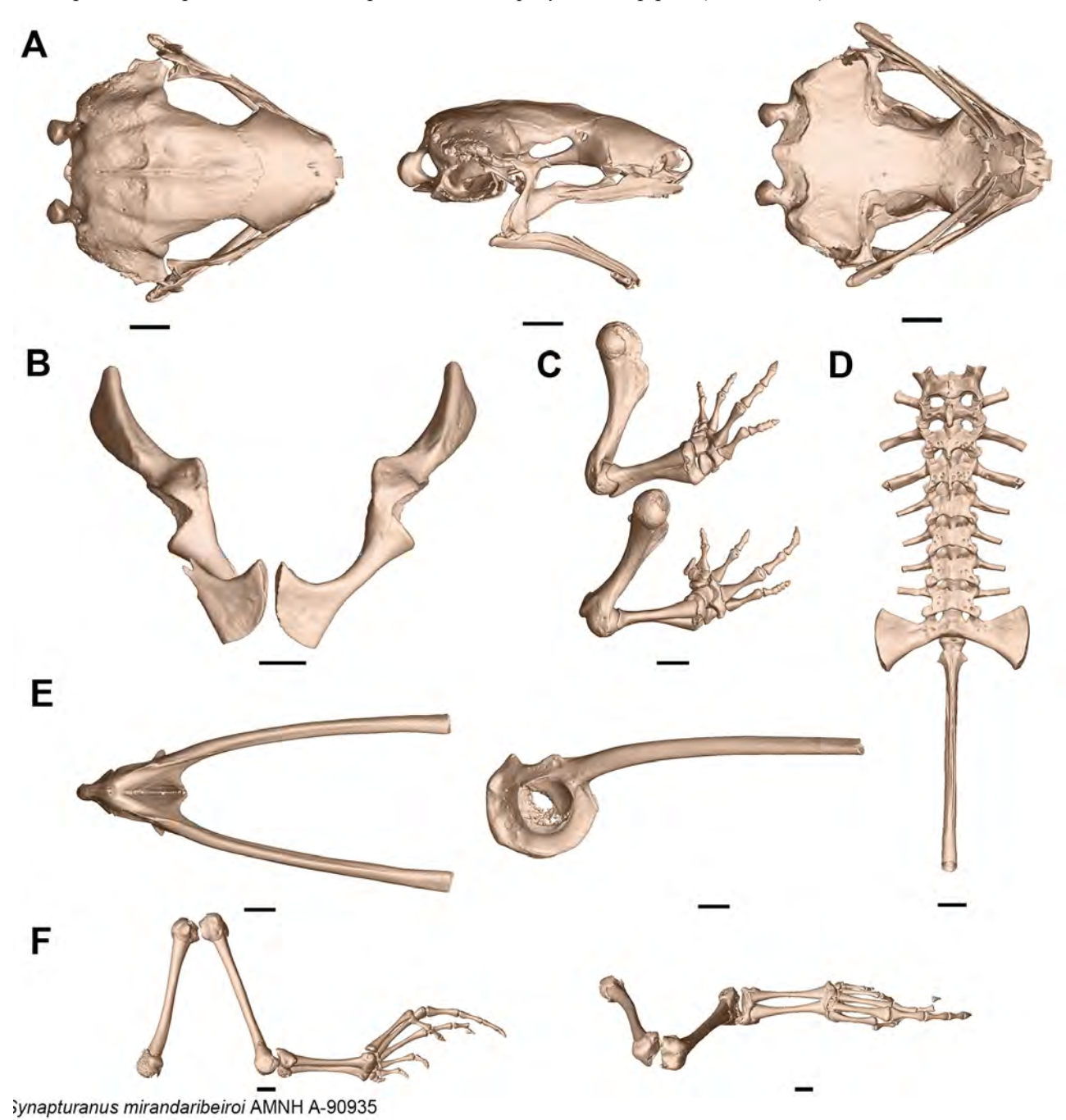


**FIGURE 13**. Colorized micro computed-tomography (microCT) scans of *Synapturanus mirandariberoi* (AMNH A-90935), illustrating major skeletal features. All scale bars equal 1 mm. (A) From left to right; dorsal, lateral, and ventral views of the skull; (B) ventral view of the pectoral girdle; (C) dorsal (upper) and medial (lower) views of the right arm; (D) dorsal view of the vertebral column; (E) from left to right; dorsal and lateral views of the pelvic girdle; and (F) from left to right; dorsal and lateral views of the left (reflected, right leg was damaged) leg.

In dorsal and ventral views of *Synapturanus salseri*, we observed what we consider to be the internasal bone (Fig. 12). This narrow element was reported in *Pternohyla fodiens* and found in the midline of the skull and on the dorsal area of the internasal septum and that it may function to reinforce the skull in burrowing frogs (Trueb 1970). This element is distinct in *Synapturanus* and represents a more extensive ossification of the internasal septum. In *S. salseri* the internasal is least developed not reaching the anterior tip of the nasal capsules. The ossification of the internasal bone is more extensive in *S. mirandariberoi* and *S. rabus* with the anterior curvature of the internasal, which in ventral view, is lying between the alary processes of the premaxillae. In lateral view, the anterior curvature of the internasal aligns with the tip of the maxillae in *S. rabus* (Fig. 14); whereas in *S. mirandariberoi*, it extends beyond the anterior tip of the maxillae (Fig. 13). Furthermore, dorsally the fusion of the internasal to the nasals is noticeable in *S. rabus* (less distinct in *S. mirandariberoi*). In *Synapturanus*, the extensive fusion of cranial bones is likely correlated, as in other taxa, with miniaturization (Hanken 1993, Scherz *et al.*. 2019, Paluh *et al.*. 2020) coupled in some taxa with fossoriality e.g. *Synapturanus*, resulting in an overall pattern of hyperossification.

In Synapturanus, the premaxillae are not found at the anterior end of the skull, but located posterior to, and between, the distal tips of the maxillae; they are not fully visible in lateral view (Figs. 9, 12-14). The premaxillae have a pars dentalis that lack teeth and a broader pars palatina that is slightly notched posteriorly. The pars alaris are inclined anteriorly and project dorsally, diverging to each other in S. salseri and S. mirandariberoi and mostly parallel to each other in S. rabus. In the ventral view, they appear flanking the anterior end of the internasal in S. mirandariberoi and S. rabus; in lateral view, their tip contact with the internasal in S. mirandariberoi. The maxillae have a well-developed pars facialis; in S. mirandariberoi and S. rabus, it has an overall broad and triangular-shaped preorbital process not contacting with the nasals, S. salseri lacks the triangular shape. The pars palatina of the maxillae is absent on the anterior quarter of the maxillae where the premaxillae are found; the pars palatina are distinctly broader anteriorly. The maxillary arches are incomplete due to the loss of the quadratojugals (Figs. 9, 12-14). The septomaxillae partially support the nasolacrimal duct (Duellman and Trueb 1994) and the homology of this bone was previously reviewed (Pugener and Maglia 2007). The septomaxillae of Synapturanus are triradiate and located slightly lateral and posterior to the pars palatina of premaxillae. They are independent from other elements in S. salseri and in S. mirandariberoi and in S. rabus the tip of the posterior ramus of the septomaxillae is fused to the anteroventral medial margins of the planum antorbitale (Fig. 12-14). Furthermore, they are located forward in the skull where their anterior ramus is found in front or parallel to the mentomeckelian.

In *Synapturanus salseri* the sphenethmoid ossifies only to form the anterior wall of the braincase and it is distinctly separated from the nasals, the frontoparietals, and the parasphenoid that underlines the braincase (Fig. 12). The braincase is completely ossified in *S. rabus* and *S. latebrosus* **sp. nov.** (Figs. 14 and 9, respectively). In *S. rabus*, the anterior wall of the orbital capsule is ossified and the posterior edge of the nasals is indistinctly continuous with this wall, whereas in *S. mirandariberoi* the posterior edges of the nasal is distinct. The braincase of *S. latebrosus* **sp. nov.** is ossified but nasals and frontoparietals are distinct from each other and from the underlying ossified braincase (Fig. 9).

The parasphenoid develops ventral to the braincase. In *Synapturanus salseri* it is triradiate with a long and anteriorly pointed cultriform process, lateral broad alae, and a short posterior tip that extends between the exoccipitals. The parasphenoid of *S. latebrosus* **sp. nov.** is similar to *S. salseri*, but lacks the lateral alae. This bone is fused with the floor of the braincase, the exoccipitals, and the sphenethmoid, but overall its boundaries are still visible in *S. mirandariberoi*; whereas in *S. rabus* it is mostly indistinct on the cranial floor (Figs. 9, 12–14).

The otic capsule of *S. salseri* is mostly cartilaginous with only its anterior and posterior walls being ossified; consequently, in CT scans the fenestra ovalis is not defined; the optic capsule is fully-ossified with a distinct fenestra ovalis in *S. rabus*, *S. mirandariberoi*, and *S. latebrosus* **sp. nov.** The fenestra ovalis in *S. mirandariberoi* located ventrally and oriented ventrolateral, whereas *S. rabus* and *S. latebrosus* show more lateral positioned fenestra ovalis. The columella is overall small and thin with a broader proximal end which bears a slight indentation in *S. salseri* and *S. mirandariberoi* and has convex edge in *S. rabus* and *S. latebrosus* **sp. nov.** 

The T-shaped squamosal consists of ventral, otic, and zygomatic rami. The ventral ramus is well developed and anteriorly inclined in all species. The otic and zygomatic rami are about equal in length except in *S. salseri* where the otic ramus is longer (Fig. 12). The otic ramus contacts with the anterolateral margin of the ossified crista parotica; in *S. latebrosus* **sp. nov.** this margin is not fully ossified (Fig. 9). The zygomatic ramus in *S. salseri* and *S. latebrosus* **sp. nov.** is overall pointed, whereas in *S. mirandariberoi* is almost rectangular and in *S. rabus* it expands down appearing as an anterior expansion of the zygomatic ramus through the top 1/3 of its length (Figs. 9, 12–14).

The anuran pterygoids are triradiate (Trueb 1970). The pterygoids of *Synapturanus* are triangular-shaped, with a distinct anterior ramus (the tip of the triangle) and the base of the triangle consisting of a flange of bone extending between the medial and posterior rami. The anterior ramus of the pterygoid overlaps the posterior part of the maxillae (about 35% in *S. salseri*, 42% in *S. mirandariberoi*, and 43% in *S. rabus* overlap of the maxillae length). During development, the squamosal and pterygoids invest the cartilaginous palatoquadrate as reported for *Hamptophryne*; in the adult, the only remains of the palatoquadrate is the ossified pars articularis quadrati that participates in the jaw articulation (de Sá and Trueb, 1991).

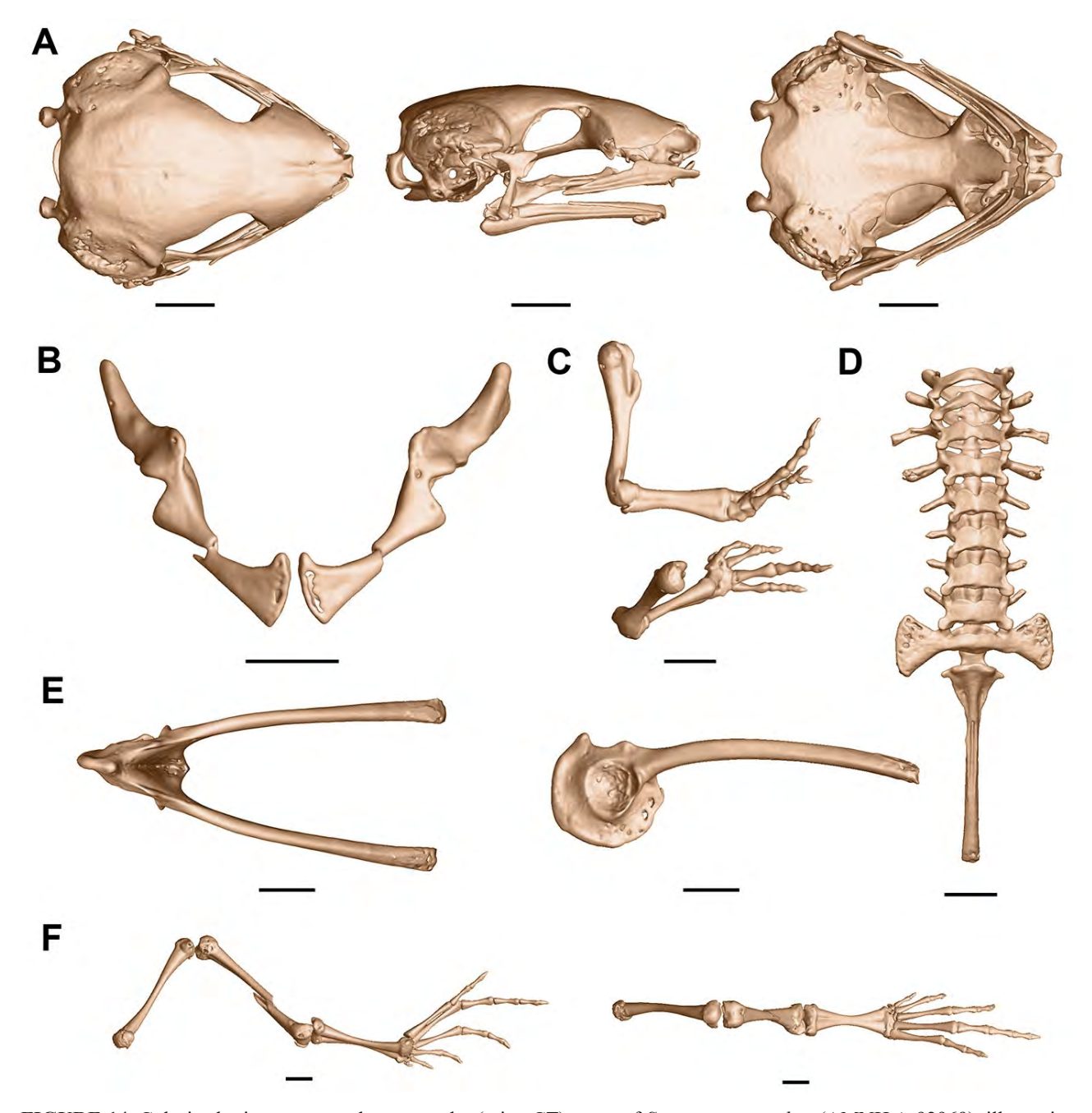


**FIGURE 14**. Colorized micro computed-tomography (microCT) scans of *Synapturanus rabus* (AMNH A-92969), illustrating major skeletal features. All scale bars equal 1 mm. (A) From left to right; dorsal, lateral, and ventral views of the skull; (B) ventral view of the pectoral girdle; (C) dorsal (upper) and medial (lower) views of the right arm; (D) dorsal view of the vertebral column; (E) from left to right; dorsal and lateral views of the pelvic girdle; and (F) from left to right; dorsal and lateral views of the right leg.

The dentaries invest the anterolateral external surface of Meckel's cartilage and the angulosplenials extend over its lateral and posterior surfaces. The ratio dentary/angulosplenial length is: 59% in *S. salseri* and *S. rabus*, 64% in *S. latebrosus* **sp. nov.**, and 65% in *S. mirandariberoi*. Mentomeckelian bones are found between, the tips of the angulosplenial, i.e., slightly recessed from the tip of the dentaries (Figs. 9, 12–14). The mentomeckelian are small bones, their anterior part lies horizontal to the edge of the mandible and then bending posteriorly and slightly outward, parallel to the anterior tip of the angulosplenial. In *S. rabus*, the posterior tip of the mentomeckelian has a pointed extension that is not present in the other species.

The vertebral column consists of 8 presacral vertebrae (Figs. 10, 12–14); in *Synapturanus* the vertebrae are non-imbricated (distinctively in *S. salseri* and *S. latebrosus* **sp. nov**., Figs. 12 and 9) and lack neural processes; transverse processes of presacral II and VIII are oriented anteriorly; transverse processes of presacral III about of equal width to the sacral diapophyses; sacral vertebra articulates with the coccyx via a bicondylar articulation. Coccyx rounded, smooth, and slightly wider anteriorly.

The pelvic girdle is V-shaped in *Synapturanus* (Figs. 10, 12–14). The ilial shaft is mostly smooth bearing only a low crest on its dorsal edge above the acetabulum, the ilium is fully ossified. The acetabulum is formed by the confluence of the ilium, ischium, and cartilaginous pubis. In *S. salseri*, the ilium is well developed, the ischium is not entirely ossified, and the pubis is not calcified. Whereas in *S. mirandariberoi* all three elements are ossified/calcified and their boundaries can be seen; furthermore, in *S. rabus* and *S. latebrosus* sp. nov. they are fully ossified and their boundaries are indistinct.

Microhylids have a firmisternal pectoral girdle. The pectoral girdle of *Synapturanus* lacks clavicles, precoracoids, procoracoids, and omosternum; the sternum is entirely cartilaginous forming a wide plate that is continuous with the epicoracoid cartilages (Figs. 10, 12–14). Coracoids are robust and fused with the scapula as reported for *Hamptophryne boliviana*; however, this species retains the procoracoid cartilages and the clavicles (de Sá and Trueb, 1991); the glenoid fossa is formed by these two fused bones. The cleithrum invests the anterior margin of the cartilaginous suprascapula in *S. latebrosus* sp. nov. Interestingly, the CT scan of the other species does not show the presence of a cleithrum.

The forelimb in *Synapturanus* consist of the proximal humerus and the fused radius and ulna distally (Figs. 10, 12–14). The humerus has a distinct and wide crest on its proximal end in *S. salseri* and *S. mirandariberoi*; however, in *S. rabus* and *S. latebrosus* **sp. nov.** the crest is narrow and less distinct.

Phalangeal formula is 2-2-3-3, terminal phalanges are pointed. Phalanges are not fused in *S. salseri*; whereas in *S. mirandariberoi* and *S. rabus* there seems to be fusion of some terminal phalanges. Carpal elements in *S. salseri* are cartilaginous and the species lacks prepollex. *Synapturanus mirandariberoi* and *S. latebrosus* **sp. nov.** have large and distinct ulnare and radiale, fused carpals 2, 3, and 4, carpal 1, distinct centrale 1 and 2, and prepollex, whereas *S. rabus* has two blocks of fused elements, one consisting of ulnare, carpals 1–4, and another consisting of fused radiale, centrale 1 and 2, prepollex, and metacarpal 1. Hindlimbs in *Synapturanus* consist, proximal to distally, of: femur, tibio-fibulae, elongated tibiale and fibulare, and a phalangeal formula 2-2-3-4-3, terminal phalanges triangular and pointed (Figs. 10, 12–14). The tibiale and fibulare are fused into a single element in *S. rabus* and *S. latebrosus* (Figs. 14 and 10, respectively). Tarsal elements in *S. salseri* are cartilaginous; in *S. mirandariberoi*, *S. rabus*, and *S. latebrosus* **sp. nov.** the prehallux, centrale, and intermedium are visible.

We include the protuberant wrist gland found in males of *Synapturanus* in the category of a multicellular "breeding glands" of anurans. These are sexually dimorphic glands, found in specific areas of the body, and likely derived from mucous gland (Noble 1929); histochemicaly they are not mucus glands but their secretion stained more similar to mucus than to granular glands (Holloway and Dapson 1971). Their function is releasing compounds that function as attractants, calming, or receptive during amplexus (Sever, 1989). Furthermore, in some genera the glands also function to "glue" the amplected pair. Gluing seems more prevalent in species with notable size difference between males and females and in fossorial species with underground nesting, but it has also evolved in aquatic species (Visser *et al.*. 1982). Overall, gluing during amplexus has evolved independently in several anuran lineages. We have found no reports or evidence of "gluing" during amplexus in *Synapturanus*.

The wrist gland in breeding males of *Synapturanus* is a synapomorphy for the genus. The coloration of this gland was described as gray-brown, similar to the rest of the arm in *S. rabus*, whereas in *S. salseri* and *S. mirandariberoi* the pale wrist gland contrast with the darker coloration of the rest of the arm (Pyburn, 1976). We cannot discard that the described scattered dots of these glands could correspond to the external opening of the glandular ducts. The surface of these gland in *Synapturanus* is always smooth, i.e. lacking spines, protuberances, or serrations.

Currently, there is no information on the hormonal function or histological structure of wrist glands in *Synapturanus* and there is no report or evidence of gluing in the genus. Breeding gland were reported for a few other microhylids. Pectoral breeding glands were reported for *Gastrophryne carolinenis* and *G. olivacea* where they function to "glue" the male to the dorsum of the female during amplexus; they were also reported in the Southeast Asian *Kaloula picta* (Conaway and Metter, 1967; Metter and Conoway, 1969; Inger 1954). The secretions of these glands stained very differently; but histochemical they are more similar to mucus than to granular glands (Holloway and Dapson 1971).

The forearm gland is present in males larger than 18.1 mm SVL in *S. latebrosus* **sp. nov.**, larger than 14.0 mm SVL in *S. sacratus* **sp. nov.**, and larger than 15.1 mm SVL in *S. artifex*; we consider those specimens as adult and reproductively active males. Males in the type series of *S. rabus* (Pyburn, 1976), and the male we collected near their type locality, exhibited the wrist gland. The photograph of a paratype of *S. salseri* (Pyburn 1975) also shows the wrist gland. Males of *S. salseri* collected close to the species type locality had this gland. We do not have specimens collected throughout the year for any of the species to relate the presence of the gland to a particular time. The wrist gland seems to be a permanent secondary character once the individual reaches sexual maturity. If the wrist gland is functional throughout the year, then the species may not have a specific "breeding season". A continuous reproductive strategy may be favored by the stable humidity below the leaflitter and within the forest's mat of rootlets.

Overall, due its fossorial and leaf litter habits, little is known about the life history and reproductive biology of *Synapturanus*. Pyburn (1976) assumed that *S. rabus* females move around on the leaf litter searching for males and that males called from underneath the layer of rootlets; our field observations cannot corroborate Pyburn's comment. At least one female of the type series (holotype and paratopotypes) of *S. latebrosus* **sp. nov.** was collected at night, below the compact "mat" of small and interweaved rootlets that characterizes the forest floor at the type locality. From the paratypes, one female and two males were collected below the leaf litter; one additional female was collected while moving above the leaf litter and three females were found inside rotten trunks. The type series of *S. sacratus* **sp. nov.**, both males and females, were collected while mingling in the leaf litter in the afternoon. The single female and three males of *S. artifex* **sp. nov.** were collected within the deep "mat" of rootlets that characterized the floor of the rainforest in the area. It is likely that the three new species are active in the afternoon and at night; both *S. artifex* **sp. nov.** and *S. latebrosus* **sp. nov.** were heard calling at those times. The advertisement calls of *Synapturanus salseri*, *S. rabus*, *S. mirandariberoi*, *S. zombie*, *S. mesomorphus*, and *S. ajuricaba* have been previously reported (Pyburn, 1975, 1976, Zimmerman and Bogart, 1984, Menin *et al.*. 2007, Fouquet *et al.*. 2021b). Unfortunately, we do not have recordings of two of the three new species here described.

Currently, there is no available information on the reproductive biology for any of the three new species described here or on those described for the Eastern Guiana Shield (Fouquet *et al.* 2021b), beyond the data previously reported for *S. salseri*, *S. mirandariberoi* and *S. rabus* (Carvalho, 1954, Pyburn, 1975, Pyburn 1976; Menin *et al..*, 2007; Hero 1990, McDiarmid and Altig 1999). *Synapturanus* was presumably listed as a direct developer by Duellman and Trueb (1986, 1994), and Hero (1990). The reported reproductive data suggest that amplexus and oviposition take place below the rootlet mantle. We did not find postures of any of the new species; however, finding the specimens under the rootlet mantle and the soil suggests that the postures could be laid at this interface. In *S. latebrosus* **sp. nov.**, as we rolled up the rootlets mat the specimens were exposed, but we found no holes from which they could emerge. Recently, it was suggested that the species of western clade would have epigean habits (Fouquet *et al.*. 2021a, b) and that they forage among the leaf litter given the less robust conformation of their humerus and the fusion between tibiale and fibulare, among other features. The depth between the rootlet layer in which we found many specimens of *S. latebrosus* **sp. nov.** and all those of *S. artifex.* **sp. nov.** do not corroborate epigean habits but they probably do not dig holes for egg deposition, as Pyburn (1976) would suggest when he describes finding the egg clutches of *S. rabus* below the ground surface, about 10 cm deep.

Synapturanus rabus females were reported to have two large-yolked eggs and a clutch had two capsulated embryos that were accompanied by an adult (Pyburn, 1976). Egg clutches of the "S. rabus species complex" may all consist of two eggs and clutch size is likely limited by overall body size.

Finally, the habitat conditions of the three species described here are quite different; *S. sacratus* **sp. nov.** and *S. artifex* **sp. nov.** are found in well-conserved forests, the former in a state protected area and the latter in an indigenous territory. On the other hand, *Synapturanus latebrosus* **sp. nov.** inhabits forested areas in the Department of Caquetá, unfortunately extensive areas of forest have been cleared to generate pastures for livestock. In 2018, according to the Sistema de Información Ambiental Territorial de la Amazonia Colombiana-SIAT-AC, the four

municipalities where this species have been reported have, in average, a forest cover of 26% versus 56% of pasture cover. *Synapturanus latebrosus* **sp. nov.** seems to be exclusively restricted to remaining small forest fragments which are still vulnerable to deforestation and severe climatic change impacts, for these reasons the evaluation of its conservation status is urgently needed.

## Acknowledgements

The authors thank to Julián Rojas and Fabián Cabrera whose participation was supported by the project Convenio 060 de 2013 Gobernación del Caquetá-Instituto Sinchi Fondo de CTeI del SGR, to its coordinator, Carlos Hernando Rodríguez; to Yunner Fabian González, Diego Huseth Ruiz, and Hernándo Trujillo for their valuable field work; to Asociación de Cabildos y Autoridades Tradicionales de la Chorrera—AZICATCH, the Okaina indigenous cabildo, its authorities, and to all the participants of the 2019 inventory for their hospitality, interest and support. We thank Parques Nacionales Naturales de Colombia and to the Indigenous Authorities of Yaigojé Apaporis, for inviting ICN-UN to carry out the biological characterization for the declaration of the Yaigojé Apaporis National Natural Park, to Jorge Kayuanari from the Jirijirimo community for his support in the field and to Julio Betancur for his help with the photos of *S. sacratus* **sp. nov.** We are thankful with our peers from SINCHI Institute, Sonia Sua, Natalia Castillo, Felipe Parra for their support with maps and data, and all our colleagues of the fauna group for their invaluable support during the field work. We are grateful to the SINCHI Institute for its financial support for inventory work and continuous commitment to document Colombian biodiversity. Rafael O. de Sá and João F. R. Tonini are supported by NSF award DEB-1949749.

#### References

- Boulenger, G.A. (1900) Batrachians. *In*: Lankester, E.R., Report on a collection made by Messrs. F. V. McConnell and J. J. Quelch at Mount Roraima in British Guiana. *Transactions of the Linnean Society of London*, Series 2, Zoology, 8, pp. 55–56.
  - https://doi.org/10.1111/j.1096-3642.1900.tb00312.x
- Callery, E.M., Fang, H. & Ellison, R.P. (2001) Frogs without polliwogs: evolution of anuran direct development. *Bioessays*, 23, 233–241.
  - https://doi.org/10.1002/1521-1878(200103)23:3%3C233::AID-BIES1033%3E3.0.CO;2-Q
- Carvalho A.L. (1954) A Preliminary Synopsis of the Genera of American Microhylid Frogs. *Occasional Papers of the Museum of Zoology University of Michigan*, 555, 1–21.
- Chávez, G., Thompson, M.E., Sánchez, D.A., Chávez-Arribasplata, J.C. & Catenazzi, A. (2022) A needle in a haystack: Integrative taxonomy reveals the existence of a new small species of fossorial frog (Anura, Microhylidae, *Synapturanus*) from the vast lower Putumayo basin, Peru. *Evolutionary Systematics*, 6 (1), 9–20. https://doi.org/10.3897/evolsyst.6.80281
- Conaway, C.H. & Metter, D.E. (1967) Skin glands associated with breeding in Microhyla carolinensis. *Copeia*, 1967, 672–673.
  - https://doi.org/10.2307/1442250
- de Sá, R.O., Streicher, J.W., Sekonyela, R., Forlani, M.C., Loader, S.P., Greenbaum, E., Richards, S. & Haddad, C.F.B. (2012) Molecular phylogeny of microhylid frogs (Anura: Microhylidae) with emphasis on relationships among New World genera. *BMC Evolutionary Biology*, 12 (241), 1–40. https://doi.org/10.1186/1471-2148-12-241
- de Sá, R.O., Riva Tonini, J.F., van Huss, H., Long, A., Cuddy, T., Forlani, M.C., Peloso, P.L.V., Zaher, H. & Haddad, C.F.B. (2019) Multiple connections between Amazonia and Atlantic Forest shaped phylogenetic and morphological diversity in the genus *Chiasmocleis* Mehely, 1904 (Anura: Microhylidae: Gastrophryne). *Molecular Phylogenetic and Evolution*, 130, 198–210.
  - https://doi.org/10.1016/j.ympev.2018.10.021
- de Sá, R.O. & Trueb, L. (1991) Osteology, skeletal development, and chondrocranial structure of *Hamptophryne boliviana* (Anura: Microhylidae). *Journal of Morphology*, 209, 311–330. https://doi.org/10.1002/jmor.1052090307
- del Pino, E.M. & Elinson, R.P. (2004) The organizer in amphibians with large eggs: Problems and Perspectives. *In*: Grunz, H. (Ed.), *The Vertebrate Organizer*. Springer–Verlag, Berlin and Heidelberg, pp. 359–374. https://doi.org/10.1007/978-3-662-10416-3 21
- Dingerkus, G. & Uhler, L.D. (1977) Enzyme clearing of Alcian blue stained whole small vertebrates for demonstration of car-

- tilage. Stain Technology, 52, 229–232.
- https://doi.org/10.3109/10520297709116780
- Duellman, W.E. & Trueb, L. (1994) *Biology of Amphibians*. 2<sup>nd</sup> Edition. Johns Hopkins University Press, Baltimore, Maryland, pp.
- Edgar, R.C. (2004) MUSCLE: multiple sequence alignment with high accuracy and high throughput. *Nucleic Acids Research*, 32 (5), 1792–1797.
  - https://doi.org/10.1093/nar/gkh340
- Elinson, R.P. & del Pino, E.M. (2012) Developmental biology of amphibians. *Wiley Interdisciplinary Reviews Developmental Biology*, 1 (3), 345–369.
  - https://doi.org/10.1002/wdev.23
- Feng, Y.-J., Blackburn, D.C.M, Liang, D., Hillis, D.M., Wake, D.B., Cannatella, D.C. & Zhang, P. (2017) Phylogenomics reveals rapid simultaneous diversification of three major clades of Gondwanan frogs at the Cretaceous-Paleogene boundary. *Proceedings of the National Academy of Sciences, USA*, 114, E5864–5870. https://doi.org/10.1073/pnas.1704632114
- Frost, D.R. (2021) Amphibian Species of the World: An Online Reference. Version 6.1. American Museum of Natural History, New York. Electronic Database accessible. Available from: https://amphibiansoftheworld.amnh.org/index.php (accessed 1 August 2021) https://doi.org/10.5531/db.vz.0001
- Frost, D.R., Grant, T., Faivovich, J., Bain, R.H., Haas, A., Haddad, C.F.B., de Sá, R.O., Channing, A., Wilkinson, M., Donnellan, S.C., Raxworthy, C.J., Campbell, J.A., Blotto, B.L., Moler, P.E., Drewes, R.C., Nussbaum, R.A., Lynch, J.D., Green, D.M. & Wheeler, W.C. (2006) The amphibian tree of life. *Bulletin of the American Museum of Natural History*, 297, 1–370. https://doi.org/10.1206/0003-0090(2006)297[0001:TATOL]2.0.CO;2
- Gosner, K.L. (1960) A simplified table for staging anuran embryos and larvae wit notes on identification. *Herpetologica*, 16, 183–190.
- Griffiths, I. (1954) On the otic element in Amphibia, Salientia. *Proceedings of the Zoological Society of London*, 124, 35–50. https://doi.org/10.1111/j.1096-3642.1954.tb01476.x
- Guindon, S., Dufayard, J.-F., Lefort, V., Anisimova, M., Hordijk, W. & Gascuel, O. (2010). New algorithms and methods to estimate maximum-likelihood phylogenies: Assessing the performance of phyml 3.0. *Systematic Biology*, 59 (3), 307–321. https://doi.org/10.1093/sysbio/syq010
- Haddad, C.F.B. & Prado, C.A.P. (2005) Reproductive modes in frogs and their unexpected diversity in the Atlantic Forest of Brazil. *BioScience*, 55 (3), 207–217. https://doi.org/10.1641/0006-3568(2005)055[0207:RMIFAT]2.0.CO;2
- Hammer, Ø., Harper, D.A.T. & Ryan, P.D. (2001) Past: Paleontological Statistics software package for education and data analy-
- sis. *Palaeontologia Electronica*, 4 (1), 1–9. Hanken, J. (1993) Model systems versus outgroups: alternative approaches to the study of head development and evolution.
  - *American Zoologist*, 33, 448–456. https://doi.org/10.1093/icb/33.4.448
- Hero, J.M. (1990) An illustrated key to tadpoles occurring in the Central Amazon rainforest, Manaus, Amazonas, Brasil. *Amazoniana*, 11 (2), 201–262.
- Hime, P.M., Lemmon, A.R. Lemmon, E.C., Prendini, E., Brown, J.M., Thomson, R.C., Kratovil, J.D., Noonan, B.P., Pyron, R.A., Peloso, P.L. & Kortyna, M.L. (2021) Phylogenomics reveals ancient gene tree discordance in the amphibian tree of life. *Systematic Biology*, 70 (1), 49–66. https://doi.org/10.1093/sysbio/syaa034
- Hoang, D.T., Chernomor, O., von Haeseler, A., Minh, B.Q. & Vinh, L.S. (2018) Ufboot2: Improving the ultrafast bootstrap approximation. *Molecular Biology and Evolution*, 35 (2), 518–522. https://doi.org/10.1093/molbev/msx281
- Inger, R.F. (1954) Systematics and zoogeography of Philippine Amphibia. *Fieldiana Zoology*, 33 (4), 185–523. https://doi.org/10.5962/bhl.title.5571
- Holloway, W.R. & Dapson, R.W. (1971) Histochemistry of integumentary secretions of the narrow–mouth toad, *Gastrophryne carolinesis*. *Copeia*, 1971, 351–353. https://doi.org/10.2307/1442855
- Kalyaanamoorthy, S., Minh, B.Q., Wong, T.K.F., von Haeseler, A. & Jermiin. L.S. (2017) ModelFinder: fast model selection for accurate phylogenetic estimates. *Nature Methods*, 14, 587–589. https://doi.org/10.1038/nmeth.4285
- Kizirian, D.A. & McDiarmid, R.W. (1998) A new species of *Bachia* (Squamata: Gymnophthalmidae) with plesiomorphic limb morphology. *Herpetologica*, 54 (2), 245–253.
- Lanfear, R., Calcott, B., Ho, S.Y.W. & Guindon, S. (2012) PartitionFinder: combined selection of partitioning schemes and substitution models for phylogenetic analyses. *Molecular Biology and Evolution*, 29 (6), 1695–1701. https://doi.org/10.1093/molbev/mss020
- Liu, K., Warnow, T.J., Holder, M.T., Nelesen, S., Yu, J., Stamatakis, A. & Linder, C.R. (2012) SATe-II: Very fast and accurate simultaneous estimation of multiple sequence alignments and phylogenetic trees. *Systematic Biology*, 61, 90–106.

- https://doi.org/10.1093/sysbio/syr095
- Lynch, J.D. (1971) Evolutionary relationships, osteology and zoogeography of leptodactyloid frogs. *Miscellaneous Publications of the Museum of Natural History, University of Kansas*, 53, 1–238.
- McDiarmid, R.W. & Altig, R. (Eds.) (1999) *Tadpoles: the biology of anuran larvae*. University of Chicago Press, Chicago, Illinois, xiv + 444 pp, figs, tables, index.
- Menin, M., Rodrigues, D.J. & Lima, A.P. (2007) Clutches, tadpoles and advertisement calls of *Synapturanus mirandariberoi* and *S. cf. salseri* in Central Amazonia, Brazil. *Herpetological Journal*, 17, 86–91.
- Metter, D.E. & Conoway, C.H. (1969) The influence of hormones on the development of breeding glands in *Microhyla*. *Copeia*, 3, 621–622.
  - https://doi.org/10.2307/1441944
- Miller, M.A., Pfeiffer W. & Schwartz, T. (2010) Creating the CIPRES Science Gateway for inference of large phylogenetic trees. *In: Gateway Computing Environments Workshop (GCE)*. IEEE, New Orleans, Louisiana, pp. 1–8. https://doi.org/10.1109/GCE.2010.5676129
- Nelson, C.E. & Lescure, J. (1975) The taxonomy and distribution of *Myersiella* and *Synapturanus* (Anura: Microhylidae). *Herpetologica* 31, 389–397.
- Nguyen, L.-T., Schmidt, H.A., von Haeseler, A. & Minh, B.Q. (2015) IQ-TREE: A fast and effective stochastic algorithm for estimating maximum-likelihood phylogenies. *Molecular Biology and Evolution*, 32 (1), 268–274. https://doi.org/10.1093/molbev/msu300
- Noble, G.K. (1929) The relation of courtship to the secondary sexual characters of the two-lined salamander, *Eurycea bislineata* (Green). *American Museum Novitates*, 362, 1–5.
- Paluh, D.J., Stanley, E.L. & Blackburn, D.C. (2020) Evolution of hyperossification expands skull diversity in frogs. *Proceedings of the National Academy of Sciences* 117 (15), 8554–8562. https://doi.org/10.1073/pnas.2000872117
- Parker, H.W. (1934) A Monograph of the Frogs of the Family Microhylidae. *Trustees of the British Museum, London*, 8, 1–208
- Pugener, L.A. & Maglia, A.M. (2007) Skeletal morphology and development of the olfactory region of *Spea* (Anura: Scaphiopodidae). *Journal of Anatomy*, 211, 754–768. https://doi.org/10.1111/j.1469-7580.2007.00826.x
- Pyburn, W.F. (1975) A new species of microhylid frog of the genus *Synapturanus* from southeastern Colombia. *Herpetologica*, 31, 439–443.
- Pyburn, W.F. (1977 "1976") A new fossorial frog from the Colombian rain forest (Anura: Microhylidae). *Herpetologica*, 32, 367–370.
- Pyron, R.A. & Wiens, J.J. (2011) A large-scale phylogeny of Amphibia including over 2800 species, and a revised classification of advanced frogs, salamanders, and caecilians. *Molecular Phylogenetics and Evolution*, 61, 543–583. https://doi.org/10.1016/j.ympev.2011.06.012
- Rambaut ,A. (2014) FigTree. Version 1.4.4. A Graphical Viewer of Phylogenetic Trees. Available from: http://tree.bio.ed.ac.uk/software/figtree/ (accessed 14 March 2023)
- Suchard, M.A., Lemey, P., Baele, G., Ayres, D.L., Drummond, A.J. & Rambaut, A. (2018) *Bayesian phylogenetic and phylodynamic data integration using BEAST 1.10. Virus Evolution*, 4, vey016. https://doi.org/10.1093/ve/vey016.
- Rambaut, A. (2014) FigTree. Version 1.4.4. A Graphical Viewer of Phylogenetic Trees. Available from: http://tree.bio.ed.ac.uk/software/figtree/ (accessed 14 March 2023)
- Ronquist, F., Teslenko, M., Van Der Mark, P., Ayres, D.L., Darling, A., Höhna, S. & Huelsenbeck, J. P. (2012) MrBayes 3.2: efficient Bayesian phylogenetic inference and model choice across a large model space. *Systematic Biology*, 61 (3), 539–542. https://doi.org/10.1093/sysbio/sys029
- Scherz, M.D., Hutter, C.R., Rakotoarison, A., Riemann, J.C., Rödel, M.O., Ndriantsoa, S. H., Glos, J., Roberts, S.H., Crottini, A., Vences, M. & Glaw, F. (2019) Morphological and ecological convergence at the lower size limit for vertebrates highlighted by five new miniaturized microhylid frog species from three different Madagascan genera. *PLoS ONE*, 14 (3), e0213314.
  - https://doi.org/10.1371/journal.pone.0213314.
- Sever, D.M. (1989) Caudal hedonic glands in salamanders of the *Eurycea bislineata* complex (Amphibia: Plethodontidae). *Herpetologica*, 44, 322–329.
- SIAT-AC (2023) Sistema de Información Ambiental Territorial de la Amazonia Colombiana. Available from: https://siatac.co/ (accessed 14 March 2023)
- Starrett, P.H. (1968) *The phylogenetic significance of the jaw musculature in anuran amphibians*. Unpublished doctoral dissertation, University of Michigan, Ann Arbor, Michigan, 179 pp.
- Streicher, J.W., Loader, S.P., Varela-Jaramillo, A., Montoya, P. & de Sá, R.O. (2020) Analysis of ultraconserved elements supports African origins of narrow–mouthed frogs. *Molecular Phylogenetics and Evolution*, 146, 1–8. https://doi.org/10.1016/j.ympev.2020.106771
- Tamura, K., Stecher, G. & Kumar, S. (2021) MEGA 11: Molecular Evolutionary Genetics Analysis Version 11. *Molecular Biology and Evolution*, 38 (7), 3022–3027.

- https://doi.org/10.1093/molbev/msab120
- Tu, N., Yang, M.-H., Liang D. & Zhang, P. (2018) A large-scale phylogeny of Microhylidae inferred from a combined dataset of 121 genes and 427 taxa. *Molecular Phylogenetics and Evolution*, 126, 85–91. https://doi.org/10.1016/j.ympev.2018.03.036
- Trueb, L. (1970) Evolutionary relationships of casque-headed tree frogs with co-ossified skulls. *University of Kansas Publications of the Museum of Natural History*, 18, 547–716. https://doi.org/10.5962/bhl.part.19992
- Trueb, L. (1973) Bones, frogs, and evolution. *In*: Vial, J.L. (Ed.), *Evolutionary Biology of the Anurans: Contemporary Research on Major Problems*. University of Missouri Press, Columbia, Missouri, pp. 65–132.
- Trueb, L. (1977) Osteology and Anuran Systematics: Intrapopulational Variation in *Hyla lanciformis*. *Systematic Zoology*, 26 (2), 165–184.
  - https://doi.org/10.2307/2412839
- Trueb, L., Diaz, R & Blackburn, D. (2011) Osteology and chondrocranial morphology of *Gastrophryne carolinensis* (Anura: Microhylidae), with a review of the osteological diversity of New World microhylids. *Phyllomedusa*, 10 (2), 99–135. https://doi.org/10.11606/issn.2316-9079.v10i2p99-135
- van der Meijden, A., Vences, M., Hoegg, S., Boistel, R., Channing, A. & Meyer, A. (2007) Nuclear gene phylogeny of narrow–mouthed toads (Family Microhylidae) and a discussion of competing hypotheses concerning their biogeographical origins. *Molecular Phylogenetics and Evolution*, 44, 1017–1030. https://doi.org/10.1016/j.ympev.2007.02.008
- Visser, J., Cei, J.M. & Gutierrez, L.S. (1982) The histology of dermal glands of mating *Breviceps* with comments on their possible functional value in microhylids (Amphibia: Anura). *South African Journal of Zoology*, 17 (1), 24–27. https://doi.org/10.1080/02541858.1982.11447773
- Zimmerman, B.L. & Bogart, J.P. (1984) Vocalizations of primary forest frog species in the central Amazon. *Acta Amazónica*, 14 (3–4),73–519. https://doi.org/10.1590/1809-43921984143519

## APPENDIX 1. Additional examined specimens.

- Synapturanus rabus. COLOMBIA: Vaupés: area "no municipalizada" Yavaraté, comunidad Yavaraté (SINCHI-A 5911), about 50Km from the type locality of *S. rabus*; (AMNH-A 92968) near the village of Yapima (paratype); los Angeles (UTA A-3975, UTA A-39758).
- Synapturanus salseri. COLOMBIA: Vaupés: area "no municipalizada" Yavaraté, Timbó (IAvH-Am (IND-AN) 3398), (UTA A-4510, A-4513, A-4463), comunidad Matapí (SINCHI-A 5712, 5713, 5714, 5734, 5735, 5736), comunidad Yavaraté (SINCHI-A 5888, 5902, 5903, 5904, 5905, 5906, 5907).
- Synapturanus mirandariberoi. GUYANA: (AMNH-A 01293, 10399, 18987, 46265, 46386, 136017), Mazaruni-Potaro: (AMNH-A 71009, 71010, 71011, 71012, 71013, 13526), Rupununi: (AMNH-A 90936 clear and stained, 90837,90945, 90946, 90947, 92020, 92021).

**APPENDIX 2**. Morphometric measurements (in mm) of specimens of *Synapturanus latebrosus* **sp. nov.**, *S. artifex* **sp. nov.**, *S. sacratus* **sp. nov.**, *S. rabus*, and *S. salseri* 

| SPECIES                       | ACRONYM       | SEX | SVL   | HL   | HW   | IO   | END  | ED   | TBL   | SOURCE       |
|-------------------------------|---------------|-----|-------|------|------|------|------|------|-------|--------------|
| S. rabus                      | SINCHI-A 5911 | 3   | 16.35 | 4.65 | 4.20 | 1.90 | 1.30 | 1.50 | 7.15  | This study   |
| S. rabus Holotype             | USNM-199674   | 9   | 17.20 | 5.10 | 4.70 |      | 1.50 | 1.10 | 7.20  | Pyburn, 1976 |
| S. artifex sp. nov            | SINCHI-A 6633 | 3   | 15.60 | 4.10 | 4.10 | 2.20 | 1.60 | 0.90 | 6.70  | This study   |
| S. artifex sp. nov            | SINCHI-A 6631 | 3   | 15.15 | 4.20 | 4.10 | 2.25 | 1.35 | 1.10 | 6.50  | This study   |
| S. artifex sp. nov            | SINCHI-A 6632 | 8   | 15.50 | 4.15 | 4.10 | 2.15 | 1.45 | 1.15 | 6.70  | This study   |
| S. artifex sp. nov            | SINCHI-A 6518 | 3   | 15.85 | 4.10 | 4.30 | 2.00 | 1.35 | 1.00 | 6.50  | This study   |
| S. artifex sp. nov            | SINCHI-A 7110 | 3   | 15.45 | 4.35 | 4.85 | 1.90 | 1.40 | 1.10 | 6.70  | This study   |
| S. artifex sp. nov            | SINCHI-A 8134 | 3   | 15.60 | 4.50 | 4.75 | 1.75 | 1.40 | 1.50 | 6.65  | This study   |
| S. artifex sp. nov            | SINCHI-A 8207 | 3   | 15.60 | 4.00 | 4.80 | 1.90 | 1.50 | 1.00 | 6.55  | This study   |
| S. artifex sp. nov            | SINCHI-A 8210 | 3   | 15.85 | 4.20 | 4.90 | 1.60 | 1.40 | 1.30 | 6.75  | This study   |
| S. artifex sp. nov            | SINCH-A 8213  | 3   | 15.60 | 4.20 | 5.10 | 1.60 | 1.40 | 1.10 | 6.40  | This study   |
| S. artifex sp. nov            | SINCHI-A 6469 | 9   | 17.60 | 5.10 | 4.50 | 2.30 | 1.60 | 1.15 | 7.15  | This study   |
| S. artifex sp. nov            | SINCHI-A 7111 | 9   | 17.00 | 4.15 | 4.90 | 1.70 | 1.50 | 1.30 | 7.05  | This study   |
| S. artifex sp. nov            | SINCHI-A7109  | \$  | 17.20 | 4.80 | 4.95 | 1.95 | 1.65 | 1.40 | 7.10  | This study   |
| S. latebrosus <b>sp. nov.</b> | SINCHI-A 5642 | 9   | 20.00 | 5.80 | 5.00 | 2.40 | 2.00 | 1.15 | 7.55  | This study   |
| S. latebrosus sp. nov.        | SINCHI-A 5643 | 9   | 21.45 | 5.40 | 5.45 | 2.60 | 2.10 | 1.00 | 8.05  | This study   |
| S. latebrosus <b>sp. nov.</b> | SINCHI-A 2703 | 9   | 20.25 | 5.40 | 5.25 | 2.20 | 2.00 | 1.15 | 7.55  | This study   |
| S. latebrosus sp. nov.        | SINCHI-A 2678 | 9   | 20.05 | 5.15 | 5.4  | 2.35 | 1.90 | 1.10 | 8.35  | This study   |
| S. latebrosus <b>sp. nov.</b> | SINCHI-A 5671 | 9   | 20.85 | 4.80 | 4.95 | 2.40 | 1.85 | 1.10 | 7.30  | This study   |
| S. latebrosus sp. nov.        | SINCHI-A 839  | 9   | 21.50 | 5.55 | 5.90 | 2.50 | 2.00 | 1.00 | 8.30  | This study   |
| S. latebrosus <b>sp. nov.</b> | SINCHI-A 841  | 9   | 20.85 | 5.50 | 5.50 | 2.70 | 2.10 | 1.00 | 7.45  | This study   |
| S. latebrosus <b>sp. nov.</b> | SINCHI-A 840  | 9   | 22.00 | 5.45 | 5.90 | 2.60 | 2.20 | 1.10 | 8.40  | This study   |
| S. latebrosus sp. nov.        | SINCHI-A 843  | 3   | 18.10 | 4.55 | 5.15 | 2.50 | 1.95 | 1.25 | 7.20  | This study   |
| S. latebrosus <b>sp. nov.</b> | SINCHI-A 844  | 8   | 19.00 | 4.70 | 4.85 | 2.30 | 1.95 | 1.15 | 6.35  | This study   |
| S. latebrosus <b>sp. nov.</b> | SINCHI-A 845  | 8   | 19.00 | 5.15 | 5.40 | 2.10 | 1.95 | 0.95 | 6.95  | This study   |
| S. sacratus sp. nov           | ICN 56890     | 9   | 16.60 | 4.45 | 4.30 | 1.90 | 1.60 | 1.10 | 6.85  | This study   |
| S. sacratus sp. nov           | ICN 56889     | \$  | 17.30 | 4.55 | 4.15 | 2.05 | 1.40 | 1.15 | 6.95  | This study   |
| S. sacratus sp. nov           | ICN 56895     | 3   | 15.10 | 4.15 | 3.95 | 1.85 | 1.55 | 1.25 | 6.70  | This study   |
| S. sacratus sp. nov           | ICN 56892     | 8   | 14.00 | 3.90 | 4.20 | 1.90 | 1.50 | 1.50 | 6.00  | This study   |
| S. salseri Holotype           | UTA A-4011    | 8   | 27.60 | 7.00 | 7.10 |      | 2.10 | 1.40 | 11.10 | Pyburn, 1975 |
| S. salseri                    | SINCHI-A 5904 | 8   | 25.95 | 5.85 | 6.40 | 3.20 | 2.20 | 1.50 | 10.60 | This study   |
| S. salseri                    | SINCHI-A 5906 | 3   | 25.15 | 6.00 | 6.95 | 2.90 | 2.15 | 1.20 | 11.50 | This study   |
| S. salseri                    | SINCHI-A 5888 | 8   | 25.85 | 6.45 | 6.00 | 2.80 | 2.45 | 1.15 | 10.65 | This study   |
| S. salseri                    | SINCHI-A 5903 | 3   | 24.85 | 6.50 | 6.15 | 3.00 | 2.00 | 1.45 | 10.30 | This study   |
| S. salseri                    | SINCHI-A 5902 | 3   | 25.30 | 6.55 | 6.75 | 2.90 | 2.10 | 1.30 | 10.35 | This study   |
| S. salseri                    | SINCHI-A 5907 | 3   | 23.60 | 6.80 | 6.90 | 3.00 | 2.20 | 1.10 | 10.15 | This study   |
| S. salseri                    | SINCHI-A 5905 | 3   | 23.75 | 6.20 | 6.20 | 2.60 | 2.25 | 1.10 | 10.30 | This study   |
| S. salseri                    | SINCHI-A 5735 | 3   | 22.65 | 6.50 | 6.05 | 2.90 | 2.10 | 1.35 | 9.30  | This study   |
| S. salseri                    | SINCHI-A 5734 | 3   | 24.10 | 6.15 | 6.00 | 2.95 | 2.00 | 1.40 | 9.80  | This study   |
| S. salseri                    | SINCHI-A 5736 | 3   | 23.90 | 5.90 | 5.95 | 2.65 | 1.95 | 1.10 | 9.40  | This study   |
| S. salseri                    | SINCHI-A 5714 | 3   | 23.70 | 5.70 | 6.30 | 2.55 | 2.10 | 1.40 | 9.15  | This study   |
| S. salseri                    | SINCHI-A 5713 | 3   | 23.40 | 5.85 | 5.85 | 2.65 | 2.00 | 1.20 | 9.95  | This study   |
| S. salseri                    | SINCHI-A 5712 | 3   | 24.80 | 6.35 | 5.80 | 2.95 | 2.20 | 1.45 | 10.50 | This study   |

| Specimen<br>voucher | Field number | Genus        | Species     | Locality                 | Country   | Latitude  | Longitude  | Accession Number     | Source  |
|---------------------|--------------|--------------|-------------|--------------------------|-----------|-----------|------------|----------------------|---------|
| MZUSP159209         | MTR40087     | Adelastes    | hylonomos   | Maturaka, AM             | Brazil    | 0.625169  | -66.117435 | MW305220.1:1069-2645 | GenBank |
| MZUSP154210         | MTR40120     | Adelastes    | hylonomos   | Maturaka, AM             | Brazil    | 0.625169  | -66.117435 | MW222085.1           | GenBank |
| ROM39677            |              | Otophryne    | steyermarki | Mt. Ayanganna            | Guyana    | 5.399508  | -59.950554 | KC180078.1           | GenBank |
| ROM42961            | PT-461       | Otophryne    | steyermarki | Mt. Wokomung             | Guyana    | 5.117497  | -59.822474 | KM509172.1           | GenBank |
| PK3778              | PK3778       | Otophryne    | steyermarki | Chimanta-Tepui           | Guyana    | 5.320278  | -62.202500 | MW305226.1:1131-2723 | GenBank |
| PK1997              | PK1997       | Otophryne    | steyermarki | Maringma-Tepui           | Guyana    | 5.206667  | -60.591667 | MW305225.1:1134-2714 | GenBank |
| ROM 39679           |              | Otophryne    | robusta     | Mt. Ayanganna            | Guyana    |           |            | KC180034             | GenBank |
| ROM 42963           | PT-459       | Otophryne    | robusta     | Mt. Wokomung             | Guyana    | 5.117497  | -59.822474 | KM509171             | GenBank |
| PK 2237             | PK 2237      | Otophryne    | robusta     | La Escalera,<br>Bolivar  | Venezuela | 5.915556  | -61.433056 | MW305221.1:1135-2713 | GenBank |
| MZUSP 159215        | MTR36115     | Synapturanus | Içá 1       | Comunidade<br>Cuiau, AM  | Brazil    | -2.883871 | -68.366997 | MW305233.1:1135-2681 | GenBank |
| MZUSP 159216        | MTR36356     | Synapturanus | Içá 1       | Comunidade<br>Cuiau, AM  | Brazil    | -2.883871 | -68.366997 | MW222082.1           | GenBank |
| MZUSP 159217        | MTR36176     | Synapturanus | Içá 1       | Comunidade<br>Cuiau, AM  | Brazil    | -2.883871 | -68.366997 | MW222081.1           | GenBank |
| MCP 13774           | SCF1838      | Synapturanus | Juami       | ESEC Juami-<br>Japur, AM | Brazil    | -1.75834  | -67.61532  | MW222075.1           | GenBank |
| MCP 13775           | SCF 1836     | Synapturanus | Juami       | ESEC Juami-<br>Japur, AM | Brazil    | -1.75834  | -67.6126   | MW222073.1           | GenBank |
| MCP 13776           | SCF 1837     | Synapturanus | Juami       | ESEC Juami-<br>Japur, AM | Brazil    | -1.75834  | -67.6126   | MW222074.1           | GenBank |
| MCP 13777           | SCF 1835     | Synapturanus | Juami       | ESEC Juami-<br>Japur, AM | Brazil    | -1.75834  | -67.6126   | MW222072.1           | GenBank |
| MZUNAP01-834        |              | Synapturanus | Nanay       |                          | Peru      | -3.204567 | -74.712067 | MW222086.1           | GenBank |

.....continued on the next page

| APPENDIX 3. (Continued) | ontinued)    |              |             |                                |          |           |             |                  |            |
|-------------------------|--------------|--------------|-------------|--------------------------------|----------|-----------|-------------|------------------|------------|
| Specimen voucher        | Field number | Genus        | Species     | Locality                       | Country  | Latitude  | Longitude   | Accession Number | Source     |
|                         | MW 1004      | Synapturanus | mesomorphus | Iwokrama                       | Guyana   | 4.6713889 | -58.685     | KC180029         | GenBank    |
| MNCN 51182              |              | Synapturanus | mesomorphus | Kaieteur National<br>Park      | Guyana   |           |             | OM291532         | This study |
|                         | FB 2007      | Synapturanus | mesomorphus |                                | Guyana   |           |             | EF017962         | GenBank    |
| SMNS12078               | RE-MABM0102  | Synapturanus | mesomorphus | Mabura hill forest<br>reserve  | Guyana   | 5.1552778 | -58.6997222 | KC180018         | GenBank    |
| SINCHI-A 5713           | MOM 6885     | Synapturanus | salseri     | Vaupés, Matap                  | Colombia | 1.075594  | -69.3628    | OP481225         | This study |
| SINCHI-A 5714           | MOM 6886     | Synapturanus | salseri     | Vaupés, Matap                  | Colombia | 1.075594  | -69.3628    | OP481218         | This study |
| SINCHI-A 5734           | MOM 6910     | Synapturanus | salseri     | Vaupés, Matap                  | Colombia | 1.076667  | -69.3629    | OP481226         | This study |
| SINCHI-A 5735           | MOM 6911     | Synapturanus | salseri     | Vaupés, Matap                  | Colombia | 1.076667  | -69.3629    | OP481224         | This study |
| SINCHI-A 5889           | MOM 7500     | Synapturanus | salseri     | Vaupés, Yavarat                | Colombia | 0.618056  | -69.2147    | OP481223         | This study |
| SINCHI-A 5888           | MOM 7502     | Synapturanus | salseri     | Vaupés, Yavarat                | Colombia | 0.618056  | -69.2147    | OP481222         | This study |
| SINCHI-A 5903           | MOM 7503     | Synapturanus | salseri     | Vaupés, Yavarat                | Colombia | 0.619833  | -69.2173    | OP481216         | This study |
| SINCHI-A 5904           | MOM 7504     | Synapturanus | salseri     | Vaupés, Yavarat                | Colombia | 0.619833  | -69.2173    | OP481219         | This study |
| SINCHI-A 5712           | MOM 6884     | Synapturanus | salseri     | Vaupés, Matap                  | Colombia | 1.075594  | -69.3628    | OP481217         | This study |
| SINCHI-A 5905           | MOM 7505     | Synapturanus | salseri     | Vaupés, Yavarat                | Colombia | 0.619833  | -69.2173    | OP481221         | This study |
| SINCHI-A 5907           | MOM 7506     | Synapturanus | salseri     | Vaupés, Yavarat                | Colombia | 0.619833  | -69.2173    | OP481220         | This study |
| SINCHI-A 5642           | JARM 220     | Synapturanus | latebrosus  | Caquet, vereda<br>Alto Caldas  | Colombia | 1.6601806 | -75.63138   | OM291533         | This study |
| SINCHI-A 5671           | JARM 254     | Synapturanus | latebrosus  | Caquet, vereda la<br>Primavera | Colombia | 1.6513528 | -75.617969  | OM291534         | This study |
| SINCHI-A 2678           | JARM 139     | Synapturanus | latebrosus  | Caquet, vereda<br>Sina         | Colombia | 1.4000278 | -75.731194  | OM291535         | This study |
|                         |              |              |             |                                |          |           |             |                  |            |

| APPENDIX 3. (Continued) | ontinued)       |              |            |  |           |            |            |                      |            |
|-------------------------|-----------------|--------------|------------|--|-----------|------------|------------|----------------------|------------|
| Specimen<br>voucher     | Field number    | Genus        | Species    | Locality   | Country   | Latitude   | Longitude  | Accession Number     | Source     |
| SINCHI-A 5643           | JARM 221        | Synapturanus | latebrosus | Caquet, vereda<br>Alto Caldas                                | Colombia  | 1.6601806  | -75.63138  | OM291536             | This study |
| QCAZ 59998              | PSO-C 3662      | Synapturanus | Colombia   | Río Indiyaco   | Colombia  | 1.177183   | -76.184689 | MW305236.1:1198-2746 | GenBank    |
| ICN 56893               | JDL 28935       | Synapturanus | sacratus   | Amazonas,<br>Jirijirimo                                      | Colombia  | -0.0416667 | -70.95     | OM291537             | This study |
| ICN 56889               | JDL 28951       | Synapturanus | sacratus   | Amazonas,<br>Jirijirimo                                      | Colombia  | -0.0416667 | -70.95     | OM291538             | This study |
| ICN 56894               | JDL 28933       | Synapturanus | sacratus   | Amazonas,<br>Jirijirimo                                      | Colombia  | -0.0416667 | -70.95     | OM291539             | This study |
| SINCHI-A 5911           | MOM 7501        | Synapturanus | rabus      | Vaupés, Yavarat  | Colombia  | 0.615972   | -69.2165   | OM274078             | This study |
| MHNLS19900              | AJC 2952-PT-214 | Synapturanus | Venezuela  | Río Cuao   | Venezuela | 5.044138   | -67.560952 | MW222055.1           | GenBank    |
| MHNL19901               | AJC 2953/PT-215 | Synapturanus | Venezuela  | Río Cuao   | Venezuela | 5.044138   | -67.560952 | MW305230.1:1124-2667 | GenBank    |
| MHNLS 19948             | AJC 3002        | Synapturanus | Venezuela  | Río Cuao   | Venzuela  | 5.044138   | -67.560952 | MW222059.1           | GenBank    |
| MHNLS 19949             | AJC 3003        | Synapturanus | Venezuela  | Río Cuao   | Venezuela | 5.044138   | -67.560952 | MW222060.1           | GenBank    |
| MHNL 20087              | AJC 3151        | Synapturanus | Venezuela  | Río Cuao   | Venezuela | 5.044138   | -67.560952 | MW222064.1           | GenBank    |
| MNCN 47881              |                 | Synapturanus | salseri    | Amazonas,<br>Tobogãn de la<br>Selva, Atures                  | Venezuela |            |            | OP481227             | This study |
| MNCN 47739              |                 | Synapturanus | salseri    | Amazonas,<br>entre rio Cuao y<br>Tobogãn del Cuao,<br>Autuna | Venezuela |            |            | OP481229             | This study |
| MNCN 47764              |                 | Synapturanus | salseri    | Amazonas,<br>entre rio Cuao y<br>Tobogãn del Cuao,<br>Autuna | Venezuela |            |            | OP481228             | This study |
|                         |                 |              |            |  |           |            |            |                      | ,          |

.....continued on the next page

| APPENDIX 3. (Continued) | ontinued)    |              |         |   |           |            |              |                      |            |
|-------------------------|--------------|--------------|---------|---|-----------|------------|--------------|----------------------|------------|
| Specimen voucher        | Field number | Genus        | Species | Locality  | Country   | Latitude   | Longitude    | Accession Number     | Source     |
| MNCN 47693              |              | Synapturanus | salseri | Amazonas, Raudal<br>de Danto, rio<br>Cuao, Autuna | Venezuela |            |              | OP481230             | This study |
| MNCN 47689              |              | Synapturanus | salseri | Amazonas, Raudal<br>de Danto, rio<br>Cuao, Autuna | Venezuela |            |              | OP481232             | This study |
| MNCN 47740              |              | Synapturanus | salseri | Amazonas, Raudal<br>de Danto, rio<br>Cuao, Autuna | Venezuela |            |              | OP481231             | This study |
| QCAZ 64258              | SC 55066     | Synapturanus | Ecuador | Río Yasun   | Ecuador   | -0.917320  | -76.16052    | MW222087.1           | GenBank    |
| QCAZ 64259              | SC55092      | Synapturanus | Ecuador | Río Yasun   | Ecuador   | -0.917320  | -76.16052    | MW305237.1:1141-2695 | GenBank    |
| SINCHI-A 6633           | SNC-H 406    | Synapturanus | artifex | Amazonas,<br>La Chorrera                          | Colombia  | -1.5288056 | -72.677361   | OM368337             | This study |
| SINCHI–A 6631           | SNC-H 404    | Synapturanus | artifex | Amazonas,<br>La Chorrera                          | Colombia  | -1.5288056 | -72.677361   | OM368338             | This study |
| SINCHI–A 6518           | MOM 7479     | Synapturanus | artifex | Amazonas,<br>La Chorrera                          | Colombia  | -1.5288056 | -72.677361   | OM368339             | This study |
| SINCHI–A 6469           | MOM 7430     | Synapturanus | artifex | Amazonas,<br>La Chorrera                          | Colombia  | -1.5288056 | -72.677361   | OM368340             | This study |
| MZUSP 159225            | MTR 35927    | Synapturanus | Içá 2   | Comunidade<br>Cuiau, A                            | Brazil    | -2.88387   | -68.366997   | MW222080.1           | GenBank    |
| MZUSP 159226            | MTR 36366    | Synapturanus | Içá 2   | Comunidade<br>Cuiau, AM                           | Brazil    | -2.88387   | -68.366997   | MW222083.1           | GenBank    |
| CORBIDI 21051           |              | Synapturanus | danta   | Quebrada<br>Federico, Loreto                      | Per       | 0.61805555 | -69.23138889 | OM488910.1           | GenBank    |
| CRBIIAP 1561            | GGU 5292     | Synapturanus | Divisor | Jenaro Herrera                                    | Peru      | -4.900434  | -73.665110   | MW222067.1           | GenBank    |
|                         |              |              |         |   |           |            |              |                      |            |

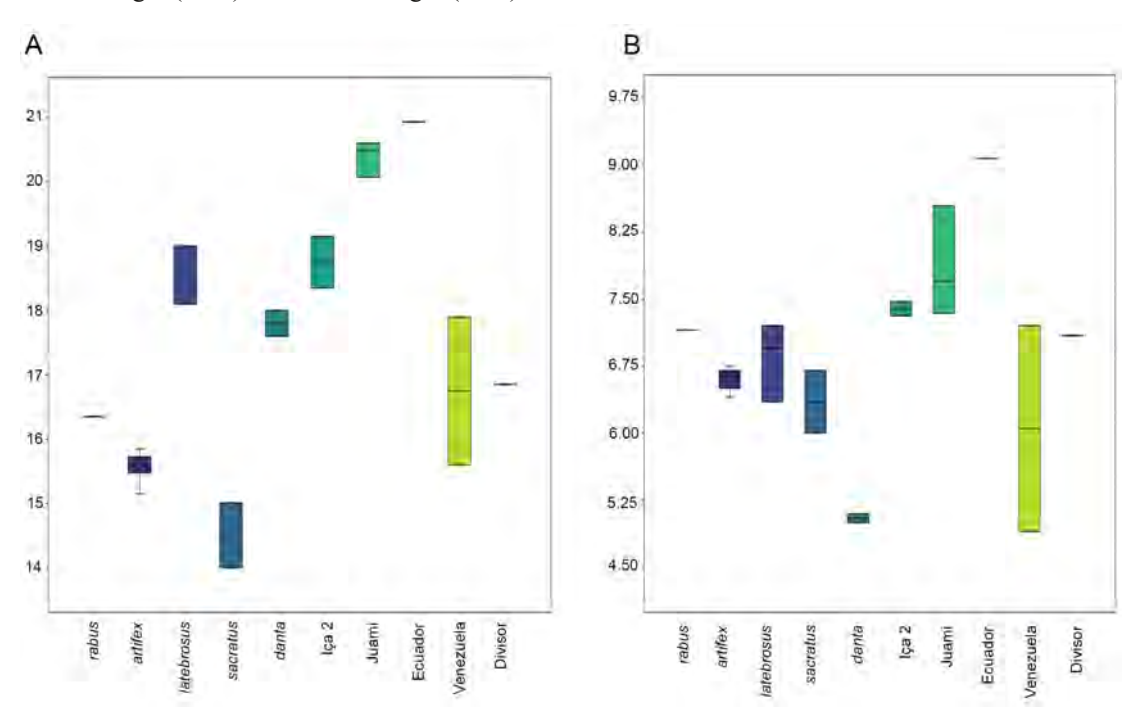
|                       | (2000)          |              |                 |  |          |           |             |                      |         |
|-----------------------|-----------------|--------------|-----------------|--|----------|-----------|-------------|----------------------|---------|
| Specimen voucher      | Field number    | Genus        | Species         | Locality                                       | Country  | Latitude  | Longitude   | Accession Number     | Source  |
| MZUSP 159223          | MTR28042/PT-606 | Synapturanus | Divisor         | Serra do Divisor                               | Brazil   | -7.437811 | -73.657109  | MW305235.1:1123-2668 | GenBank |
| MZUSP 159224          | MTR28524-PT-613 | Synapturanus | Divisor         | Serra do Divisor                               | Brazil   | -7.437811 | -73.657109  | MW222079.1           | GenBank |
| MZUSP 159221          | MTR39811        | Synapturanus | Neblina         | Maturac, AM.                                   | Brazil   | 0.625169  | -66.117435  | MW305234.1:1119-2671 | GenBank |
| MZUSP 159222          | MTR 39989       | Synapturanus | Neblina         | Maturac, AM.                                   | Brazil   | 0.625169  | -66.117435  | MW222084.1           | GenBank |
| SMNS 12078            | RE-MABM0102     | Synapturanus | mesomorphus     | Mabura hill<br>forest reserve                  | Guyana   | 5.1552778 | -58.6997222 | KC180018.1           | GenBank |
|                       | MW 1004         | Synapturanus | mesomorphus     | Iwokrama                                       | Guyana   | 4.671388  | -58.685     | KC180029.1           | GenBank |
| USNM 588793           | BPN3762         | Synapturanus | mesomorphus     | Bay Camp                                       | Guyana   | 5.01155   | -59.64308   | KDQF01002099.1       | GenBank |
| MNCN 51182            |                 | Synapturanus | mesomorphus     | Kinky backdam<br>#2, Kaieteur<br>National Park | Guyana   |           |             | OP806494             | GenBank |
|                       | FB2007          | Synapturanus | mesomorphus     |  | Guyana   | I         | I           | EF017962.1           | GenBank |
| MTD48012              | RE-040          | Synapturanus | mesomorphus     | Iwokrama                                       | Guyana   | 4.6713889 | -58.685     | MW222077.1           | GenBank |
| ROM44167              | PT-460          | Synapturanus | mesomorphus     | Plateau above<br>Meamu River                   | Guyana   | 6.3019444 | -60.478333  | MW222088.1           | GenBank |
| CTMZ7473              | GB 118          | Synapturanus | mesomorphus     | Kuribrong                                      | Guyana   | 5.34195   | -59.54223   | KDQF01002383.1       | GenBank |
| IRSNB 14906           | PK1397          | Synapturanus | mesomorphus     | Kaieteur NP                                    | Guyana   | 5.132663  | -59.416838  | KDQF01003985.1       | GenBank |
| INPA 3505             | DT 3635         | Synapturanus | Tapajos         | Middle Tapajós<br>RiveR, PA                    | Brazil   | -4.684055 | -56.444861  | MW202070.1           | GenBank |
| INPAH29574            | INPA-HT1656     | Synapturanus | Taboca          | Mineração Taboca,<br>AM                        | Brazil   | -0.72762  | -60.16744   | MW305229.1:1120-2677 | GenBank |
| MZUSP159218           | MTR18822        | Synapturanus | Purus           | rio Purus, AM                                  | Brazil   | -4.18314  | -61.48801   | KDQF01003401.1       | GenBank |
| MNHN-RA-<br>2020.0083 | AF3732          | Synapturanus | mirandaribeiroi | Voltzberg                                      | Suriname | 4.68169   | -56.18568   | KDQF01001463.1       | GenBank |
|                       |                 |              |                 |  |          |           |             | ,                    | ,       |

| APPENDIX 3. (Continued) | Continued)             |              |                 |   |           |           |            |                      |         |
|-------------------------|------------------------|--------------|-----------------|---|-----------|-----------|------------|----------------------|---------|
| Specimen voucher        | Field number           | Genus        | Species         | Locality  | Country   | Latitude  | Longitude  | Accession Number     | Source  |
| INPAH18572              | INPA-HT121             | Synapturanus | mirandaribeiroi | Parque Estadual<br>Rio Negro AM                       | Brazil    | -2.725467 | -60.40455  | HW222068.1           | GenBank |
| MNHN-<br>RA2020.0079    | AF2791<br>(APA-973-1-) | Synapturanus | mirandaribeiroi | Mitaraka  | F. Guiana | 2.23577   | -54.44928  | MW305231.1:1120-2671 | GenBank |
| MNHN-<br>RA2020.0082    | AF3975                 | Synapturanus | mirandaribeiroi | Mitaraka  | F. Guiana | 2.243153  | -54.464699 | MW222054.1           | GenBank |
| SSPCTGA-AN-<br>5465     | CTGA-N-5465            | Synapturanus | mirandaribeiroi | Experimental farm of the Federal University, Amazonas | Brazil    | -2.6333   | -60.050    | MG806096.1           | GenBank |
| MNHN-<br>RA2020.0087    | AF 3573                | Synapturanus | zombie          | Itoupe  | F. Guiana | 3.02302   | -53.09547  | MW305232.1:1121-2678 | GenBank |
| MNHN-RA-<br>2020.0085   | AF0525                 | Synapturanus | zombie          | Saul  | F. Guiana | 3.637633  | -53.213704 | KDQF010001128.1      | GenBank |
| MNHN<br>RA2020.0086     | AF1315                 | Synapturanus | zombie          | Manare  | F. Guiana | 4.183333  | -52.15     | MW222052.1           | GenBank |
| MZUSP159220             | MTR24135               | Synapturanus | zombie          | Oiapoque, AP  | Brazil    | 3.8794167 | -51.770972 | KDQF01003577.1       | GenBank |
|                         | AF238                  | Synapturanus | ajuricaba       | Manaos, AM  | Brazil    | -3.041269 | -60.043573 | MW305228.1:1117-2670 | GenBank |
|                         | AF237                  | Synapturanus | ajuricaba       | Manaos, AM  | Brazil    | -3.041269 | -60.043573 | KM509207.1           | GenBank |
| INPAH35751              | AFP341/<br>INPA-HT7069 | Synapturanus | ajuricaba       | Ilha Sapupara AM,                                     | Brazil    | -1.892436 | -59.448716 | MW222069.1           | GenBank |
| MPEG29454               | CN373/PT-007           | Synapturanus | ajuricaba       | Trombetas, PA   | Brazil    | -1.381772 | -56.863028 | MW222066.1           | GenBank |
| MPEG23273               | CN230/PT-144           | Synapturanus | ajuricaba       | Flota Faro, Pa  | Brazil    | -1.713889 | -57.213333 | MW222065.1           | GenBank |
| MPEG23271               | CN064/PT-145           | Synapturanus | ajuricaba       | Flota Faro, Pa  | Brazil    | -1.713889 | -57.213333 | MW222076.1           | GenBank |
|                         |                        |              |                 |   |           |           |            |                      |         |

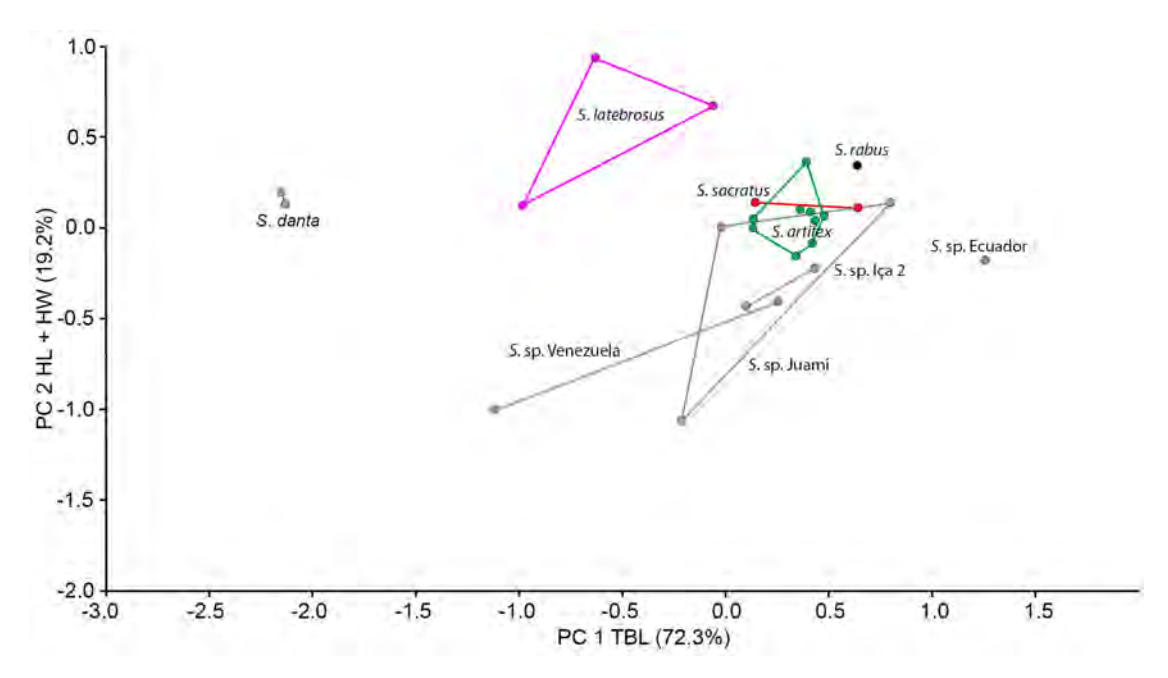
APPENDIX 4a. Results from PCA using uncorrected external morphometric data Abbreviations as in legend to Table 1.

|     | PC 1           | PC 2           | PC 3    | PC 4    | PC 5    | PC 6    | PC | Eigenvalue | % variance |
|-----|----------------|----------------|---------|---------|---------|---------|----|------------|------------|
| SVL | <b>94.88</b> 9 | -2.052         | -20.939 | -11.678 | 43.662  | -15.338 | 1  | 4,43339    | 83,442     |
| HL  | 5.072          | -81.659        | 68.688  | -68.415 | -22.468 | -20.396 | 2  | 0,627065   | 11,802     |
| HW  | 13.041         | -38.853        | 58.603  | 68.698  | -12.833 | -14.273 | 3  | 0,164149   | 3,0895     |
| END | 34.396         | -39.852        | 24.867  | -60.532 | 96.508  | 18.541  | 4  | 0,0579897  | 1,0914     |
| ED  | 1.757          | 37.331         | 31.284  | 6.996   | -25.886 | 9.983   | 5  | 0,0215525  | 0,40564    |
| TL  | 28.025         | <b>89.29</b> 1 | 27.948  | 20.652  | -31.228 | -49.338 | 6  | 0,00902078 | 0,16978    |

**APPENDIX 4c**. Boxplots for males of described and undescribed species of the *Synapturanus rabus* species complex. A. For Snout–vent length (SVL) B. For tibia length (TBL)



APPENDIX 4d. PCA using residuals of the regression of each variable on SVL



**APPENDIX 5**. Full maximum likelihood phylogenetic tree of *Synapturanus* using 16S. Node values represent SH-aLRT support (%) / ultrafast bootstrap support (%).